ornl

ORNL/TM-12908

OAK RIDGE
NATIONAL
LABORATORY

MARTIN MARIETTA

Analysis of Source Term Modeling for Low-Level Radioactive Waste Performance Assessments

Alan S. Icenhour

MANAGED BY
MARTIN MARIETTA ENERGY SYSTEMS, INC.
FOR THE UNITED STATES
DEPARTMENT OF ENERGY

ORNL/TM-12908

ANALYSIS OF SOURCE TERM MODELING FOR LOW-LEVEL RADIOACTIVE WASTE PERFORMANCE ASSESSMENTS

Alan S. Icenhour

Date Published: March 1995

Prepared by the
OAK RIDGE NATIONAL LABORATORY
Oak Ridge, Tennessee 37831-6495
managed by
MARTIN MARIETTA ENERGY SYSTEMS, INC.
for the
U.S. DEPARTMENT OF ENERGY
under contract DE-AC05-84OR21400

CONTENTS

Page

LIST OF FIGURES vii

LIST OF TABLES xi

LIST OF ABBREVIATIONS, ACRONYMS, AND INITIALISMS xiii

LIST OF SYMBOLS xv

ACKNOWLEDGMENTS xxi

ABSTRACT xxiii

1. INTRODUCTION 1

2. OVERVIEW OF PERFORMANCE ASSESSMENT METHODOLOGY 7

    2.1 INTRODUCTION 7
    2.2 DISPOSAL SYSTEM CHARACTERIZATION 8
    2.3 SOURCE TERM 11
    2.4 TRANSPORT TO RECEPTOR LOCATIONS 13
    2.5 DOSE CALCULATIONS 13
    2.6 SUMMARY 15

3. DESCRIPTION OF THE SOURCE1 AND SOURCE2 COMPUTER CODES ... 17

    3.1 INTRODUCTION 17
    3.2 OVERVIEW OF THE SOURCE CODES 17
    3.3 CONCRETE DEGRADATION 21
        3.3.1 Sulfate Attack 29
        3.3.2 Calcium Hydroxide Leaching 30
        3.3.3 Corrosion of Steel Reinforcement 31
        3.3.4 Corrosion of Metal Barriers 32
    3.4 CONCRETE STRUCTURAL AND CRACKING ANALYSES 32
        3.4.1 Concrete Structural Analysis 32
        3.4.2 Concrete-Cracking Analysis 33
    3.5 CONTAMINANT LEACHING MODELS 35
    3.6 SUMMARY 35

4. CONTAMINANT TRANSPORT THEORY 37

4.1 INTRODUCTION 37
4.2 ADVECTION-DIFFUSION EQUATION 38
4.3 MODIFICATION OF ADVECTION-DIFFUSION EQUATION FOR TRANSPORT OF RADIONUCLIDES IN A POROUS BODY 41
4.4 COEFFICIENTS IN THE ADVECTION-DIFFUSION EQUATION 46
4.5 UNSATURATED POROUS MEDIA 47
4.6 SEMIANALYTICAL SOLUTION OF THE ADVECTION-DIFFUSION EQUATION 48
4.6.1 Advection Analytical Solution 48
4.6.2 Diffusion Analytical Solution 57
4.6.3 Total Leaching Solution 61
4.7 SUMMARY 61

5. COMPARISON OF ADVECTION MODELS 63

5.1 INTRODUCTION 63
5.2 OVERVIEW OF ZERO-ORDER ADVECTION MODEL 63
5.3 OVERVIEW OF FIRST-ORDER ADVECTION MODEL 64
5.4 COMPARISON OF MODELS 66
5.4.1 Tumulus-Type Disposal 68
5.4.2 Silo-Type Disposal 75
5.4.3 Unlined Trench-Type Disposal 81
5.5 HALF-LIFE EFFECTS ON ADVECTIVE MODELS 87
5.6 DISTRIBUTION COEFFICIENT EFFECTS ON ADVECTIVE MODELS 89
5.7 SUMMARY OF RESULTS 95

6. APPLICATION OF THE SOURCE1 CODE TO THE DEVELOPMENT OF AN INTRUDER SCENARIO 97

6.1 INTRODUCTION 97
6.2 SENSITIVITY AND UNCERTAINTY ANALYSES 99
6.3 EVALUATION OF TIME OF INTRUSION 101
6.4 EVALUATION OF REMAINING INVENTORY AT TIME OF INTRUSION 105
6.5 SUMMARY OF METHOD 105

7. CONCLUSIONS 107

8. RECOMMENDATIONS 111

8.1 INTRODUCTION 111
8.2 RECOMMENDATION 1: ALTERNATIVE SOLUTION OF THE ADVECTION-DIFFUSION EQUATION 111

8.3 RECOMMENDATION 2: ACCOUNTING FOR RADIOACTIVE DAUGHTERS 112
8.4 RECOMMENDATION 3: CONCRETE-DEGRADATION MECHANISMS 112
8.5 RECOMMENDATION 4: CORROSION MODELS OF METAL BARRIERS 113
8.6 RECOMMENDATION 5: EVALUATION OF THE RELATIONSHIP BETWEEN MOBILE AND IMMOBILE CONTAMINANTS 113
8.7 RECOMMENDATION 6: VARIATION OF DIFFUSION COEFFICIENTS AND DISTRIBUTION COEFFICIENTS FOR SENSITIVITY AND UNCERTAINTY ANALYSES 114
8.8 RECOMMENDATION 7: UNCERTAINTY IN SOURCE TERM MODELS USED IN INTRUDER SCENARIO DEVELOPMENT 114
8.9 RECOMMENDATION 8: SOURCE TERM CODES AS DESIGN TOOLS 115

REFERENCES 117

APPENDIX A. RELATIONSHIP OF THE DIMENSIONLESS DISTRIBUTION COEFFICIENT TO OTHER COMMONLY MEASURED DISTRIBUTION COEFFICIENTS 123

APPENDIX B. GRAPHS OF ADVECTIVE MODEL COMPARISONS 127

LIST OF FIGURES

Figure		Page
2.1	Components of a performance assessment.	9
2.2	Examples of pathways for contaminant release to the environment.	12
2.3	Examples of exposure pathways to humans from environmental contaminants	14
3.1	Representative tumulus-type disposal facility modeled by SOURCE1	18
3.2	Representative silo-type disposal facility modeled by SOURCE2	19
3.3	Logic flow in the SOURCE computer codes	20
3.4	Logic flow in the concrete degradation and cracking subroutines for the SOURCE codes	34
4.1	Representation of the system modeled by the FLOTHRU computer code	57
5.1	Comparison of the cumulative fraction of ^{137}Cs leached from a tumulus (SOURCE1 with first-order advection model) with and without decay after release	69
5.2	Comparison of ^{137}Cs fractional leach rates from a tumulus (SOURCE1) using zero-order and first-order advection models	74
5.3	Comparison of the undecayed cumulative fraction of ^{137}Cs leached from a tumulus (SOURCE1) using zero-order and first-order advection models	74
5.4.	Comparison of ^{137}Cs fractional leach rates from a silo (SOURCE2) using zero-order and first-order advection models.	80
5.5	Comparison of the undecayed cumulative fraction of ^{137}Cs leached from a silo (SOURCE2) using zero-order and first-order advection models	80
5.6	Comparison of ^{137}Cs fractional leach rates from an unlined trench (SOURCE2) using zero-order and first-order advection models	86

5.7 Comparison of the undecayed cumulative fraction of ^{137}Cs leached from an unlined trench (SOURCE2) using zero-order and first-order advection models 86

5.8 Comparison of the undecayed cumulative fraction of ^{135}Cs leached from a tumulus (SOURCE1) using zero-order and first-order advection models . . . 88

5.9 Comparison of the undecayed cumulative fraction of ^{135}Cs leached from a silo (SOURCE2) using zero-order and first-order advection models 88

5.10 Comparison of the undecayed cumulative fraction of ^{135}Cs leached from an unlined trench (SOURCE2) using zero-order and first-order advection models 89

5.11 Comparison of the undecayed cumulative fraction of ^{137}Cs leached from a tumulus (SOURCE1) using zero-order and first-order advection models for $K_d = 1.99$ 92

5.12 Comparison of the undecayed cumulative fraction of ^{137}Cs leached from a tumulus (SOURCE1) using zero-order and first-order advection models for $K_d = 199$ 92

5.13 Comparison of the undecayed cumulative fraction of ^{137}Cs leached from a silo (SOURCE2) using zero-order and first-order advection models for $K_d = 1.99$ 93

5.14 Comparison of the undecayed cumulative fraction of ^{137}Cs leached from a silo (SOURCE2) using zero-order and first-order advection models for $K_d = 199$ 93

5.15 Comparison of the undecayed cumulative fraction of ^{137}Cs leached from an unlined trench (SOURCE2) using zero-order and first-order advection models for $K_d = 1.99$ 94

5.16 Comparison of the undecayed cumulative fraction of ^{137}Cs leached from an unlined trench (SOURCE2) using zero-order and first-order advection models for $K_d = 199$ 94

6.1 Relative frequency of vault-wall thickness reaching 0.0 m for a tumulus-type disposal facility 104

6.2 Relative frequency of ^{137}Cs inventory remaining after 322 years for a tumulus-type disposal facility 106

B.1 Comparison of the undecayed cumulative fraction of ^{3}H leached from a tumulus (SOURCE1) using zero-order and first-order advection models 129

B.2 Comparison of the undecayed cumulative fraction of ^{14}C leached from a tumulus (SOURCE1) using zero-order and first-order advection models 129

B.3 Comparison of the undecayed cumulative fraction of ^{90}Sr leached from a tumulus (SOURCE1) using zero-order and first-order advection models 130

B.4 Comparison of the undecayed cumulative fraction of ^{152}Eu leached from a tumulus (SOURCE1) using zero-order and first-order advection models 130

B.5 Comparison of the undecayed cumulative fraction of ^{238}U leached from a tumulus (SOURCE1) using zero-order and first-order advection models 131

B.6 Comparison of the undecayed cumulative fraction of ^{3}H leached from a silo (SOURCE2) using zero-order and first-order advection models 131

B.7 Comparison of the undecayed cumulative fraction of ^{14}C leached from a silo (SOURCE2) using zero-order and first-order advection models 132

B.8 Comparison of the undecayed cumulative fraction of ^{90}Sr leached from a silo (SOURCE2) using zero-order and first-order advection models 132

B.9 Comparison of the undecayed cumulative fraction of ^{152}Eu leached from a silo (SOURCE2) using zero-order and first-order advection models 133

B.10 Comparison of the undecayed cumulative fraction of ^{238}U leached from a silo (SOURCE2) using zero-order and first-order advection models 133

B.11 Comparison of the undecayed cumulative fraction of ^{3}H leached from an unlined trench (SOURCE2) using zero-order and first-order advection models 134

B.12 Comparison of the undecayed cumulative fraction of ^{14}C leached from an unlined trench (SOURCE2) using zero-order and first-order advection models 134

B.13 Comparison of the undecayed cumulative fraction of ^{90}Sr leached from an unlined trench (SOURCE2) using zero-order and first-order advection models 135

B.14 Comparison of the undecayed cumulative fraction of ^{152}Eu leached from an unlined trench (SOURCE2) using zero-order and first-order advection models 135

B.15 Comparison of the undecayed cumulative fraction of ^{238}U leached from an unlined trench (SOURCE2) using zero-order and first-order advection models 136

LIST OF TABLES

Table		Page
2.1	Examples of performance objectives for low-level radioactive waste disposal	7
3.1	Sample input data for the SOURCE1 code	22
3.2	Sample output data (abridged) for the SOURCE1 code	26
5.1	Summary of radionuclide data used in advective model comparisons	67
5.2	Example of physicochemical parameters used in the SOURCE1 simulation of a tumulus-type waste disposal facility	70
5.3	Monthly water infiltration values for a tumulus	73
5.4	Example of physicochemical parameters used in the SOURCE2 simulation of a silo-type waste disposal facility	76
5.5	Monthly water infiltration values for a silo	79
5.6	Example of physicochemical parameters used in the SOURCE2 simulation of a trench-type waste disposal facility	82
5.7	Monthly water infiltration values for an unlined trench	85
5.8	Distribution coefficients and diffusion coefficients for cesium used in the analysis of the effect of K_d on the first-order and zero-order advective models	91
5.9	Comparison of maximum undecayed cumulative fraction leached values for ^{137}Cs using two advective models	95
6.1	SOURCE1 code sensitive parameters and range of uncertainty	102
A.1	Relationship of the dimensionless distribution coefficient (K) to some other commonly measured distribution coefficients	125

LIST OF ABBREVIATIONS, ACRONYMS, AND INITIALISMS

BLT	Breach-Leach-Transport
BNL	Brookhaven National Laboratory
$Ca(OH)_2$	Calcium Hydroxide
DOE	U.S. Department of Energy
DUST	Disposal Unit Source Term
EPRI	Electric Power Research Institute
FD	Finite Difference
FEMWATER	Finite Element Model of Water Flow
INEL	Idaho National Engineering Laboratory
KOH	Potassium Hydroxide
LLW	Low-Level Radioactive Waste
MCMC	Multi-Cell Mixing Cascade
NaOH	Sodium Hydroxide
ORNL	Oak Ridge National Laboratory
RAE	Rogers and Associates Engineering
S/S	Solidification/Stabilization
SOURCE	Used when referring to both the SOURCE1 and SOURCE2 codes
SWSA	Solid Waste Storage Area

LIST OF SYMBOLS

English

A	=	cross-sectional area of the porous body (cm^2)
A_o	=	surface area over which oxygen diffuses to the reinforcement (cm^2)
C	=	mass of mobile contaminant per unit volume fluid (g/cm^3)
Ca_l	=	groundwater release rate of $Ca(OH)_2$ ($year^{-1}$)
Ca_c	=	$Ca(OH)_2$ concentration in concrete (mol/L)
Ca_p	=	$Ca(OH)_2$ concentration in concrete pore solution (mol/L)
C_e	=	concentration of sulfate as ettringite (mol/m^3)
C_I	=	mass of immobile contaminant per unit volume of the porous body (g/cm^3)
C_M	=	mass of mobile contaminant per unit volume of the porous body (g/cm^3)
c_o	=	groundwater sulfate concentration (mol/m^3)
C_{sl}	=	solubility limit of the radionuclide in the pore fluid (g/cm^3)
C_T	=	total mass of contaminant in the porous body per unit volume of the porous body (g/cm^3)
C_t	=	concrete member thickness (m)
$\frac{\partial C_v}{\partial x}$	=	concentration gradient of the contaminant (g/cm^4)
$C_v(x,t) = C_v$	=	mass of contaminant (at spatial position x and time t) per unit volume (g/cm^3)
D	=	diffusion coefficient (cm^2/s)
D_i	=	"intrinsic" diffusion coefficient (m^2/s)

D_o	=	diffusion coefficient of oxygen through concrete (cm^2/s)
D_s	=	self-diffusion coefficient (cm^2/s)
E	=	Young's modulus (Pa)
F_{ax}	=	advective flux of the contaminant in the x direction ($g\ cm^{-2}\ s^{-1}$)
G	=	geometry factor (dimensionless)
H	=	fraction of pcre capacity to hold liquid that is filled (dimensionless)
h	=	relative saturation (dimensionless)
I	=	water percolation rate through concrete (m/year)
J_o	=	oxygen flow rate at the steel reinforcement (g/s)
J_x	=	diffusive flux of the contaminant in the x direction ($g\ cm^{-2}\ s^{-1}$)
K	=	partition coefficient (dimensionless)
k	=	an empirical constant (units depend on the value of N)
K_d	=	radionuclide distribution coefficient (mL/g)
L	=	mass of radionuclide leached because of advection (g)
L_a	=	total mass of radionuclide released during a time step (g)
$\frac{dL_a}{dt}$	=	radionuclide release rate caused by advection in year a (g/year)
$\frac{dL_i}{dt}$	=	radionuclide release rate caused by advection during month i (g/month)
$\frac{dL_o(t)}{dt}$	=	leach rate calculated in Version 1.0 SOURCE codes (g/s)
$\frac{dL(t)}{dt}$	=	advective leach rate at time t (g/s)

N	=	an empirical constant (dimensionless)
n	=	effective porosity (volume of interconnected pores per unit volume of the porous body) (cm^3/cm^3)
$\frac{d[O_2]}{dx}$	=	dissolved oxygen concentration gradient (g/cm^4)
Q	=	total mass of contaminant in the porous body (g)
q	=	fluid infiltration rate (cm/s)
Q_0	=	initial mass of radionuclide in the porous body (g)
Q_a	=	radionuclide inventory available for leaching at the beginning of year a (g)
Q_i	=	mass of radionuclide in the contaminated volume at the beginning of month i (g)
q_i	=	water percolation rate through the waste during month i (cm/month)
$Q(t)$	=	mass of radionuclide in the porous body (g) at time t
R	=	degradation rate (m/s)
R_d	=	retardation factor (unitless)
R_s	=	solubility limited release rate during the period of interest (g/s)
S	=	mass of immobile contaminant per unit mass of porous body (g/g)
T_R	=	average residence time of contaminants in the porous body (s)
t	=	time (s)
Δt	=	length of time step (year)
t'	=	time (month)
$t_{1/2}$	=	half-life (s)

$t_{\frac{1}{2}}'$	=	half-life (year)
t_1, t_2	=	the bounds of the time period of interest (s)
t_1', t_2'	=	the bounds of the time period of interest (month)
t_a	=	duration of leaching interval (one year)
u_x	=	the fluid velocity in the x direction (cm/s)
v	=	pore fluid velocity (cm/s)
v_n	=	effective velocity of the mobile radionuclides in the porous body (cm/s)
W	=	width of the porous body (cm)
WA	=	the total volume of the porous body (cm^3)
x	=	distance (cm)

Greek

α	=	roughness factor for fracture path (dimensionless)
β	=	linear strain caused by a mole of sulfate reacted in a m^3 (unitless)
γ	=	constrictivity (dimensionless)
λ_a	=	decay constant ($year^{-1}$)
λ_d	=	radioactive decay constant (s^{-1})
λ_d'	=	decay constant ($month^{-1}$)
λ_L	=	leach rate constant (s^{-1})
$\lambda_{L,i}$	=	leach rate constant for month i ($month^{-1}$)
ρ_b	=	bulk density (mass of porous body per unit volume of the porous body) (g/cm^3)

σ	=	fracture surface energy of concrete (J/m^2)
μ_c	=	Poisson's ratio for concrete (dimensionless)
τ	=	tortuosity (dimensionless)

ACKNOWLEDGMENTS

This work was originally produced as an M.S. degree thesis in nuclear engineering at the University of Tennessee. Larry Miller, Peter Groer, and Raphael Perez, all of the University of Tennessee, each provided excellent review and comment. At the Oak Ridge National Laboratory, Herschel Godbee, Jerry Klein, John Begovich, and Don Lee were each a source of advice, critical review, and support. Lynn Tharp provided expert assistance and guidance in the use of the SOURCE and PRISM computer codes. Steve Loghry assisted in the final figure preparation. Ralph Sharpe provided insightful and timely editorial review and comment. Finally, the outstanding efforts and expert word processing of Sue McDaniel resulted in the preparation of this manuscript.

ABSTRACT

Site-specific radiological performance assessments are required for the disposal of low-level radioactive waste (LLW) at both commercial and U.S. Department of Energy facilities. The purpose of these assessments is to provide the technical basis for demonstrating compliance with performance objectives for LLW disposal as set forth by appropriate authorities. Performance assessments are used to evaluate potential doses to individuals as a result of the release of radionuclides to the environment and intrusion into the disposal facility. Complex computer models are often used to calculate the release of radionuclides from a facility and the transport of these radionuclides through the environment. The calculated releases constitute the source term for a performance assessment.

This work explores source term modeling of LLW disposal facilities by using two state-of-the-art computer codes, SOURCE1 and SOURCE2. An overview of the performance assessment methodology is presented, and the basic processes modeled in the SOURCE1 and SOURCE2 codes are described.

A detailed derivation of contaminant transport equations for a waste disposal facility results in a first-order advective model which can be compared with the zero-order model used in the SOURCE1 and SOURCE2 codes. The derivation accounts for radioactive decay, radionuclide sorption/desorption, and unsaturated transport in a porous medium. The concept of the leach rate constant is used as a basis for the first-order advective model.

Comparisons are made between the two advective models for a variety of radionuclides, transport parameters, and waste-disposal technologies. These comparisons show that, in general, the zero-order model predicts undecayed cumulative fractions leached that are slightly greater than or equal to those of the first-order model. For long-lived radionuclides, results from the two models eventually reach the same value. By contrast, for short-lived radionuclides, the zero-order model predicts a slightly higher

undecayed cumulative fraction leached than does the first-order model. Variation of the distribution coefficient produces small differences between the two advective models.

A new methodology, based on sensitivity and uncertainty analyses, is developed for predicting intruder scenarios. This method is demonstrated for ^{137}Cs in a tumulus-type disposal facility. The sensitivity and uncertainty analyses incorporate input-parameter uncertainty into the evaluation of a potential time of intrusion and the remaining radionuclide inventory.

Finally, conclusions from this study are presented, and recommendations for continuing work are made. From the work presented, it is clear that source term modeling presents a large number of areas for investigation. The work presented in this report enhances the understanding of source term modeling. Continued work in the recommended areas should lead to further improvement in source term codes.

1. INTRODUCTION

Low-level radioactive wastes (LLW) generated in government and commercial operations need to be isolated from the environment almost in perpetuity (at least minimally for 300 to 500 years and, in some cases, even longer). An increasing number waste disposal sites use facilities with engineered barriers (e.g., concrete, metal, and plastic) to isolate these wastes from the environment.[1] However, little actual data are available concerning whether the engineered barriers in these facilities can contain LLW over long periods of time. In the absence of such data, computer codes are generally used to analyze the expected performance of a facility with time. This analysis, termed a *performance assessment*, provides insight into potential radionuclide releases from the facilities at a disposal site and ultimately aids in the prediction of doses to individuals from these releases. A performance assessment is conducted as a check to determine whether the facility performs as designed (i.e., to demonstrate that the facility can meet the criteria established by appropriate authority). In addition, performance assessments can be used to set limits on the amounts of specific radionuclides that may be disposed of at an LLW disposal facility in order not to exceed regulatory constraints.

Source terms (i.e., estimates of the release of radionuclides from disposal facilities over time) are needed to provide input information for the hydrogeological models used in performance assessments. For the most part, computer models are used to evaluate the source term for a facility. These models attempt to describe mathematically the complex interaction of water with LLW and the transport of radionuclides away from the disposal facility. In addition, some sophisticated source-term computer codes include routines that model the performance (degradation) of engineered barriers, over time. Several examples of more commonly used computer codes that have been developed to evaluate source terms include GWSCREEN,[2] BLT (Breach-Leach-Transport),[3] DUST (Disposal Unit Source Term),[4] BARRIER,[5] as well as SOURCE1 and SOURCE2.[6]

GWSCREEN was developed at Idaho National Engineering Laboratory (INEL) to assess the release of contaminants to groundwater from both surface and subsurface

sources. This code does not address the degradation of engineered barriers. Contaminant transport is modeled as a first-order leaching process that accounts for radioactive decay and sorption/desorption of contaminants by solids. Diffusive transport is not modeled in GWSCREEN.

The BLT code was written at Brookhaven National Laboratory (BNL) to evaluate releases of radionuclides from LLW disposal facilities. This code calculates radionuclide releases as a result of water infiltration, waste-container degradation, and waste form leaching. The water-infiltration input for BLT is estimated by using FEMWATER (Finite Element Model of Water Flow),[7] a two-dimensional unsaturated flow code. Two types of container degradation models are available in BLT: general failure, which is a function of the container thickness and a user-specified corrosion rate, and local failure, which is based on a semiempirical relationship. Because both of the degradation mechanisms focus on metal corrosion, the BLT code is not usually applicable to facilities with concrete barriers. Leaching of contaminants from the waste form by three mechanisms is considered: diffusion through pores in the form, dissolution of the form, and surface rinse of the form. Each of these release mechanisms is calculated independently and then summed to evaluate the total release. The total release is scaled by the fraction of the waste container that has degraded.

The DUST code was also written at BNL. This code simulates waste container degradation and contaminant transport, and is used to predict releases from disposal facilities that utilize shallow-land burial. Container degradation is simulated by a method similar to that used in the BLT code (i.e., metallic corrosion). Two types of degradation are modeled: general failure, which occurs at a user-specified time, and localized failure, which allows containers to partially fail over time because of localized corrosion (e.g., pitting and stress corrosion cracking). Contaminant release is initiated when container failure begins. Two methods to evaluate contaminant releases are available in the code: the Finite Difference (FD) model and the Multi-Cell Mixing Cascade (MCMC) model. The FD model uses the method of finite differences and specified initial and boundary conditions to solve an advection-diffusion equation. The MCMC model

divides the disposal facility into a number of mixing cells of uniform size and concentration. The MCMC model considers only advective transport for the release of contaminants from these mixing cells. Four types of release mechanisms can be simulated through the use of the FD and MCMC models: solubility-limited release, surface rinse with partitioning, diffusion release (FD model only), and uniform release (equivalent to dissolution modeled in BLT). Based on the type of waste form, the user can specify a release mechanism to be used by the code.

The BARRIER code was developed by Rogers and Associates Engineering Corporation (RAE) with the sponsorship of the Electric Power Research Institute (EPRI). This code not only provides a source term but also calculates radionuclide transport in the environment and subsequent doses to individuals. BARRIER was one of the first attempts at modeling the long-term performance of barriers used in LLW disposal. This code can be used to model above- and below-ground vault disposal, disposal using modular concrete canisters, and facilities which have no engineered barriers. The concrete degradation mechanisms modeled are sulfate attack, calcium hydroxide leaching, freeze-thaw cycling, and corrosion of metal reinforcement. Rates of water infiltration increase as the engineered barriers degrade. Four options are available to calculate the release of radionuclides from a disposal facility: constant leach rate, nuclide specific leach rate, advection with partitioning of contaminants between a liquid and solid, and diffusion.

The SOURCE1 and SOURCE2 codes, collectively called the SOURCE codes, were prepared by RAE for the Oak Ridge National Laboratory (ORNL). The SOURCE1 code is used to model releases from tumulus-type waste disposal facilities. SOURCE2 is used to predict releases from silo, well, well-in-silo, and trench-type waste disposal facilities. Both of these source term codes predict the performance of engineered barriers, over time. Concrete degradation mechanisms included in the SOURCE codes are sulfate attack, calcium hydroxide leaching, and corrosion of metal reinforcement. Additionally, these codes model the corrosion of metal containers (e.g., steel boxes and pipes) that may be used in a waste disposal facility. Degradation of the engineered barriers results in

increased water flow through a disposal facility. Two transport mechanisms, advection and diffusion, are modeled by the SOURCE codes. The total radionuclide release is the sum of the calculated releases by advection and diffusion.

As this brief overview brings out, all available models/codes considered viable have limitations in terms of developing (1) algorithms to describe the time-response for complex physicochemical phenomena and (2) computer codes to integrate or couple these phenomena and evaluate them. The existing codes are being upgraded, and new, more advanced ones are being developed. It is generally conceded that all have shortcomings and other inherent problems that can be overcome, but correcting these deficiencies will require considerable time. Given the current state of the art in code development, the classical conservative approach applied in the BARRIER code may make it the most viable and defensible code available (e.g., see Ref. 8). The SOURCE codes used in this study are spinoffs of the source term portions of the BARRIER code.

The purpose of this work is to explore source term modeling for performance assessments of LLW disposal facilities. The SOURCE1 and the SOURCE2 codes are used as the source term models. This study focuses on three areas: development of contaminant transport theory (Chapter 4), comparison of advective transport models (Chapter 5), and development of a method to predict doses to an inadvertent intruder into an LLW disposal facility (Chapter 6).

In Chapter 2, the general methodology used in performance assessments is described. Each of the major steps in a performance assessment is discussed to provide insight into this complex process. These steps include disposal system characterization, source term determination, calculation of the transport of radionuclides to receptor locations, and the evaluation of doses to individuals.

In Chapter 3, the SOURCE1 and the SOURCE2 computer codes are described. These codes, either in original form or with modifications, are used for the computations performed as part of this work. The degradation and structural failure mechanisms modeled by the codes are discussed. Additionally, an overview of the contaminant transport mechanisms modeled in the SOURCE1 and the SOURCE2 codes is presented.

In Chapter 4, contaminant transport theory is discussed. First, a basic advection-diffusion equation for transport of stable (i.e., nonradioactive) contaminants in a fluid is derived. The equation is then modified to describe transport in a saturated porous body (e.g., concrete) and to account for a radioactive contaminant. Next, this equation is modified for the case in which the porous body is not saturated. Finally, situations that are dominated by either advective or diffusive transport are discussed, and methods of solution are presented. For the case dominated by advection, an advective transport equation, which is different from the one used in Version 1.0 of the SOURCE codes,[6] is derived. The solution of the advective transport equation is based on the use of a leach rate constant.

In Chapter 5, comparisons are made between the advective transport model derived in Chapter 4 (first-order model) and the advective model used in Version 1.0 of the SOURCE codes (zero-order model). Six radionuclides are used for the comparisons to provide a broad range of contaminant properties. Comparisons between the two advective models are performed for each of these radionuclides for three types of disposal facilities: tumulus, silos, and unlined trenches. In addition, the effects of two properties, half-life and distribution coefficient, are examined for each of the two advective models. The results of these comparisons show that, in general, the zero-order advective model predicts an undecayed cumulative fraction leached that is slightly greater than or equal to the first-order advective model prediction. For long-lived radionuclides, both models eventually reach the same undecayed cumulative fraction leached. On the other hand, for short-lived radionuclides, the results form the zero-order model are slightly greater than the results from the first-order model. Variation of the distribution coefficient produced small differences between the two advective models.

In Chapter 6, a different perspective on source term modeling is examined. Up to this point, the discussion has focused on the radionuclide release and transport from a waste disposal facility. These types of calculations allow for an evaluation of doses to an individual who is located away from the disposal site. However, an individual who intrudes into a facility would also receive a dose from the radionuclide inventory

remaining in the facility. Parameters used in source term models are often selected to maximize the estimated release of radionuclides. Hence, using these parameters may quickly deplete the radionuclide inventory and, depending on the time of intrusion, may lead to little or no calculated dose to an intruder. In Chapter 6, a new method is presented to predict a reasonable time at which inadvertent intrusion into a tumulus-type facility might occur and the remaining radionuclide inventory at this time of intrusion. This method, based on sensitivity and uncertainty analyses, combines parameter uncertainties with the degradation and the transport models in SOURCE1 to aid in the prediction of a time of intrusion and the remaining inventory.

In Chapter 7, conclusions from this study are provided. In Chapter 8, the final chapter, recommendations for further work in the area of source term modeling for LLW disposal facility performance assessments are offered.

2. OVERVIEW OF PERFORMANCE ASSESSMENT METHODOLOGY

2.1 INTRODUCTION

Performance assessments are conducted to demonstrate the compliance of LLW disposal facilities with performance objectives that are established by an appropriate authority. These objectives are designed to protect public safety and health and to protect the environment. Examples of performance objectives for LLW disposal are presented in Table 2.1. These objectives were established for U.S. Department of Energy (DOE) sites in DOE Order 5820.2A.[9]

Table 2.1. Examples of performance objectives for low-level radioactive waste disposal

Objective	Limit/requirement	Comment
Protection of public safety and health	As specified in DOE Orders	Example: DOE Order 5400.5, "Radiation Protection of the Public and the Environment"
Limitation of external dose to public	25 mrem/year	Doses are from contaminants in surface water, groundwater, soil, plants, and animals
Limitation of atmospheric releases	Specified in 40CFR61	
Limitation in releases of radioactivity in effluents to the environment	As low as reasonably achievable	As commonly defined by the Nuclear Regulatory Commission
Limitation of the committed effective dose equivalent to inadvertent intruders		After loss of active institutional control (100 years)
Continuous exposure	100 mrem/year	
Acute exposure	500 mrem	
Protection of groundwater resources	As specified in federal, state, and local requirements	

Performance assessments can be used also as tools to maintain a disposal facility in compliance with performance objectives. Disposal limits for various radionuclides can be established through performance assessments to meet these objectives. These limits then become part of the waste acceptance criteria for a particular disposal facility. In addition, performance assessments may present insight into different types of disposal options that may ultimately be used in the design of a disposal facility.

Figure 2.1 provides a basic overview of the performance assessment methodology. First, the disposal system must be characterized. Then, potential releases (i.e., a *source term*) of radionuclides from the disposal facility are evaluated. Next, calculations are performed for the transport of the released radionuclides to locations at which compliance with the performance objectives must be evaluated (i.e., *receptor locations*). Finally, various exposure pathways to individuals are evaluated to aid in the calculation of potential radiological doses. These doses can be compared with the performance objectives to determine if the disposal facility is in compliance with the requirements. Each of these components is described in this chapter.

2.2 DISPOSAL SYSTEM CHARACTERIZATION

To develop reasonable models for contaminant release and transport from a waste disposal facility, it is important to gather as much detail about the disposal system as possible. The disposal system includes a broad spectrum of components which impact contaminant transport from a facility. These components include the waste streams, the waste forms, the immobilization agents, the surrounding site, and the engineered disposal facility. Hence, the characterization of each of these components is necessary to characterize the entire disposal system.

Waste stream characterization results in the identification of the types and amounts of radionuclides in a disposal system. In addition, characterization should also identify the chemical form (e.g., compound, ion, colloid, complex, etc.) of the radionuclide. This

ORNL-DWG 95-5639

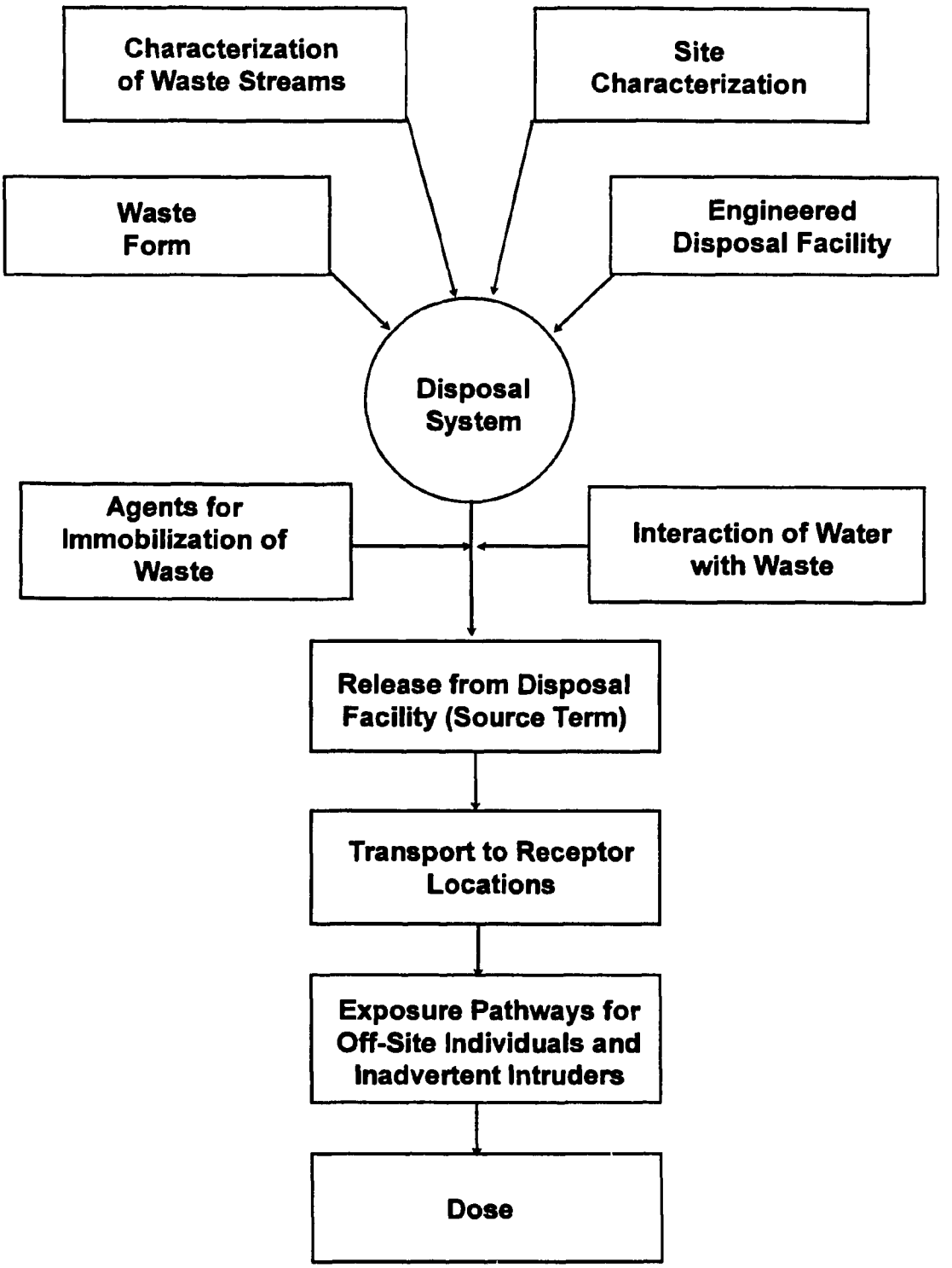

Fig. 2.1. Components of a performance assessment.

information is important to aid in the prediction of chemical interactions of a given species with both the waste and the environment.

The form of the waste affects its ability to prevent the release of radionuclides. Waste may be loosely placed in a disposal facility with no other containers. On the other hand, before its disposal, waste may be placed into containers such as drums or boxes. These containers can be made of metal, concrete, cardboard, or other materials. Waste may also be incorporated into concrete, asphalt, or some other solidification/stabilization (S/S) agent.

Special materials (or agents) may be added to the waste to immobilize (or slow the release of) radionuclides. This addition is sometimes performed as part of a waste S/S process (e.g., S/S of waste in concrete, asphalt, etc.). These agents may be effective only for selected radionuclides. Some types of agents that have been added to concrete-solidified waste include conasaga shale for cesium and blast furnace slag for technetium.[10-12] The particular mix of S/S agents can be specifically formulated for a given waste stream to minimize the release of radionuclides. The composition of these mixtures can be used to establish parameters that describe the transport of the radionuclide from the waste form.

The site characterization includes a description of the site location, topography, geology, soils, hydrogeology, surface water, and climate. A knowledge of these data helps with the establishment of the water flow field and also the amount of water available to infiltrate the disposal facility. Hence, the amount of water that may contact the waste can be estimated. In addition, site characterization also aids in the evaluation of the transport of radionuclides away from the disposal facility.

The description of the engineered disposal facility is important to identify barriers that may prevent or delay the release of radionuclides. The complexity of a facility may range from an unlined trench to a facility that contains multiple barriers, leachate collection systems, and sophisticated monitoring systems. In addition to presenting a physical barrier to release, the materials comprising a disposal facility can also act as a chemical barrier (e.g., sorption of radionuclides onto facility materials). Thus, the

chemical properties of a facility must be considered in addition to its construction details. The effects of both physical and chemical barriers can be incorporated into computer models that describe the release of radionuclides.

2.3 SOURCE TERM

The estimation of the release of contaminants from a disposal facility is referred to as a *source term determination.* This source term provides an estimate, as a function of time, of the amount of contaminants that are released and available for transport to receptor locations. Contaminant release can occur through numerous pathways, as is illustrated in Fig. 2.2. Gaseous or particulate contaminants can become airborne. Water runoff that has contacted the waste may contaminate surface water or the surrounding soil. Finally, contaminants can be released directly to groundwater from the disposal facility.

It is very important that the disposal system be well characterized to calculate the source term. Then, decisions can be made regarding the types of releases that will be modeled. For example, if it is not likely that gaseous contaminants will be present or that particulates could become suspended, then airborne releases might be ignored. In addition, decisions on the types of models to be used can be made based on the disposal system characterization. The complexity of the disposal system may warrant the use of specific models to reasonably describe the system.

Numerous computer models have been developed to calculate the source term from radioactive waste disposal facilities.[2-6] These models are often specifically created for certain types of facilities and, as a result, are often unique in their application. Computer models provide an estimate of the release of contaminants from a disposal facility. Normally, both radioactive decay and chemical interactions of contaminants are incorporated into these calculations. Results from source term models are used to predict the transport of contaminants to receptor locations.

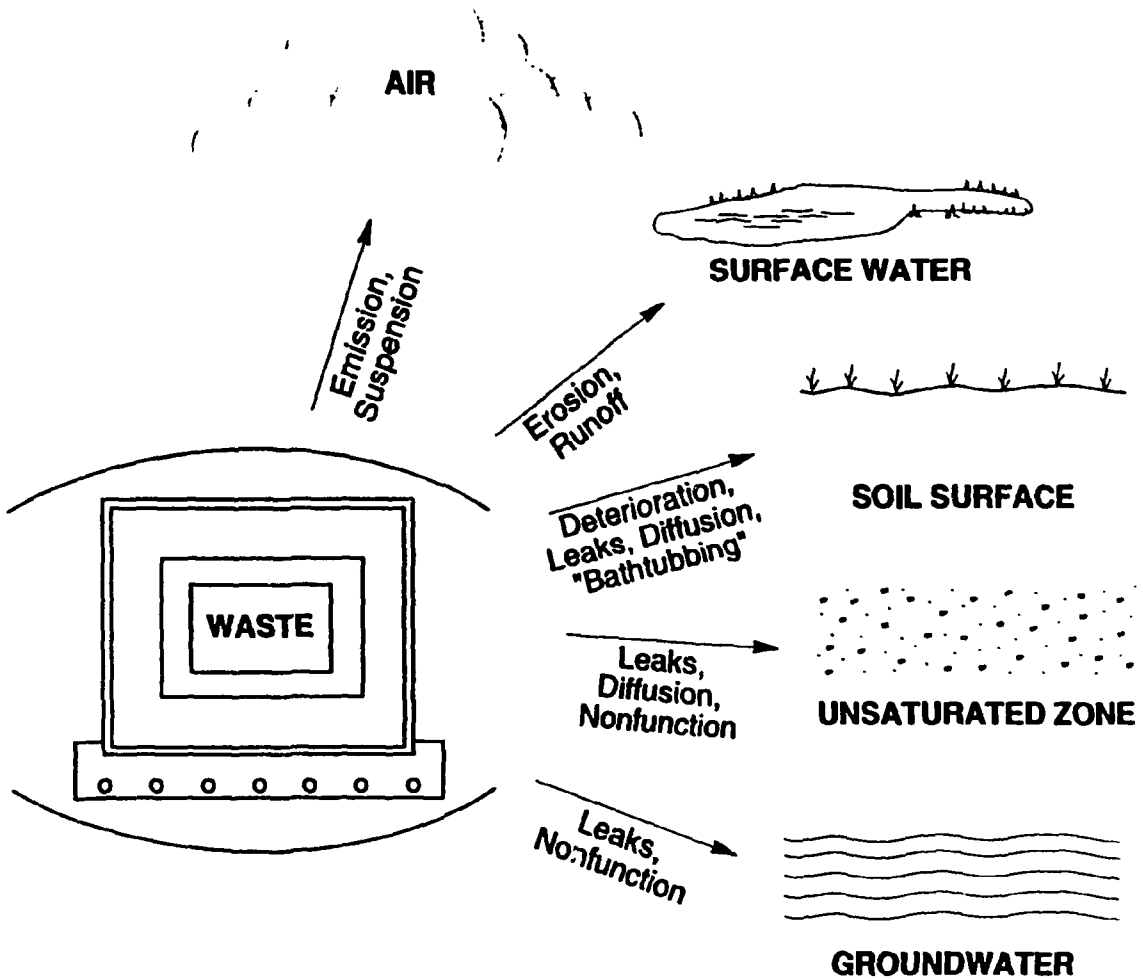

Fig. 2.2. Examples of pathways for contaminant release to the environment.
(Courtesy of ORNL Waste Management and Remedial Action Division)

2.4 TRANSPORT TO RECEPTOR LOCATIONS

Once the source term has been evaluated, the transport of the radionuclides to receptor locations can be calculated. The type of transport depends on the release path and the location of the receptor. Air-dispersion models may be used to calculate releases to the atmosphere. These models may contain routines that both estimate the deposition of contaminants on the ground and calculate concentrations in the plume. An appropriate surface-water model may be selected to calculate the transport of contaminants released to a stream, lake, or river. Finally, available transport models account for the movement of contaminants through the groundwater in both the unsaturated (vadose) and saturated zones. Reference 13 provides an overview of the types of models (for transport to receptor locations) that may be encountered in a performance assessment.

The selection of an appropriate model should be made only after careful evaluation of the disposal system characterization and the potential release pathways. The results from these models can then be used to estimate the amount of a given radionuclide reaching a receptor as a function of time.

2.5 DOSE CALCULATIONS

The amount or concentration of a radionuclide at a receptor location can be used to estimate the dose to an exposed individual. The calculated dose is a function of the exposure pathway. Potential exposure pathways for humans are presented in Fig. 2.3. Airborne releases can result in internal doses from inhalation and external doses from immersion within a plume. Similarly, internal and external doses can be received from surface waters, biota, soils, and groundwater (e.g., wells). Finally, an individual may receive a dose as a result of direct exposure to a waste disposal facility. This could occur, for example, if a person breached the integrity of the waste containment by digging into a disposal facility.

The evaluation of the internal dose to an individual is often the result of many assumptions regarding the uptake of the contaminant and the physiology of the individual. This individual is often referred to as a "reference man."[14] For example, a

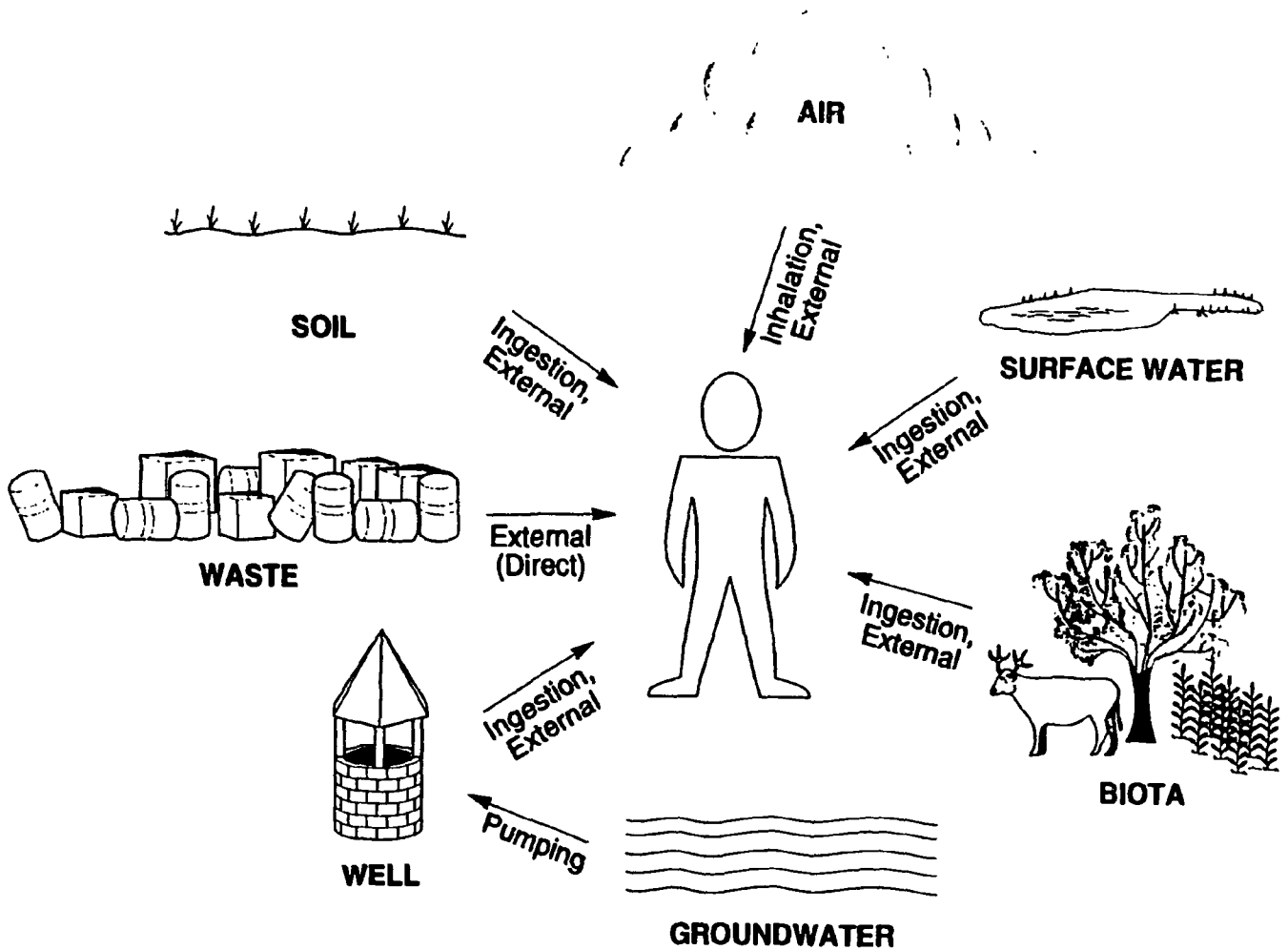

Fig. 2.3. Examples of exposure pathways to humans from environmental contaminants. (Courtesy of ORNL Waste Management and Remedial Action Division)

fish-consumption rate may be assumed for fish that are taken from a contaminated lake. Similarly, drinking rates, breathing rates, and other ingestion rates may be assumed to estimate the uptake of contaminants. Once the contaminant is inside the body, it may be preferentially transported to selected organs. Hence, consideration must be given to the partitioning of the radionuclide within the body. Finally, the amount of time that the contaminant is retained within the body must also be considered. This time is a function of both the radioactive and biologic half-lives. After consideration of the above factors, an estimation of the internal dose to a reference man can be made.

Radionuclides may also cause an external dose to an individual . To evaluate the external dose, the following information must be known:[15] concentration of the radionuclide as a function of time and distance from the receptor, energy and intensity of radiation emitted by the radionuclide, types and amounts of shielding between the radiation source and the individual, and the amount of transmission of the radiation through the body. This information can be estimated through the performance assessment process.

2.6 SUMMARY

A performance assessment is a tool that can be used to estimate potential contaminant releases from LLW disposal facilities and the effect of these contaminants in the environment. A performance assessment requires an extensive disposal system characterization; a source term determination; a calculation of the transport of released radionuclides to a receptor location; and finally, an estimation of doses to individuals. The results of these analyses can be used to verify that a facility is in compliance with established performance objectives which are designed to protect human safety and health and the environment.

3. DESCRIPTION OF THE SOURCE1 AND SOURCE2 COMPUTER CODES

3.1 INTRODUCTION

As stated in Chapters 1 and 2, a number of computer codes are available to predict the source terms from waste disposal facilities. Two of these codes, SOURCE1 and SOURCE2 (collectively called the SOURCE codes),[6] are used in this study. These codes can be used to model the release of radionuclides from waste disposal facilities including the degradation of engineered barriers, if such barriers are employed.

In this chapter, a description of the SOURCE code methodology is presented. First, a general overview of these codes is given. This overview is followed by descriptions of the major components of the codes: concrete degradation modeling, concrete structural and cracking analyses, and contaminant-leaching models. The following description of the codes is adapted from work presented in Ref. 6.

3.2 OVERVIEW OF THE SOURCE CODES

The SOURCE computer codes are used to estimate the source term, or radionuclide release rate, from various types of disposal facilities. SOURCE1 simulates releases from a tumulus-type disposal facility (Fig. 3.1). SOURCE2 simulates releases from silo, well, well-in-silo, and trench disposal facilities. A typical silo-type disposal facility modeled in SOURCE2 is presented in Fig. 3.2. Figure 3.3 shows the logic flow of the SOURCE computer codes. This logic flow is common to both SOURCE1 and SOURCE2.

Radionuclide release rates from waste disposal facilities are a function of the integrity of the waste (or waste form) and the engineered barriers used in construction of the facility. When intact, these barriers minimize the contact of water with the waste, thereby minimizing releases of radionuclides. As the barriers deteriorate over time, water can more readily contact the waste and mobilize radionuclides, thereby accelerating releases to the environment.

The SOURCE codes predict the long-term performance of engineered barriers used in waste disposal facilities. Changes in the material properties of the barriers caused by

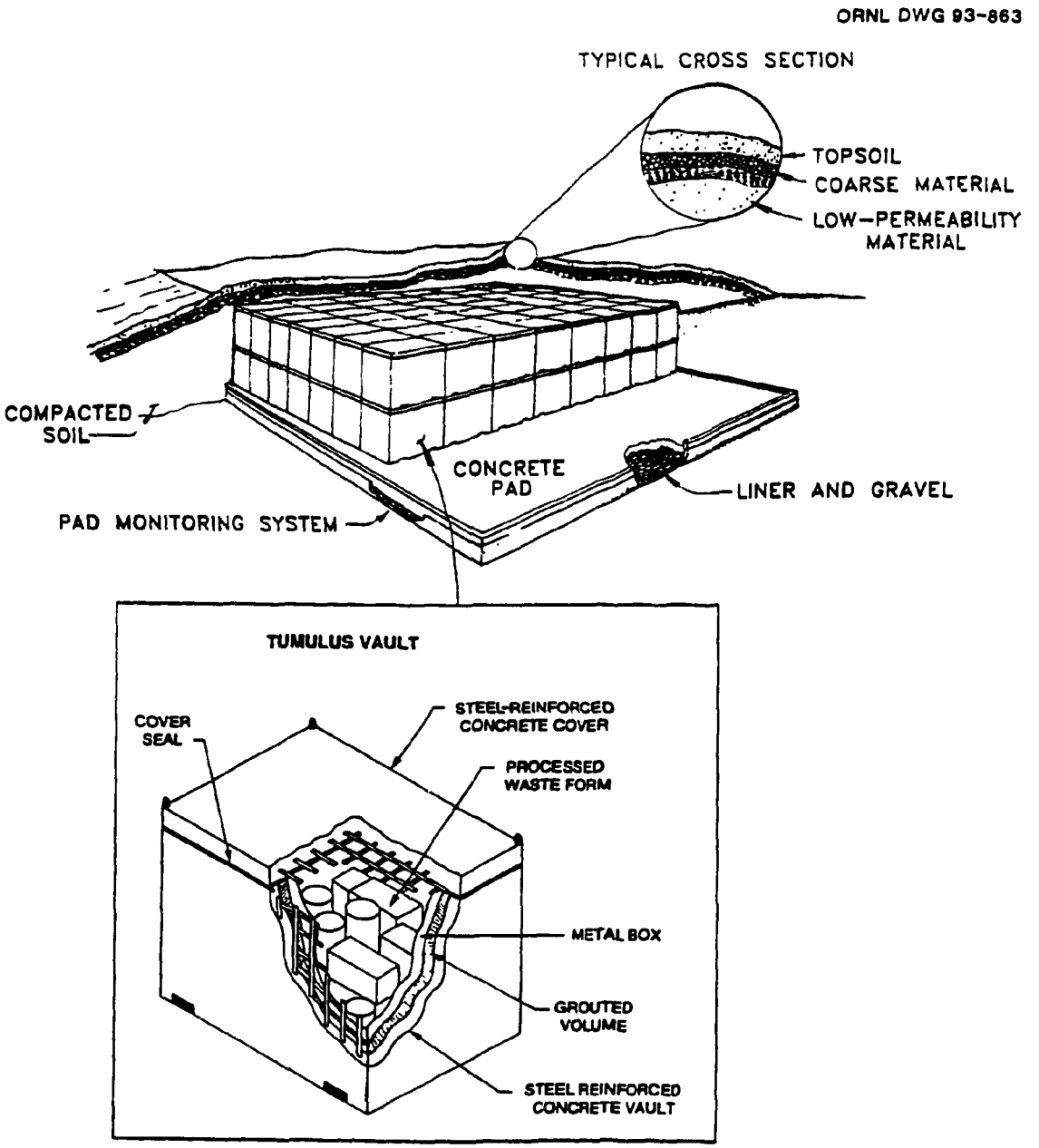

Fig. 3.1. Representative tumulus-type disposal facility modeled by SOURCE1.

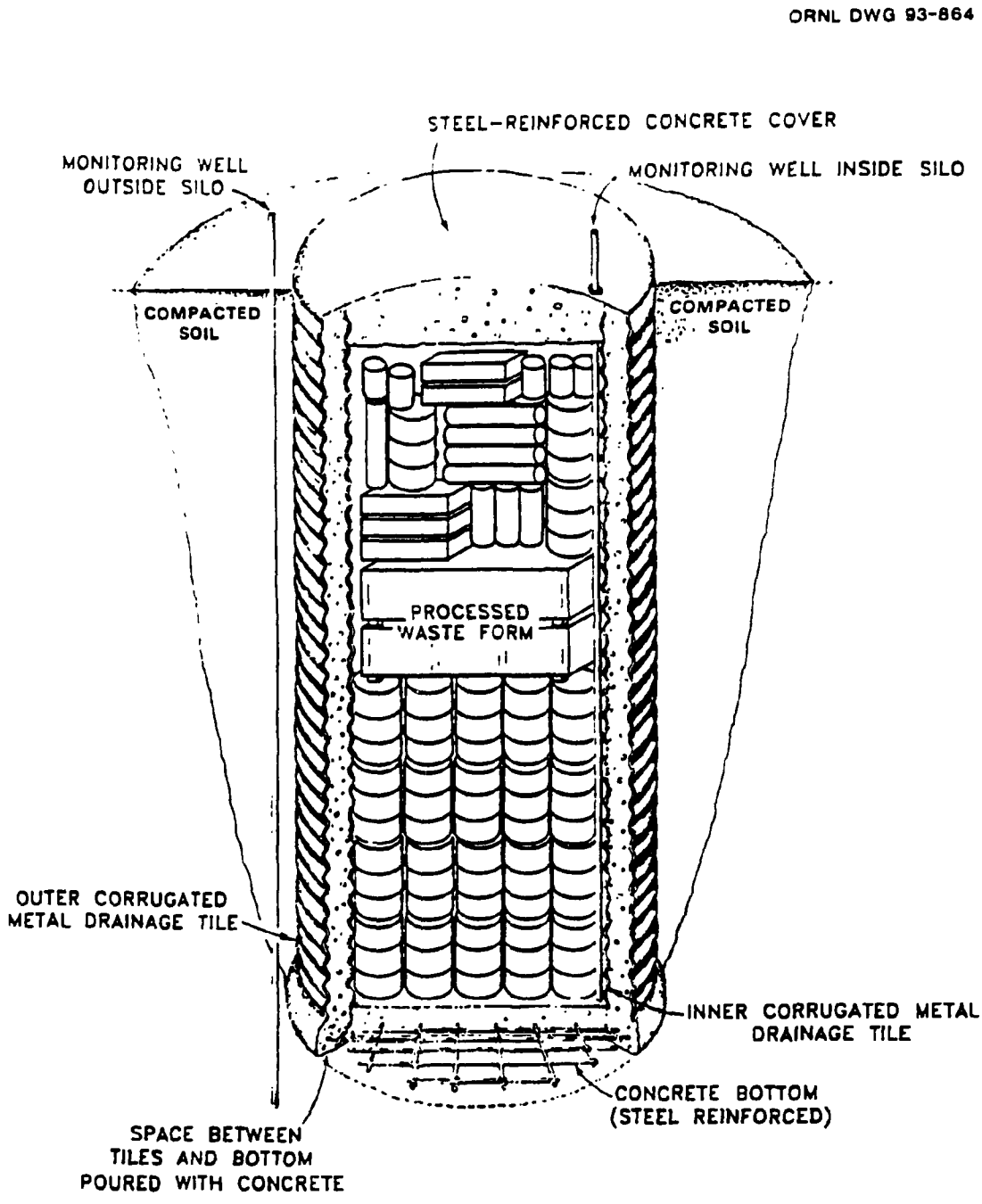

Fig. 3.2. Representative silo-type disposal facility modeled by SOURCE2.
(SOURCE2 is applicable to silo, well-in-silo, and unlined trench disposal technologies.)

ORNL DWG 93A-738

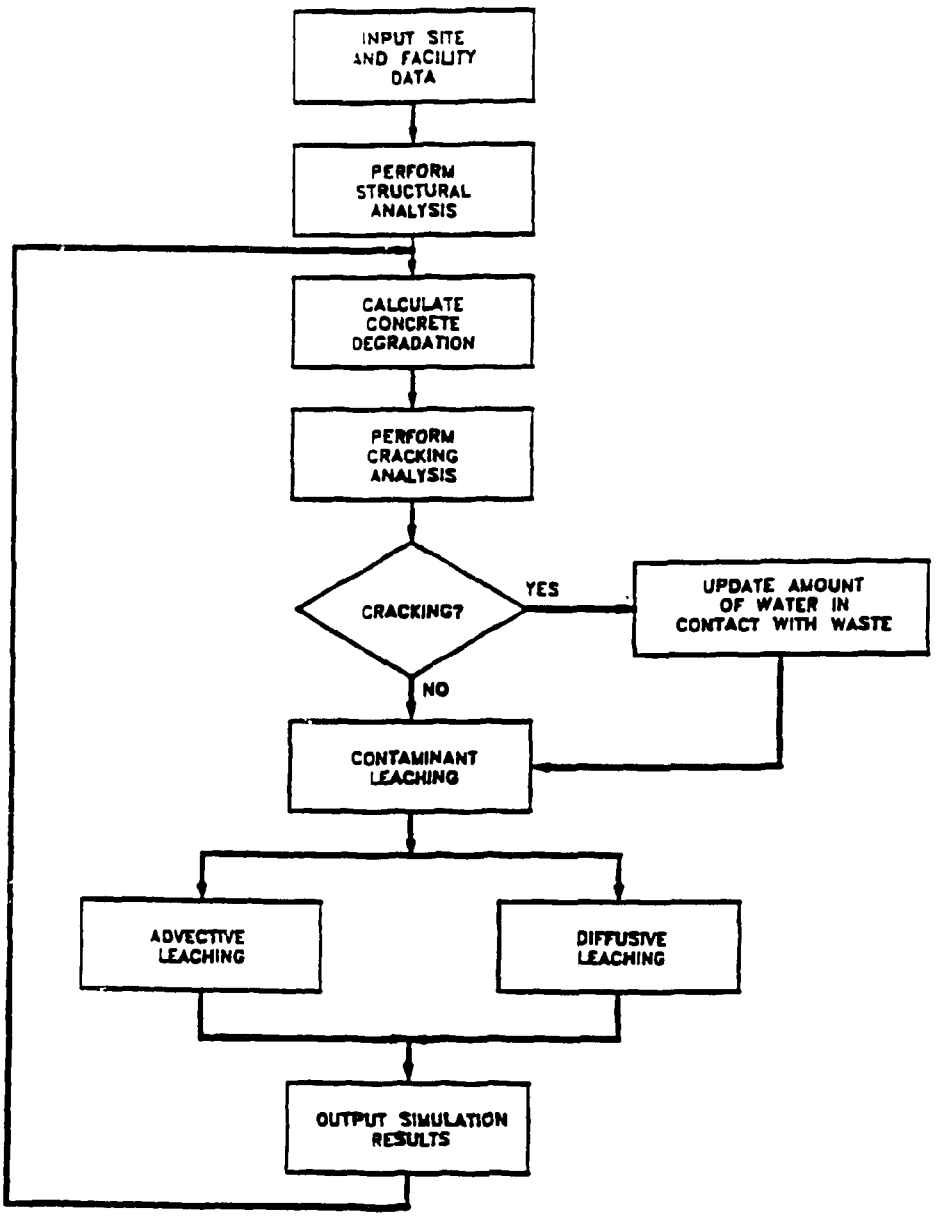

Fig. 3.3. Logic flow in the SOURCE computer codes.

chemical attack and physical stress are modeled. The projected material properties are then considered in structural and cracking analyses of the disposal facility. These analyses are performed to assess the ability of the disposal facilities to bear the loads placed upon them. As the ability to bear design loads is compromised and the structures crack or fail, rates of infiltration of water through the waste are adjusted.

The SOURCE computer codes consider two mechanisms through which waste radionuclides are released to the environment; advection (bulk flow driven by hydraulic pressure differences) and diffusion (nuclide movement driven by concentration differences). The calculated total release rate resulting from advection and diffusion is compared with the solubility limit of the nuclide in water. If this limit is exceeded, the release rate is adjusted to the value dictated by the solubility limit. As the disposal facility degrades, the rate of percolation of water through the waste increases. Thus, except for cases constrained by solubility, advective releases will increase with degradation and, in general, dominate the total release.

The output of the SOURCE codes includes summaries of the barrier degradation and failure analyses, and contaminant release rates as a function of time. The generation of a source term with these codes requires more than 100 input parameters to describe the physical and chemical characteristics of the disposal unit and waste type under consideration. An example of the input parameters required is presented in Table 3.1. Table 3.2 provides an abridged example output listing for a SOURCE1 simulation for ^{137}Cs.

3.3 CONCRETE DEGRADATION

Concrete is widely used in waste storage and disposal; thus, computer codes to predict the long-term behavior of concrete under service conditions are highly desirable. A number of codes (e.g., Refs. 5, 6, 8, and 16) have been and are being developed. The degree to which such codes mimic the real-world, long-term behavior of concrete is generally acknowledged to depend upon numerous factors. These factors can be grouped broadly as chemical attack, physical stress, and microbial action.[8,16-18] Degradation

Table 3.1. Sample input data for the SOURCE1 code

Simulation length: 1000 years Output edit frequency: 50 years

Flux entering trench (cm/month)

January	9.58×10^{0}	February	8.56×10^{0}	March	8.30×10^{0}
April	5.77×10^{0}	May	7.43×10^{0}	June	7.60×10^{-1}
July	2.00×10^{-1}	August	2.50×10^{-1}	September	1.60×10^{-1}
October	1.00×10^{-1}	November	7.00×10^{-2}	December	6.86×10^{0}

Waste trench area	4.66E+02 m^2
Groundwater total dissolved solids	3.49E+02 ppm
Groundwater temperature	1.50E+01 °C
Groundwater pH	6.75E+00
Saturated Hydraulic Conductivity:	
Recharge	5.80E-07 cm/s
Soil backfill	3.50E-03 cm/s
Concrete	1.00E-10 cm/s
Groundwater constituent concentrations:	
Ca^{2+}	2.10E-03 mol/L
Cl^-	2.04E-04 mol/L
CO_3^{2-}	1.00E-03 mol/L
Mg^{2+}	5.21E-04 mol/L
SO_4^{2-}	2.62E-04 mol/L
O_2	1.63E-04 mol/L
Constituent solubilities:	
$Ca(OH)_2$	2.00E-02 mol/L
CO_3^{2-}	1.20E-03 mol/L
Mg^{2+}	1.20E-03 mol/L
Concrete constituent concentrations:	
Calcium concentration in C-S-H system	1.75E+00 mol/L
Calcium concentration in pore fluid	2.00E-02 mol/L
CaO content in cement	2.11E+00 mol/L
Free Cl^-	1.00E-02 mol/L
Silica concentration in C-S-H system	7.10E-01 mol/L

Table 3.1. (continued)

Diffusion coefficients in concrete:	
NaOH, KOH	2.12E-11 m^2/s
$Ca(OH)_2$	1.82E-11 m^2/s
Cl^-	5.08E-11 m^2/s
CO_2	1.92E-10 m^2/s
O_2	2.10E-10 m^2/s
SO_4^{2-}	1.06E-11 m^2/s
Concrete design specifications:	
Compressive strength at 28 d	3.52E+02 kg/cm^2
Poisson's ratio of concrete	1.50E-01
Modulus of elasticity of steel	2.04E+06 kg/cm^2
Yield strength of steel	4.22E+03 kg/cm^2
Modulus of subgrade reaction	1.41E+02 kg/cm^2
Young's modulus of elasticity	2.04E+05 kg/cm^2
Concrete water/cement ratio	4.00E-01
Concrete density	2.40E+00 g/cm^3
Concrete porosity	1.50E-01
Cement content	3.85E+02 kg/m^3
Initial pH	1.25E+01
Tumulus design specifications:	
Layers of vaults	2
Number of vaults wide	8
Number of vaults long	18
Vault dimensions:	
Vault width	1.52E+00 m
Vault length	2.13E+00 m
Vault height	1.65E+00 m
Concrete member thickness:	
Roof	1.78E+01 cm
Walls	1.78E+01 cm
Floor	1.78E+01 cm
Steel reinforcement radius:	
Roof	7.94E-01 cm
Walls	6.35E-01 cm
Floor	6.35E-01 cm

Table 3.1. (continued)

Spacing of steel reinforcement:	
Roof	2.54E+01 cm
Walls	3.05E+01 cm
Floor	3.05E+01 cm
Concrete cover thickness on tension face:	
Roof:	
X-direction	7.77E+00 cm
Y-direction	9.37E+00 cm
Walls:	
Horizontal direction	8.26E+00 cm
Vertical direction	9.52E+00 cm
Floor:	
X-direction	5.08E+00 cm
Y-direction	6.35E+00 cm
Soil and waste properties:	
Earthen cover thickness	1.83E+00 m
Earthen cover density	1.76E+00 g/cm^3
Friction angle of waste backfill	4.00E+01 degrees
Friction angle of soil backfill	3.00E+01 degrees
Density of waste backfill	1.76E+00 g/cm^3
Density of soil backfill	1.76E+00 g/cm^3
Waste density	1.76E+00 g/cm^3
Average moisture content of waste	9.90E-01 vol. frac.
Static load:	
Vault layer 1	3.65E-01 kg/cm^2
Vault layer 2	7.10E-01 kg/cm^2
Concrete and waste package failure rates:	
Waste container:	
Start of failure	0.00E+00 years
Time to complete failure	6.00E+01 years
Epoxy coating:	
Start of failure	0.00E+00 years
Time to complete failure	2.00E+01 years

Table 3.1. (continued)

Nuclide-Specific Parameters

Nuclide	Half-life (year)	Solubility (mol/L)	Waste K_d (mL/g)	Diffusion coefficients		Initial inventory (g)
				Waste (m^2/s)	Concrete (m^2/s)	
Cs-137	3.00E+01	1.60E+01	1.99E+01	6.80E-12	5.12E-13	5.81E-04

Table 3.2. Sample output data (abridged) for the SOURCE1 code

Nuclide: ^{137}Cs

Year	Vault inventory (g)		Leaching rate (g/year)		
	Intact	Cracked	Advection	Diffusion	Total
1	0.567730E-03	0.000000E+00	0.562810E-11	0.000000E+00	0.562810E-11
2	0.554763E-03	0.000000E+00	0.109991E-10	0.000000E+00	0.109991E-10
3	0.542092E-03	0.000000E+00	0.161218E-10	0.000000E+00	0.161218E-10
4	0.529711E-03	0.000000E+00	0.519010E-11	0.000000E+00	0.519010E-11
5	0.517612E-03	0.000000E+00	0.256563E-10	0.000000E+00	0.256563E-10
.					
.					
.					
100	0.575915E-04	0.000000E+00	0.342576E-10	0.368914E-08	0.372340E-08
101	0.562723E-04	0.000000E+00	0.334730E-10	0.383311E-08	0.386658E-08
102	0.274915E-04	0.268883E-04	0.607502E-06	0.397833E-08	0.611480E-06
103	0.265668E-04	0.259839E-04	0.587071E-06	0.407941E-08	0.591150E-06
104	0.256731E-04	0.251098E-04	0.567325E-06	0.417874E-08	0.571503E-06
105	0.248094E-04	0.242650E-04	0.548240E-06	0.427617E-08	0.552516E-06
.					
.					
.					
169	0.271749E-05	0.265781E-05	0.601015E-07	0.500926E-08	0.651108E-07
170	0.262379E-05	0.256617E-05	0.580305E-07	0.495572E-08	0.629862E-07
171	0.000000E+00	0.495526E-05	0.112056E-06	0.490143E-08	0.116958E-06
172	0.000000E+00	0.473106E-05	0.106989E-06	0.479262E-08	0.111781E-06
173	0.000000E+00	0.451689E-05	0.102148E-06	0.468501E-08	0.106833E-06

Table 3.2. (continued)

Year	Vault inventory (g)		Leaching rate (g/year)		
	Intact	Cracked	Advection	Diffusion	Total
⋮					
200	0.000000E+00	0.127984E-05	0.289655E-07	0.232333E-08	0.312888E-07

Concrete degradation summary for year 200

Concrete member thickness	
Roof	7.57E+00 cm
Walls	7.57E+00 cm
Floor	7.57E+00 cm

Concrete loss due to sulfate attack	
Roof	1.02E+01 cm
Walls	1.02E+01 cm
Floor	1.02E+01 cm

Fractional loss of yield strength due to $Ca(OH)_2$ leaching	
Roof	8.52E-02
Walls	8.52E-02
Floor	8.52E-02

Corrosion results

Year of onset of corrosion	
Roof	0 years
Walls	0 years
Floor	0 years

Corrosion product layer thickness	
Roof	0.00E+00 cm
Walls	0.00E+00 cm
Floor	0.00E+00 cm

Remaining steel reinforcement	
Roof	7.94E-01 cm
Walls	6.35E-01 cm
Floor	6.35E-01 cm

Table 3.2. (continued)

Concrete cracking analysis for year 200

Cracking due to corrosion of steel	
Vault roof	None
Vault walls	None
Vault floor	None

Cracking due to loading and shear	
Vault roof	Cracked
Vault walls	None
Vault floor	Cracked

Crack characteristics	Upper vault	Lower vault
Vault roof		
Average crack width (cm)	7.44E-04	2.80E-02
Fractional volume of cracks	1.72E-05	5.54E-04
Vault floor		
Average crack width (cm)	0.00E+00	2.09E-02
Fractional volume of cracks	0.00E+00	4.95E-04

caused by chemical attack includes the effects of sulfate attack, calcium hydroxide leaching, alkali-aggregate reaction, salt crystallization, and metal-reinforcement corrosion. Degradation caused by physical stress includes the effects of freeze-thaw cycles, wet-dry cycles, and osmotic pressure. Degradation caused by microbial action includes the effects of sulfur-oxidizing and nitrifying bacteria and heterotrophic organisms. Radiation damage to concrete incorporating LLW is not expected to be of concern because the doses received are low when compared with those required to produce significant changes in concrete products.

The SOURCE codes include the chemical degradation mechanisms of sulfate attack, calcium hydroxide leaching, and steel reinforcement corrosion. The codes assume that initially water flow through concrete barriers is described by the permeability of the concrete and that cracks are caused by subsequent degradation. Data on original cracks in concrete (i.e., those formed during curing and aging before a disposal facility is put into service) are, for the most part, not available. This observation can be extended to include data on the initial quality of the concrete used in construction of a disposal facility, on the skill with which the concrete is placed, and on the conditions to which the concrete is exposed after placement but before a performance assessment begins.

3.3.1 Sulfate Attack

Sulfate attack occurs when sulfate ions from the environment penetrate concrete and react expansively with the concrete. The resulting internal expansion causes stress, cracking, and exfoliation. The sulfate attack model is based on the work given in Ref. 19. The rate of degradation can be expressed as:

$$R = \frac{E\beta^2 c_o C_e D_i}{\alpha\sigma(1-\mu_c)} \quad , \tag{3.1}$$

where

R = degradation rate (m/s),

E = Young's modulus (Pa),

β = linear strain caused by a mole of sulfate reacted in a m^3 (unitless),

c_o = groundwater sulfate concentration (mol/m^3),

C_e = concentration of sulfate as ettringite (mol/m^3),

D_i = "intrinsic" diffusion coefficient (m^2/s),

α = roughness factor for fracture path (dimensionless),

σ = fracture surface energy of concrete (J/m^2), and

μ_c = Poisson's ratio for concrete (dimensionless).

3.3.2 Calcium Hydroxide Leaching

As NaOH, KOH, and $Ca(OH)_2$ are leached from the concrete, the pH of the concrete is adjusted within the computer model. The pH declines linearly in direct proportion to the reduction in NaOH and KOH. After NaOH and KOH are totally leached from the concrete, changes in pH are modeled as a polynomial function of the $Ca(OH)_2$ content. As the $Ca(OH)_2$ is leached, the strength of the concrete declines. The calcium-hydroxide-leaching model includes advective and diffusive flow and is based on the work described in Refs. 6, 20–23. If the groundwater is not saturated with calcium carbonate, advective leaching of $Ca(OH)_2$ is calculated using[21]

$$Ca_l = I \frac{Ca_p}{C_t Ca_c} \quad , \tag{3.2}$$

where

Ca_l = groundwater release rate of $Ca(OH)_2$ ($year^{-1}$),

I = water percolation rate through concrete (m/year),

Ca_p = $Ca(OH)_2$ concentration in concrete pore solution (mol/L),

C_t = concrete member thickness (m), and

Ca_c = $Ca(OH)_2$ concentration in concrete (mol/L).

3.3.3 Corrosion of Steel Reinforcement

Corrosion of steel reinforcement is initiated upon depassivation of the steel by carbonation or chloride penetration. The corrosion propagates at a rate determined by the rate of diffusion of oxygen to the steel. The corrosion-of-steel-reinforcement model is based on work reported in Refs. 24 and 25. The flow rate of oxygen to the surface of the steel reinforcement is modeled using Fick's first law of diffusion[26]

$$J_o = -D_o A_o \left(\frac{d[O_2]}{dx} \right) , \tag{3.3}$$

where

J_o = oxygen flow rate at the steel reinforcement (g/s),

D_o = diffusion coefficient of oxygen through concrete (cm^2/s),

A_o = surface area over which oxygen diffuses to the reinforcement (cm^2), and

$\frac{d[O_2]}{dx}$ = dissolved oxygen concentration gradient (g/cm^4).

The rate of oxygen consumption by the corrosion reaction is assumed to be greater than the rate of oxygen diffusion to the reaction surface. Under these conditions, the corrosion rate is limited by the oxygen flow rate at the steel reinforcement.

Steel that is epoxy-coated may delay the onset of corrosion by providing isolation from aggressive ions and oxygen. The epoxy coating is not assumed to delay depassivation of the steel reinforcement caused by carbonation or chloride penetration. However, upon depassivation, the assumption is made that corrosion is prevented as long

as the coating remains intact. The epoxy coating is predicted to fail as a linear function of time since data for more sophisticated modeling of epoxy are not available.

3.3.4 Corrosion of Metal Barriers

Corrosion of components other than steel reinforcement also affects the long-term performance of an engineered disposal facility. Specifically, metal boxes placed inside vaults, corrugated-steel liners used in the construction of silos, and cast-iron pipes used in well construction will all fail eventually because of corrosion. The SOURCE codes consider corrosion of steel and iron barriers used in tumulus, silo, well, well-in-silo, and trench disposal technologies. Failure of these barriers is modeled as a linear function of time because sufficient site-specific data (applicable to corrosion modeling) are not generally available. Thus, in the SOURCE codes, the time at which corrosion of the metal component begins and the number of years required (following this time) for the member to fail completely are estimated based on best available data and used as input to the codes. Using these data, a failure fraction is calculated for each time step of the simulation.

3.4 CONCRETE STRUCTURAL AND CRACKING ANALYSES

Two distinct analyses are carried out to evaluate the long-term performance of the disposal units caused by chemical attack and physical stress. First, a structural analysis is carried out, and then a cracking analysis is performed. These analyses are of such complexity and length that they are described only generically. A detailed description is provided in Refs. 6 and 27.

3.4.1 Concrete Structural Analysis

The structural analysis (based upon the loads placed on the disposal facility) is used to determine shear, bending moments, axial tension, and compressive forces placed on the various structural components. As these loads vary with the structural component under consideration, this analysis is carried out for the roof, wall(s), and floor of each

disposal unit (e.g., tumulus vault, silo, etc.). The analysis for the roof is used to evaluate shear forces and bending moments caused by uniform loads. For the wall(s), the structural analysis is used to calculate shear forces caused by uniform and hydrostatic loads, bending moments caused by uniform and hydrostatic loads, compressive forces caused by roof reaction and wall weight, as well as axial and ring compressive forces for the silo wall. Finally, the floor structural analysis is used to determine shear forces and bending moments caused by concentrated loads.

3.4.2 Concrete-Cracking Analysis

The concrete-cracking analysis is used to monitor the structural integrity of the disposal unit by comparing shears, bending moments, axial tensions, and compressive forces to loads and forces at which structural or cracking failure will occur. Cracking caused by shear occurs if the shear force on a concrete component exceeds the cracking shear of the member. Cracking caused by bending occurs if bending moments for a concrete member exceed the cracking moment for the component. These cracks are assumed to penetrate the member if the bending moment exceeds the ultimate strength of the member. Cracking caused by compression occurs if the compressive forces on the wall exceed the ultimate strength of the wall. Finally, cracking caused by corrosion of steel reinforcement occurs if the tension stress at the steel-concrete interface exceeds the tensile strength of the concrete.

Changes in concrete properties caused by chemical attack and physical stress must be taken into account in the cracking analysis. Therefore, the cracking analysis is closely coupled to the concrete degradation analysis throughout the simulation. This coupling is illustrated in the concrete degradation and cracking logic flow presented in Fig. 3.4.

ORNL DWG 83A-737

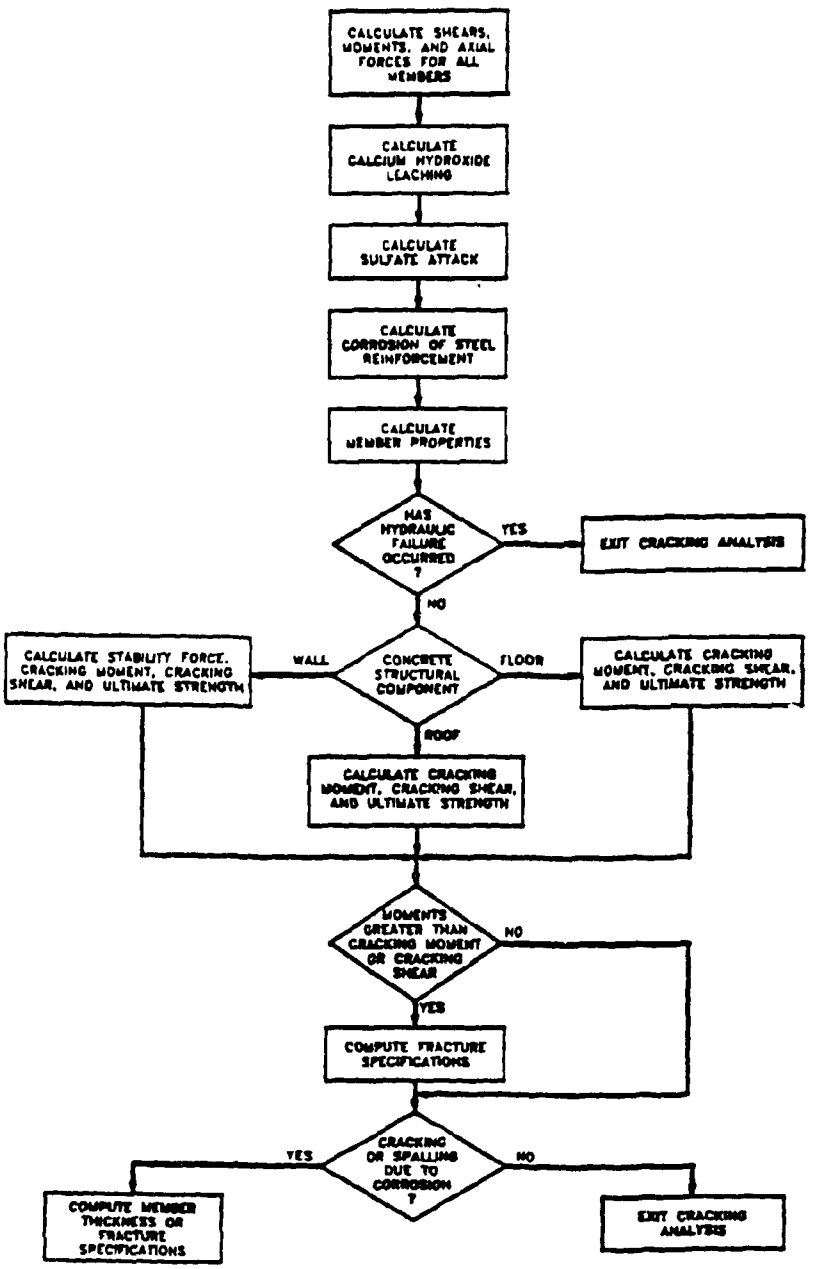

Fig. 3.4. Logic flow in the concrete degradation and cracking subroutines for the SOURCE codes.

3.5 CONTAMINANT LEACHING MODELS

The SOURCE codes incorporate two mass transport mechanisms (advection and diffusion) that are modeled in one dimension. The concentration that is calculated to be released by these two mechanisms cannot exceed the solubility limit of a nuclide. Rates of release from disposal facilities which have not undergone significant structural failure will generally be low, that is, below detection limits. These releases are dependent largely on the relative water saturation of the waste and concrete and, for the most part, are by diffusion. As a facility deteriorates and undergoes cracking, water may more easily percolate through the waste. Under these conditions, leaching of radionuclides by advection can accelerate and may overshadow leaching by diffusion.

Leaching of radionuclides by advection is directly proportional to the amount of water contacting the waste and inversely proportional to the degree to which radionuclides are sorbed by the waste matrix. An analytical expression in which the radionuclide inventory is updated at preset time steps is used to evaluate advective leaching. Leaching by diffusion is calculated using the FLOTHRU computer program (a subroutine in the SOURCE codes).[27] A description of these two leaching mechanisms is provided in Chapters 4 and 5.

3.6 SUMMARY

The SOURCE computer codes provide a one-dimensional model for nuclide (stable and radioactive) transport that can be applied to several disposal technologies. The codes account for the degradation of concrete as well as the corrosion of metal waste containers and other metal barriers. These effects are closely coupled to concrete-structural and concrete-cracking analyses. The results of these analyses are used to determine the amount of water passing through the disposal facility. Advective and diffusive transport are both modeled to evaluate the leaching of nuclides from a disposal facility. These leach rates, along with barrier degradation and failure analyses, are provided as outputs of the codes.

4. CONTAMINANT TRANSPORT THEORY

In this chapter, the general concepts of contaminant transport in, through, and along with a fluid are discussed (Sect. 4.1). Then an equation describing transport of contaminants in a fluid is developed (Sect. 4.2). This equation is modified to account for a solid phase, dispersed or continuous, mixed with a continuous fluid phase (Sects. 4.3 through 4.5). Finally, a method of solution for the derived equation is presented (Sect. 4.6). Although the equations developed can apply to any fluid at constant temperature, only an incompressible one (water) is addressed.

4.1 INTRODUCTION

In general, the transport of contaminants in a fluid is treated by three mechanisms: forced flow, advection, and diffusion. Normally, forced flow (i.e., transport caused by a mechanical device such as a fan or pump) is not a factor in the escape of radionuclides from a waste disposal facility. Thus, the transport of radionuclides (or any nuclide or substance for that matter) through and from these disposal facilities is usually described mathematically by advection-diffusion equations. In these equations, *advection* is taken as meaning transport via the mass motion of a fluid brought about by natural forces (e.g., rain, wind, tide, etc.). Thus, a contaminant that is dissolved or suspended in a fluid will be transported from one point to another by the motion of the fluid. Advection can be characterized as the movement of a contaminant on a macroscopic scale. On the other hand, *diffusion* describes the transport of a contaminant in or through a fluid by molecular motion. The contaminant may be moving in the form of an atom, a hydrated ion, a molecule, a colloid, etc. Diffusion can be characterized as the movement of a contaminant on a microscopic scale.

At a waste disposal facility, advection is primarily driven by the hydraulic gradients caused by rain, melting ice or snow, as well as the hydrostatic head in the aquifers formed by these natural phenomena. Diffusion is driven by the concentration differences

between two regions in a continuum. Note that diffusion is not restricted to a stationary fluid because diffusion can occur within a moving fluid as well.

Advection-diffusion equations may describe other mechanisms in addition to advection and diffusion. Depending on the system (fluid plus solid) being modeled, such an equation also may include other mechanisms for contaminant loss from (e.g., precipitation, sorption, and radioactive decay) and addition to (e.g., dissolution, desorption, and generation as a radioactive decay product) the fluid or system. A complex system, such as a radioactive waste disposal facility, requires the incorporation of loss and addition mechanisms such as those just mentioned.

An advection-diffusion equation, with appropriate initial and boundary conditions, can be solved analytically; numerically; or, as in the case of the SOURCE1 and SOURCE2 models, a combination of the two techniques (frequently referred to as semianalytically). The basis for a semianalytical solution of an advection-diffusion equation is developed in this chapter. Particular emphasis is placed on the advection portion of the equation. First, an elementary mass balance is used to develop a basic advection-diffusion equation for a fluid. This equation is then modified to reflect the effects of sorption/desorption in a saturated porous medium. In addition, the equation is modified to account for radioactive decay of the contaminant. Contaminant generation (e.g., the contaminant is formed as a decay product) is not considered. Next, the effect of an unsaturated porous medium is incorporated into the equation. Finally, using this modified equation, the basis for an advective model is developed. This advective model, coupled with a diffusive model, comprises the semianalytical solution of the advection-diffusion equation.

4.2 ADVECTION-DIFFUSION EQUATION

The following derivation of an advection-diffusion equation is for an incompressible fluid at constant temperature and considers transport in one dimension (x direction) only. A three-dimensional solution for a compressible fluid is considerably more complex, but

is tractable if required. Consider an elementary volume of thickness Δx. Assume that the volume contains a contaminant of concentration $C_v(x, t)$,

where

$C_v(x, t) = C_v$ = mass of contaminant (at spatial position x and time t) per unit volume (g/cm^3),

x = distance (cm), and

t = time (s).

In the absence of sources (e.g., a daughter product) and sinks (e.g., radioactive decay), the one-dimensional rate of change of contaminant concentration in the volume can be evaluated by performing a mass balance on the volume. This rate can be quantified through calculation of the net diffusion and advection rates from the volume. The derivation considers transport through a unit cross-sectional area at time t.

As stated, mass diffusion is contaminant movement driven by concentration differences. For example, larger contaminant concentration inside a volume than outside can cause a flow of contaminant out of the volume. The diffusive flux (amount flowing per unit of area per unit of time) is represented by Fick's Law[26] (frequently referred to as Fick's First Law); namely,

$$J_x = -D\frac{\partial C_v}{\partial x} \quad , \tag{4.1}$$

where

J_x = diffusive flux of the contaminant in the x direction ($g\ cm^{-2}\ s^{-1}$),

D = diffusion coefficient (cm^2/s), and

$\frac{\partial C_v}{\partial x}$ = concentration gradient of the contaminant (g/cm^4).

As mentioned, advection is contaminant transport resulting from bulk flow driven by fluid (hydraulic) pressure differences. The advective flux can be represented by

$$F_{ax} = C_v u_x \quad , \tag{4.2}$$

where

F_{ax} = advective flux of the contaminant in the x direction (g cm^{-2} s^{-1}), and

u_x = the fluid velocity in the x direction (cm/s).

The net rate of change of the contaminant concentration in the elementary volume can be evaluated by performing a mass balance (i.e., change = input - output) using Eqs. (4.1) and (4.2). This results in the following equation:

$$\frac{\partial C_v}{\partial t}\Delta x = \left[-D\frac{\partial C_v}{\partial x}\bigg|_x - \left(-D\frac{\partial C_v}{\partial x}\bigg|_{x+\Delta x}\right)\right] + \left[C_v(x,t) - C_v(x+\Delta x,t)\right]u_x \quad . \tag{4.3}$$

Dividing both sides of Eq. (4.3) by Δx yields

$$\frac{\partial C_v}{\partial t} = \frac{D\left(\frac{\partial C_v}{\partial x}\bigg|_{x+\Delta x} - \frac{\partial C_v}{\partial x}\bigg|_x\right)}{\Delta x} + u_x\left[\frac{C_v(x,t) - C_v(x+\Delta x,t)}{\Delta x}\right] \quad . \tag{4.4}$$

Here, the assumption has been made that the material is isotopic. Taking $\lim_{\Delta x \to 0}$ of both sides of Eq. (4.4) results in

$$\lim_{\Delta x \to 0}\frac{\partial C_v}{\partial t} = \lim_{\Delta x \to 0}\left[\frac{D\left(\frac{\partial C_v}{\partial x}\bigg|_{x+\Delta x} - \frac{\partial C_v}{\partial x}\bigg|_x\right)}{\Delta x} + u_x\left[\frac{C_v(x,t) - C_v(x+\Delta x,t)}{\Delta x}\right]\right] \tag{4.5}$$

or

$$\frac{\partial C_v}{\partial t} = D\frac{\partial^2 C_v}{\partial x^2} - u_x\frac{\partial C_v}{\partial x} \quad . \tag{4.6}$$

This expression, extended to three dimensions, can be written as

$$\frac{\partial C_v}{\partial t} = D\nabla^2 C_v - \nabla \cdot (u C_v) \quad , \tag{4.7}$$

where ∇^2 is the Laplacian operator; u is the velocity vector; ∇ is the differential operator; and C_v is a function of x, y, and z.

4.3 MODIFICATION OF ADVECTION-DIFFUSION EQUATION FOR TRANSPORT OF RADIONUCLIDES IN A POROUS BODY

Equation (4.6) describes one-dimensional transport of a stable contaminant in a single-phase medium. If the medium consists of more than one phase, such as a porous body (e.g., concrete), and the contaminant is radioactive, then Eq. (4.6) must be modified. Here, it is important to clearly define the term *porosity*. In the broadest sense, the absolute or total porosity is the ratio of the pore volume of the medium to the total volume of the medium. However, because only the interconnected pores of sufficient diameter allow flow, an effective pore volume should be used in the porosity calculation. An *effective porosity*, n, can then be defined as the ratio of the effective (interconnected) pore volume of the medium to the total volume of the medium.[28]

Consider a porous body of effective porosity, n, in which the pores are full of fluid (saturated). This body is assumed to contain a radioactive contaminant which can be exchanged between the fluid in the pores and the solid. The contaminant contained in the fluid phase is referred to as *mobile*. The contaminant held by the solid phase is referred to as *immobile*.

The total concentration of contaminant in the porous body is given by

$$C_T = C_M + C_I \quad , \tag{4.8}$$

where

C_T = total mass of contaminant in the porous body per unit volume of the porous body (g/cm^3),

C_M = mass of mobile contaminant per unit volume of the porous body (g/cm^3), and

C_I = mass of immobile contaminant per unit volume of the porous body (g/cm^3).

A mass balance similar to that developed in Sect. 4.2 can be applied to describe the rate of change of the contaminants in the porous body. For this case, the mobile contaminants can be transported from the body by both advection and diffusion. The immobile contaminants can not be transported by advection. In addition, diffusion of the immobile contaminants through the solid is expected to be so slow (compared to diffusion and advection in the pore fluid) that it is considered to be nil. Finally, both the mobile and immobile contaminants will be lost because of radioactive decay. With these constraints, the following equation is derived:

$$\frac{\partial C_T}{\partial t} = D\frac{\partial^2 C_M}{\partial x^2} - v\frac{\partial C_M}{\partial x} - \lambda_d C_T \quad , \tag{4.9}$$

where

v = pore fluid velocity (cm/s),

λ_d = radioactive decay constant (= $\ln 2/t_{½}$) (s^{-1}), and

$t_{½}$ = half-life (s).

Note that Eq. (4.9) is similar to Eq. (4.6) with radioactive decay (a sink) and that this decay is accounted for using the rate term $\lambda_d C_T$.

Substituting Eq. (4.8) into Eq. (4.9) results in the following expression:

$$\frac{\partial (C_M + C_I)}{\partial t} = D\frac{\partial^2 C_M}{\partial x^2} - v\frac{\partial C_M}{\partial x} - \lambda_d (C_M + C_I) \tag{4.10}$$

or

$$\frac{\partial C_M}{\partial t} + \frac{\partial C_I}{\partial t} = D\frac{\partial^2 C_M}{\partial x^2} - v\frac{\partial C_M}{\partial x} - \lambda_d C_M - \lambda_d C_I \quad . \tag{4.11}$$

The mobile contaminant, C_M, is the quantity of interest in Eq. (4.11) since it can be transported from the porous body (i.e., leached into the environment). To express this equation in terms of C_M only, a relationship is needed between C_M and C_I. This relationship is commonly established by using isotherms in which C_I is some function of C_M.[16,29-34] The isotherm represents mathematically a relationship between the concentration of the radionuclide in the solid and fluid phases at a reference temperature. The use of isotherms implies that local equilibrium has been assumed. In the environment, this local equilibrium assumption means that the rate of geochemically-induced changes (e.g., sorption/desorption) in the concentration of the radionuclide in the pore fluid is much greater than the rate of fluid-flow induced changes (e.g., advection).[29] The Freundlich isotherm is commonly used in groundwater-contaminant studies[29-33] and is of the form

$$S = kC^N \quad , \tag{4.12}$$

where

- S = mass of immobile contaminant per unit mass of porous body (g/g),
- k = an empirical constant (units depend on the value of N),
- C = mass of mobile contaminant per unit volume fluid (g/cm^3), and
- N = an empirical constant (dimensionless).

To apply Eq. (4.12) to Eq. (4.11), C_I and C_M must be written in terms of S and C, respectively. These relationships can be expressed as follows:

$$C_I = \rho_b S \quad , \tag{4.13}$$

and

$$C_M = nC \quad , \tag{4.14}$$

where

ρ_b = bulk density (mass of porous body per unit volume of the porous body) (g/cm^3) and

n = effective porosity (volume of interconnected pores per unit volume of the porous body) (cm^3/cm^3).

Substituting Eqs. (4.13) and (4.14) and their derivatives with time into Eq. (4.11) results in

$$n\frac{\partial C}{\partial t} + \rho_b\frac{\partial S}{\partial t} = nD\frac{\partial^2 C}{\partial x^2} - nv\frac{\partial C}{\partial x} - n\lambda_d C - \rho_b\lambda_d S \quad . \tag{4.15}$$

It is assumed that n is independent of time and spatial position.

The time derivative term for the immobile contaminant can be written as

$$\rho_b\frac{\partial S}{\partial t} = \rho_b\frac{\partial C}{\partial t}\frac{dS}{dC} \quad . \tag{4.16}$$

Eq. (4.15) then becomes

$$n\frac{\partial C}{\partial t} + \rho_b\frac{\partial C}{\partial t}\frac{dS}{dC} = nD\frac{\partial^2 C}{\partial x^2} - nv\frac{\partial C}{\partial x} - n\lambda_d C - \rho_b\lambda_d S \quad , \tag{4.17}$$

or simplifying,

$$\frac{\partial C}{\partial t}\left(1 + \frac{\rho_b}{n}\frac{dS}{dC}\right) = D\frac{\partial^2 C}{\partial x^2} - v\frac{\partial C}{\partial x} - \lambda_d\left(C + \frac{\rho_b}{n}S\right) \quad . \tag{4.18}$$

Substitution of Eq. (4.12) and its derivatives into Eq. (4.18) yields

$$\frac{\partial C}{\partial t}\left(1 + \frac{\rho_b}{n} NkC^{N-1}\right) = D\frac{\partial^2 C}{\partial x^2} - v\frac{\partial C}{\partial x} - \lambda_d\left(C + \frac{\rho_b}{n} kC^N\right) \quad . \tag{4.19}$$

The relationship between the mobile and immobile concentrations of a contaminant is often treated as linear (i.e., N = 1), and k is defined as K_d.[4,8,29,30,32,33,35-41] The term K_d is referred to as a distribution coefficient or an equilibrium constant and is the ratio of the mass of immobile radionuclide per unit mass of the porous body to the mass of the mobile radionuclide per unit volume fluid. By this definition, K_d has units of $\frac{g/g}{g/mL}$ which is typically reported as mL/g. Note, however, that the value of K_d used must be carefully chosen as K_d is measured by a variety of methods and is reported in a variety of units. Table A.1 (Appendix A) illustrates relationships among several sets of units used for K_d.

For N = 1 and k = K_d, Eq. (4.19) becomes

$$\frac{\partial C}{\partial t}\left(1 + \frac{\rho_b}{n} K_d\right) = D\frac{\partial^2 C}{\partial x^2} - v\frac{\partial C}{\partial x} - \lambda_d\left(C + \frac{\rho_b}{n} K_d C\right) \quad . \tag{4.20}$$

Simplifying Eq. (4.20) results in

$$R_d\frac{\partial C}{\partial t} = D\frac{\partial^2 C}{\partial x^2} - v\frac{\partial C}{\partial x} - \lambda_d R_d C \quad , \tag{4.21}$$

where

$$R_d = 1 + \frac{\rho_b}{n} K_d \quad . \tag{4.22}$$

The term R_d is referred to as a retardation factor and is frequently used in transport equations for liquid/solid systems.[2,4,8,29-31,33,35,36,38,40,42,43] If divided by R_d, Eq. (4.21) can be written as

$$\frac{\partial C}{\partial t} = \frac{D}{R_d}\frac{\partial^2 C}{\partial x^2} - \frac{v}{R_d}\frac{\partial C}{\partial x} - \lambda_d C \quad . \tag{4.23}$$

This is the common form of the one-dimensional advection-diffusion equation reported in the literature.[4,8,29,35,40,42,44] It describes the transport of mobile radionuclides from a porous body (e.g., leaching from a waste disposal facility) and is the cornerstone of many source term codes, including SOURCE1 and SOURCE2.

4.4 COEFFICIENTS IN THE ADVECTION-DIFFUSION EQUATION

Equation (4.23) describes the rate of change in the concentration of a mobile radionuclide as a function of diffusive and advective transport and radioactive decay. The transport terms are affected by the interaction of the radionuclide between the fluid and solid phases of the porous body. This is reflected by the introduction of a retardation factor into Eq. (4.23). The role of the retardation factor is clearly illustrated through examination of the coefficients of the transport terms in the advection-diffusion equation.

The term $\frac{D}{R_d}\frac{\partial^2 C}{\partial x^2}$ in Eq. (4.23) describes the diffusive transport of the mobile radionuclide. The ratio $\frac{D}{R_d}$ is called a retarded diffusion coefficient. With larger values of R_d, this ratio becomes smaller. This reflects an apparent slowing, or retardation, of diffusion because of sorption/desorption on the solid.

The term $\frac{v}{R_d}\frac{\partial C}{\partial x}$ in Eq. (4.23) describes the advective transport of a mobile radionuclide. Hence, $\frac{v}{R_d}$ is essentially the effective velocity of the mobile radionuclides in the porous body. Mathematically, this can be expressed as

$$v_n = \frac{v}{R_d} \quad , \tag{4.24}$$

where

v_n = effective velocity of the mobile radionuclides in the porous body (cm/s).

Equation (4.24) provides an alternative definition (i.e., based on velocities) of the retardation factor which is often used in the literature.[29,36-38,43] The retardation factor provides a measure of the migration velocity of the mobile radionuclide relative to the pore fluid velocity. Again, as R_d becomes larger, v_n becomes smaller, thus reflecting slower advective transport because of interactions of the mobile radionuclide with the solid.

4.5 UNSATURATED POROUS MEDIA

Recall that the advection-diffusion equation [Eq. (4.23)] was derived using the assumption that the porous body is saturated (i.e, the interconnected pores are completely filled with fluid). However, in general, this may not be the case. If the pores are not saturated, then the advection-diffusion equation must be modified because transport of the mobile radionuclide occurs only in the fluid phase. This modification is frequently accomplished by introducing a parameter called the relative saturation.[2,4,6,38,43] The *relative saturation* , h, is defined as the volume of liquid in the interconnected pores per unit volume of the porous body. Hence, h may range in value from zero (for a completely dry body) to the effective porosity, n (for a saturated body). Replacing the porosity, n, in Eq. (4.22) with the relative saturation, h, results in the following equation for the retardation factor:

$$R_d = 1 + \frac{\rho_b}{h} K_d \quad , \tag{4.25}$$

where

h = relative saturation (dimensionless).

Note that if pores of the body are dry (i.e., h = 0), there would be no transport as reflected in Eq. (4.25).

4.6 SEMIANALYTICAL SOLUTION OF THE ADVECTION-DIFFUSION EQUATION

As noted in Sect. 4.1, an advection-diffusion equation may be solved analytically, numerically, or semianalytically. The SOURCE codes use a semianalytical approach in that the diffusive and advective contributions to transport are solved separately at each time step and then simply added together. The approach is justifiable if one of the transport mechanisms clearly dominates the other in a given time step. This type of behavior is expected for disposal facilities modeled in the SOURCE codes. Initially, when engineered barriers are intact, there should be little or no water flow through the facility, and diffusion will be the dominate mechanism for radionuclide transport. However, as water flow rates increase, and especially after the concrete in a disposal unit cracks, advective transport is expected to be much greater than diffusive transport. Section 4.6.1 focuses on the algorithms used to represent advective transport. The algorithms employed in the SOURCE codes for representing diffusive transport are described in Sect. 4.6.2. However, major emphasis is placed on advection because it is judged to be the primary transport mechanism for the waste disposal facilities modeled.

4.6.1 Advection Analytical Solution

Consider an unsaturated porous body, contaminated with a stable (i.e., $\lambda_d = 0$) nuclide, in which the dominant transport mechanism is advection. For these conditions, Eq. (4.23) can be written as

$$\frac{\partial C}{\partial t} = - \frac{v}{R_d} \frac{\partial C}{\partial x} \quad . \tag{4.26}$$

If the right side of Eq. (4.26) is multiplied and divided by C, then the following equation is obtained:

$$\frac{\partial C}{\partial t} = - \left(\frac{v}{R_d} \frac{1}{C} \frac{\partial C}{\partial x} \right) C \quad . \tag{4.27}$$

Equation (4.27) is similar to first-order expressions that are often used to describe processes in nature (e.g., radioactive decay, many biological processes, and numerous simple chemical reactions). Although it is not first-order, Eq. (4.27) is frequently reduced to mimic such by assuming that the net effect of the processes represented by the term $\left(\frac{v}{R_d} \frac{1}{C} \frac{\partial C}{\partial x} \right)$ can be approximated reasonably well by a constant. This quantity (since it has dimensions of reciprocal time) is generally called a *leach rate constant* and is usually expressed in terms of an average residence time;[2,38,43] namely,

$$\lambda_L = \frac{1}{T_R} \quad , \tag{4.28}$$

where

λ_L = leach rate constant (s^{-1}) and

T_R = average residence time of contaminants in the porous body (s).

A continuity equation can be written to evaluate T_R. In words, this equation is

$$\frac{\text{Mass mobile contaminant}}{\text{Residence time}} = \left(\begin{matrix} \text{Contaminant} \\ \text{velocity} \end{matrix} \right) \left(\begin{matrix} \text{Effective} \\ \text{cross-sectional} \\ \text{flow area} \end{matrix} \right) \left(\frac{\text{Mass mobile contaminant}}{\text{Pore fluid volume}} \right) . \tag{4.29}$$

Cancelling common terms and solving for the residence time results in

$$\text{Residence time} = \frac{\text{Pore fluid volume}}{\left(\begin{matrix} \text{Contaminant} \\ \text{velocity} \end{matrix} \right) \left(\begin{matrix} \text{Effective} \\ \text{cross-sectional} \\ \text{flow area} \end{matrix} \right)} \quad . \tag{4.30}$$

Substituting symbols into Eq. (4.30) yields

$$T_R = \frac{WAh}{v_n Ah} \quad , \tag{4.31}$$

where

W = width of the porous body (cm) and

A = cross-sectional area of the porous body (cm^2).

Remember that Eq. (4.24) relates the pore fluid velocity to the contaminant velocity as

$$v = R_d v_n \quad . \tag{4.32}$$

In addition, since the volumetric flow rate infiltrating the porous body is equal to the volumetric flow rate in the pores, the pore fluid velocity is related to the fluid infiltration rate by

$$v = \frac{q}{h} \quad , \tag{4.33}$$

where

q = fluid infiltration rate (cm/s).

Combining Eqs. (4.31), (4.32), and (4.33) results in the following expression for residence time:

$$T_R = \frac{WhR_d}{q} \quad . \tag{4.34}$$

The leach rate constant, λ_d, can be evaluated by substituting Eq. (4.34) into Eq. (4.28).

$$\lambda_L = \frac{q}{WhR_d} \quad . \tag{4.35}$$

As stated previously, the leach rate constant is often taken to represent the term $\left[\frac{v}{R_d}\frac{1}{C}\frac{\partial C}{\partial x}\right]$; hence,

$$\frac{v}{R_d}\frac{1}{C}\frac{\partial C}{\partial x} = \lambda_L \quad . \tag{4.36}$$

Rearrangement of Eq. (4.36) with integration over the width of the porous body at time t gives

$$\frac{v}{R_d}\int_{C(0,t)}^{C(W,t)}\frac{\partial C}{C} = \lambda_L\int_0^W dx \quad , \tag{4.37}$$

which yields

$$\frac{v}{R_d}\ln\left[\frac{C(W,t)}{C(0,t)}\right] = \lambda_L W \quad . \tag{4.38}$$

Substituting Eqs. (4.33) and (4.35) into Eq. (4.38) results in

$$\frac{q}{hR_d}\ln\left[\frac{C(W,t)}{C(0,t)}\right] = \frac{qW}{WhR_d} \quad , \tag{4.39}$$

which, upon canceling like terms, shows that

$$\ln\left(\frac{C(W,t)}{C(0,t)}\right) = 1 \quad . \tag{4.40}$$

Hence, expressing Eq. (4.27) as a first-order equation, as described above, leads to the conclusion that the contaminant concentrations at two points, separated by a distance of W, differ by a factor of e in a time span T_R.

Equation (4.27) can be written as the following linear first-order differential equation

$$\frac{\partial C}{\partial t} = -\lambda_L C \quad , \tag{4.41}$$

where λ_L is defined by Eq. (4.35). If the contaminant is radioactive (i.e., $\lambda_d \neq 0$), then Eq. (4.41) can be modified to account for this loss as follows:

$$\frac{\partial C}{\partial t} = -\lambda_L C - \lambda_d C \tag{4.42}$$

or, on factoring,

$$\frac{\partial C}{\partial t} = -(\lambda_L + \lambda_d) C \quad . \tag{4.43}$$

Equation (4.43) describes the rate of change of the mobile radionuclide concentration in the porous body. To calculate the total mass of the radionuclide in the porous body, a mass balance can be performed. Recalling that C_T is the total contaminant mass per unit volume of the porous body, the total contaminant mass in the porous body is given by

$$Q = C_T WA \quad , \tag{4.44}$$

where

Q = total mass of contaminant in the porous body (g) and

WA = the total volume of the porous body (cm^3).

Because the total contaminant concentration is the sum of the mobile and immobile contaminant concentrations [Eq. (4.8)], Eq. (4.44) can be rewritten as

$$Q = (C_M + C_I) WA \quad . \tag{4.45}$$

Substituting Eqs. (4.13) and (4.14) (with the relative saturation replacing the porosity) for the mobile and immobile concentrations results in

$$Q = (hC + S\rho_b)WA \quad . \tag{4.46}$$

Recall that the relationship between C and S is assumed to be represented by a Freundlich isotherm [Eq. (4.12)] (with N = 1 and k = K_d); namely,

$$S = K_d C \quad . \tag{4.47}$$

Substituting Eq. (4.47) into Eq. (4.46) and solving for C results in

$$C = \frac{Q}{WA(h + K_d\rho_b)} \quad . \tag{4.48}$$

From the definition of the retardation factor [Eq. (4.25)], Eq. (4.48) can be rewritten as

$$C = \frac{Q}{WAhR_d} \quad . \tag{4.49}$$

Substituting Eq. (4.49) into Eq. (4.43) results in

$$\frac{1}{WAhR_d}\frac{\partial Q}{\partial t} = -(\lambda_L + \lambda_d)\frac{Q}{WAhR_d} \tag{4.50}$$

and, cancelling common terms, yields

$$\frac{\partial Q}{\partial t} = -(\lambda_L + \lambda_d)Q \quad . \tag{4.51}$$

Equation (4.51) describes the advective release of a radioactive contaminant from an unsaturated porous body as a function of time in terms of first-order leaching and decay constants. It should be kept in mind that the use of a leaching constant is an approach that allows reasonable approximations to be made of very complex physicochemical situations.

Equation (4.51) is a first-order linear differential equation that, given an appropriate initial condition, is readily solved. Consider the case where $Q(0) = Q_0$. Then the following integral equation can be formed:

$$\int_{Q_0}^{Q(t)} \frac{dQ}{Q} = -\int_0^t (\lambda_L + \lambda_d) dt \quad . \tag{4.52}$$

The solution is

$$Q(t) = Q_0 e^{-(\lambda_L + \lambda_d)t} \quad , \tag{4.53}$$

where

$Q(t)$ = mass of radionuclide in the porous body (g) at time t and

Q_0 = initial mass of radionuclide in the porous body (g).

An instantaneous advective leach rate, following the lead given in Ref. 2, is defined by

$$\frac{dL(t)}{dt} = \lambda_L Q(t) = \lambda_L Q_0 e^{-(\lambda_L + \lambda_d)t} \quad , \tag{4.54}$$

where

$\frac{dL(t)}{dt}$ = advective leach rate at time t (g/s) and

L = mass of radionuclide leached because of advection (g).

The total radionuclide release, L, during a period of interest is given by the integration of Eq. (4.54) with respect to time:

$$L = \int_{t_1}^{t_2} \left(\frac{dL(t)}{dt} \right) dt = \int_{t_1}^{t_2} \lambda_L Q_0 e^{-(\lambda_L + \lambda_d)t} dt \quad , \tag{4.55}$$

$$L = \frac{\lambda_L}{\lambda_L + \lambda_d} Q_0 \left[e^{-(\lambda_L + \lambda_d)t_1} - e^{-(\lambda_L + \lambda_d)t_2} \right] \quad , \tag{4.56}$$

where

t_1, t_2 = the bounds of the time period of interest (s).

Note that throughout this derivation no assumption was stated regarding the solubility of the radionuclide in the pore fluid. However, it is clear that if the amount leached calculated by Eq. (4.56) exceeds the solubility limit, then Eqs. (4.51), (4.54), and (4.56) no longer hold. For this case, the mass balance of the contaminant in the porous body becomes[2]

$$Q(t) = Q_o e^{-\lambda_d t} - R_s t \quad , \tag{4.57}$$

where

R_s = solubility limited release rate during the period of interest (g/s).

The solubility-limited release rate is evaluated based on the solubility limit of the radionuclide and the amount of pore fluid available. R_s can be evaluated by the following equation:[2]

$$R_s = C_{sl} q A \quad , \tag{4.58}$$

where

C_{sl} = solubility limit of the radionuclide in the pore fluid (g/cm^3).

If the solubility limit is exceeded, Eq. (4.58) must be used to calculate the leach rate of the radionuclide from the porous body. For this case, the leach rate is said to be solubility controlled. For a given flow rate, after a sufficient period of time, the radionuclide inventory will be depleted to an amount at which the solubility limit is no longer exceeded. Alternatively, for a given inventory, the rate of fluid flow through the porous body may increase (e.g., cracking of a waste disposal unit) causing the solubility limit to no longer be exceeded. In either of these cases, once solubility is not exceeded, Eq. (4.54) is applicable and the leach rate is said to be K_d limited.

Equation (4.54) is referred to as a first-order leach rate equation because it was developed from a first-order ordinary differential equation. This equation allows for the continuous update of the inventory during the time period of interest.

Version 1.0 of the SOURCE codes[6] uses an advective leach rate equation of the form

$$\frac{dL_o(t)}{dt} = \lambda_L Q_o e^{-\lambda_d t} \quad , \tag{4.59}$$

where

$\frac{dL_o(t)}{dt}$ = leach rate calculated in Version 1.0 SOURCE codes (g/s).

Equation (4.59) is called a zero-order model. This model differs from the first-order model [Eq. (4.54)] by the absence of the term $e^{-\lambda_L t}$. This exponential term allows for the continuous update of the contaminant inventory as a result of advective leaching. Hence, the zero-order model does not continuously update the contaminant inventory as a result of advective leaching.

In Version 1.0 of the SOURCE codes, the total mass of radionuclide leached by advection is evaluated by

$$L_o = \lambda_L Q_o e^{-\lambda_d (t_2 - t_1)} (t_2 - t_1) \quad . \tag{4.60}$$

If solubility is exceeded, then Eqs. (4.57) and (4.58) are applicable.

The zero-order and first-order advective models form the basis for the model comparisons presented in Chapter 5.

4.6.2. Diffusion Analytical Solution

The following diffusive transport derivation is a résumé of the work by Nestor presented in Ref. 27. Consider the two-layer slab representation of a waste disposal unit presented in Fig. 4.1. The inner layer, which is of half-thickness a, initially contains a contaminant with concentration C_o. The outer layer, which has thickness b-a, is initially uncontaminated. This situation is analogous to the grouted waste initially placed inside an uncontaminated concrete vault (e.g., tumulus-type disposal). If there is little bulk fluid flow through this system, then diffusion will be the dominant transport mechanism. Diffusion equations can then be written for the inner and outer layers of the disposal unit. The concentration of contaminant in the inner layer is denoted by C_1, while that in the outer layer is denoted by C_2.

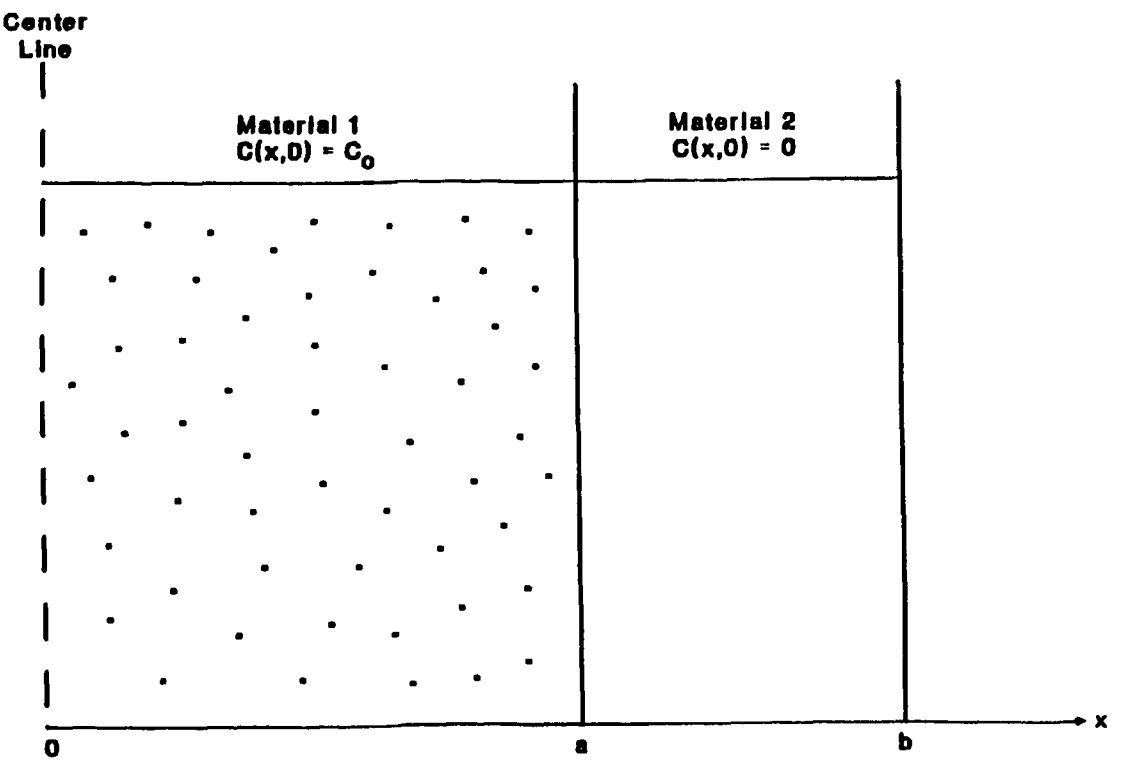

Fig. 4.1 Representation of the system modeled by the FLOTHRU computer code.

Equation (4.23) can be modified to describe the contaminant transport in the inner layer. This results in the following equation:

$$\frac{\partial C_1}{\partial t} = \frac{D_1}{R_{d1}} \frac{\partial^2 C_1}{\partial x^2} - \lambda_d C_1 \quad , \tag{4.61}$$

where the subscript 1 indicates properties associated with layer 1.

Similarly, a diffusion equation can be written for the outer layer:

$$\frac{\partial C_2}{\partial t} = \frac{D_2}{R_{d2}} \frac{\partial^2 C_2}{\partial x^2} - \lambda_d C_2 \quad , \tag{4.62}$$

where subscript 2 indicates properties associated with layer 2.

Here it is important to discuss the retarded diffusion coefficients used in Eqs. (4.61) and (4.62) (D_1/R_{d1} and D_2/R_{d2}). In Ref. 27, the retarded diffusion coefficient is given by

$$\frac{D_i}{R_{di}} = \frac{D_s}{G(1 + K)H^{-1}} \quad , \tag{4.63}$$

where

i = layer number (i = 1,2),

D_s = self-diffusion coefficient (cm^2/s),

G = geometry factor (dimensionless),

K = partition coefficient (dimensionless), and

H = fraction of pore capacity to hold liquid that is filled (dimensionless).

The self-diffusion coefficient is that which would be observed in an infinite or a free volume of pore fluid. In other words, the diffusing material is not retarded by physical or chemical interactions with a porous body. However, for a waste disposal unit, these interactions must be considered.

The geometry factor, G, is defined by

$$G = \frac{\tau^2}{\gamma} \quad , \tag{4.64}$$

where

τ = tortuosity (dimensionless) and

γ = constrictivity (dimensionless).

The tortuosity accounts for the tortuous diffusion path through the pores of the solid body. Because pores are not straight, diffusion effectively takes place over a distance longer than a mathematical solution predicts.[45] The constrictivity is a measure of the choking effect of the pores.[27] Both of the factors involve the physical slowing of diffusion; hence, G can be viewed as a physical retardation.

Chemical retardation (e.g., sorption/desorption) is described in Sect. 4.3. In Eq. (4.63), the retardation factor is represented by the term (1 + K). Recall that from Eq. (4.22) $R_d = 1 + \frac{\rho_b}{n} K_d$. From the definition of K_d in Sect. 4.3, the following relationship applies:

$$K = \frac{\rho_b}{n} K_d \quad . \tag{4.65}$$

Equation (4.22) can then be rewritten as

$$\begin{aligned} R_d &= 1 + \frac{\rho_b}{n}\left(\frac{n}{\rho_b} K\right) \\ &= 1 + K \quad . \end{aligned} \tag{4.66}$$

This is equivalent to the chemical retardation term presented in Eq. (4.63). The relationship between the dimensionless K and K_d is described in Appendix A.

Finally, if the pores are not saturated, then the entire pore volume is not available for diffusion. Hence, the apparent or effective diffusion coefficient is reduced to account for the fraction of pore capacity that is not filled with fluid. This is accomplished in

Eq. (4.63) by dividing by H^{-1}. This is tantamount to a simple linear relationship between the amount leached by diffusion and the amount of water in the pores.

Equations (4.61) and (4.62) can be solved with appropriate initial and boundary conditions. In this case, the initial conditions are

$$C_1(x, 0) = C_0 \quad 0 \le x < a \tag{4.67}$$

and

$$C_2(x, 0) = 0 \quad a \le x < b \quad . \tag{4.68}$$

The boundary conditions are

$$\left.\frac{\partial C_1}{\partial x}\right|_{x=0} = 0 \quad , \tag{4.69}$$

$$C_2(b, t) = 0 \quad , \tag{4.70}$$

$$C_1(a, t) = C_2(a, t) \quad , \tag{4.71}$$

and

$$\left.\frac{D_1}{R_{d1}}\frac{\partial C_1}{\partial x}\right|_{x=a} = \left.\frac{D_2}{R_{d2}}\frac{\partial C_2}{\partial x}\right|_{x=a} \quad . \tag{4.72}$$

The solution to Eqs. (4.61), (4.62), and (4.67) through (4.72) is implemented through the FLOTHRU computer code as described in Ref. 27. This code is incorporated as a subroutine into the SOURCE codes.

4.6.3 Total Leaching Solution

In order to calculate the total amount of radionuclide leaching from a disposal facility using the SOURCE codes, the advective and diffusive components are determined separately. These two components are then added together (hence, the use of the descriptor semianalytical) to calculate the total release. This calculated total is compared to the solubility limit of the radionuclide for the amount of water flowing through the facility. If this limit is exceeded, then the release is limited to the amount determined by solubility.

4.7 SUMMARY

In this chapter, the basis for the advective and diffusive contaminant transport algorithms used in the SOURCE codes was developed. First, a mass balance was performed to derive an advection-diffusion equation for a single-phase system. This equation was modified for a two-phase (i.e., fluid/solid) saturated system that contains a radioactive contaminant. Further modification to the advection-diffusion equation was made for the case where the system is unsaturated.

A semianalytical solution approach to the advection-diffusion equation was discussed. The advective and diffusive portions of the equation were solved separately. The solution of the advective transport problem resulted in the first-order advective model. This model was contrasted with the zero-order advective model used in the SOURCE codes. In addition, the solution of the diffusive transport problem by the FLOTHRU computer code was outlined. Finally, the total contaminant transport was given as the sum of the advective and diffusive contributions. This total was limited to the amount dictated by the solubility limit of the contaminant under consideration.

5. COMPARISON OF ADVECTION MODELS

5.1 INTRODUCTION

In Chapter 4, the bases for two advection models were developed. The zero-order model, which was used in Version 1.0 of the SOURCE codes,[27] does not continuously update the contaminant inventory during time steps. By comparison, the first-order model[2,38,43] continuously updates the contaminant inventory. In this chapter the application of each of these two models to the SOURCE codes is examined. SOURCE code results for each of these models are then compared. Next, the effects of half-life are explored. Finally, model results from variation of the distribution coefficient are presented.

5.2 OVERVIEW OF ZERO-ORDER ADVECTION MODEL

The advective leach rate equation used in Version 1.0 of the SOURCE codes is similar to Eq. (4.59). Recall that Eq. (4.59) was derived for an unsaturated porous body. For a performance assessment, this body is the waste. The advective equation used in Version 1.0 of the SOURCE codes is[27]

$$\frac{dL_a}{dt} = \left[\frac{Q_a}{W(h + K_d\rho_b)}\sum_{i=1}^{12} q_i\right] e^{-\lambda_a t_a} \quad , \tag{5.1}$$

where

$\frac{dL_a}{dt}$ = radionuclide release rate caused by advection in year a (g/year),

Q_a = radionuclide inventory available for leaching at the beginning of year a (g),

W = width of the waste (cm),

h = relative saturation of waste (volume water/volume waste),

K_d = radionuclide distribution coefficient (mL/g),

ρ_b = bulk density of waste (g/cm^3),

q_i = water percolation rate through the waste during month i (cm/month),

λ_a = decay constant (ln $2/t'_{½}$) (year^{-1}),

$t'_{½}$ = half-life of a radionuclide (year), and

t_a = duration of leaching interval (one year)

The total amount of radionuclide released during a time step is given by

$$L_a = \frac{dL_a}{dt} \Delta t \quad , \tag{5.2}$$

where

L_a = total mass of radionuclide released during a time step (g) and

Δt = length of time step (year).

Since the length of the time steps in the original SOURCE codes is one year, then L_a equals $\frac{dL_a}{dt}$. Note that the term $\frac{q_i}{W(h + K_d\rho_b)}$ is equivalent, if the time units are made consistent, to the leach rate constant, λ_L [Eq. (4.35)]. The inventory, Q_a, is revised at the end of each time step to reflect losses due to leaching and radioactive decay.

5.3 OVERVIEW OF FIRST-ORDER ADVECTION MODEL

The first-order model introduces time dependence within a time step for the leach rate calculation. That is, this model accounts for the continuously changing inventory due to leaching and radioactive decay. For the zero-order model, the inventory is only revised once per year.

To evaluate the first-order model, the instantaneous leach rate equation developed in Chapter 4 [Eq. (4.54)] is used in the following form in the SOURCE codes:

$$\frac{dL_i}{dt} = \left[\lambda_{L,i} Q_i e^{-\lambda_{L,i} t'}\right] e^{-\lambda_d' t'} \quad , \tag{5.3}$$

where

$\frac{dL_i}{dt}$ = radionuclide release rate caused by advection during month i (g/month),

$\lambda_{L,i}$ = leach rate constant for month i ($month^{-1}$) = $\frac{q_i}{W(h + K_d \rho_b)}$,

Q_i = mass of radionuclide in the contaminated volume at the beginning of month i (g),

λ_d' = decay constant ($month^{-1}$), and

t' = time (month).

The total amount of radionuclide released during a time step (between t_1' and t_2') is given by integration of Eq. (5.3). This integration was performed in Chapter 4 [Eqs. (4.55) and (4.56)] and the result is repeated here:

$$L = \frac{\lambda_{L,i}}{\lambda_{L,i} + \lambda_d'} Q_i \left[e^{-(\lambda_{L,i} + \lambda_d')t_1'} - e^{-(\lambda_{L,i} + \lambda_d')t_2'}\right] \quad . \tag{5.4}$$

Note that the zero-order and first-order leach rate equations are applicable only if the solubility limit of the radionuclide species is not exceeded. If the results of either of these models exceeds the solubility limit, then the leach rate is limited to the solubility of the species in the pore fluid.

5.4 COMPARISON OF MODELS

To compare the two advective models, a number of simulations were performed using the SOURCE1 and SOURCE2 codes. These simulations allowed for examination of various radionuclides, half-lives, distribution coefficients, and contaminant inventories. Six radionuclides were selected for use in the comparisons. These radionuclides were [numbers in parentheses are half-lives (years)]: ^{3}H (12.33), ^{14}C (5730), ^{90}Sr (28.5), ^{137}Cs (30.17), ^{152}Eu (13.33), and ^{238}U (4.468×10^{9}). In addition, three types of disposal technologies were examined: tumulus, silos, and unlined trenches. Typical radionuclide inventories for these types of disposal facilities were developed after a review of Refs. 27 and 46–48. Physiochemical parameters describing the three disposal technologies and water infiltration rates were taken from Ref. 27. Table 5.1 provides a summary of the radionuclide-specific parameters used in each of the simulations. Physiochemical parameters and water infiltration rates for each of the disposal technologies are presented as each technology is discussed.

The results from the comparison simulations just discussed are quite extensive. Hence, the results for only one radionuclide, ^{137}Cs, are presented in this chapter. The results for the other five radionuclides are discussed in this chapter; however, their graphs are presented in Appendix B. Two graphs are presented for ^{137}Cs for each disposal technology. The first graph depicts the fractional leach rate versus time for the zero-order and first-order advective models. The *fractional leach rate* is defined as the leach rate at a given time divided by the original radionuclide inventory. The second graph depicts the undecayed cumulative fraction leached versus time. The *undecayed cumulative fraction leached* is the integration of the fractional leach rate with respect to time. Note that radioactive decay is accounted for during leaching from the disposal facility. However, the graph presented is a sum of the amount of radionuclide leached from the facility. This sum is termed *undecayed* because it is not subsequently (i.e., once outside the waste) decayed with time. Normally, this undecayed output is used as an input to a groundwater

Table 5.1. Summary of radionuclide data used in advective model comparisons

Radionuclide	Formula	Disposal technology	Inventory (g/disposal unit)[a]	Solubility (mol/L)	K_d (mL/g)	Diffusion coefficient	
						Waste (m^2/s)	Concrete (m^2/s)
^{3}H	T_2O	Tumulus	1.42×10^{-6}	1.11×10^{2}	1.99×10^{-1}	3.88×10^{-9}	1.86×10^{-9}
^{14}C	$BaCO_3$	Tumulus	1.11×10^{-2}	1.11×10^{-4}	1.09×10^{0}	1.44×10^{-11}	2.18×10^{-12}
^{90}Sr	$SrCO_3$	Tumulus	1.38×10^{-4}	7.45×10^{-5}	8.74×10^{0}	1.17×10^{-11}	1.34×10^{-12}
^{137}Cs	Cs_2CO_3	Tumulus	5.81×10^{-4}	1.60×10^{1}	1.99×10^{1}	6.80×10^{-12}	5.12×10^{-13}
^{152}Eu	Eu_2O_3	Tumulus	4.87×10^{-6}	2.84×10^{-6}	3.78×10^{0}	7.95×10^{-13}	9.17×10^{-14}
^{238}U	UO_2	Tumulus	6.87×10^{2}	1.46×10^{-6}	5.56×10^{1}	3.11×10^{-14}	3.50×10^{-15}
^{3}H	T_2O	Silo	3.14×10^{-5}	1.11×10^{2}	1.99×10^{-1}	3.88×10^{-9}	1.86×10^{-9}
^{14}C	$BaCO_3$	Silo	2.72×10^{-4}	1.11×10^{-4}	1.09×10^{0}	1.44×10^{-11}	2.18×10^{-12}
^{90}Sr	$SrCO_3$	Silo	7.80×10^{-2}	7.45×10^{-5}	8.74×10^{0}	1.17×10^{-11}	1.34×10^{-12}
^{137}Cs	Cs_2CO_3	Silo	8.15×10^{-3}	1.60×10^{1}	1.99×10^{1}	6.80×10^{-12}	5.12×10^{-13}
^{152}Eu	Eu_2O_3	Silo	1.04×10^{-4}	2.84×10^{-6}	3.78×10^{0}	7.95×10^{-13}	9.17×10^{-14}
^{238}U	UO_2	Silo	9.91×10^{2}	1.46×10^{-6}	5.56×10^{1}	3.11×10^{-14}	3.50×10^{-15}
^{3}H	T_2O	Trench[b]	1.87×10^{-7}	1.11×10^{2}	1.99×10^{-1}	3.88×10^{-9}	3.88×10^{-9}
^{14}C	$BaCO_3$	Trench[b]	2.16×10^{-1}	1.11×10^{-4}	1.09×10^{0}	1.44×10^{-11}	1.44×10^{-11}
^{90}Sr	$SrCO_3$	Trench[b]	2.64×10^{-4}	7.45×10^{-5}	8.74×10^{0}	1.17×10^{-11}	1.17×10^{-11}
^{137}Cs	Cs_2CO_3	Trench[b]	5.17×10^{-6}	1.60×10^{1}	1.99×10^{1}	6.80×10^{-12}	6.80×10^{-12}
^{152}Eu	Eu_2O_3	Trench[b]	4.02×10^{-1}	2.84×10^{-6}	3.78×10^{0}	7.95×10^{-13}	7.95×10^{-13}
^{238}U	UO_2	Trench[b]	2.20×10^{-1}	1.46×10^{-6}	5.56×10^{1}	3.11×10^{-14}	3.11×10^{-14}

[a]Inventory is g/vault (tumulus technology), g/silo (silo technology), or g/trench (trench technology).

[b]Trench modeled as a right circular cylinder (e.g., silo) with equivalent surface area. Diffusion coefficients in waste and concrete are set to the same value.

transport code, which will account properly for further radioactive decay in the environment. Figure 5.1 contrasts the undecayed cumulative fraction leached and the decayed cumulative fraction leached for ^{137}Cs in a tumulus-type disposal facility.

5.4.1 Tumulus-Type Disposal

The tumulus facility modeled consists of concrete vaults stacked in two layers with 144 vaults in each layer. Each vault is filled with LLW and the void space is grouted (see Fig. 3.1). The inner volume of each vault is assumed to be a homogeneous mixture of waste and grout. Table 5.2 provides a summary of the physicochemical parameters used in modeling a tumulus disposal unit. Assumed water infiltration rates are presented in Table 5.3.

Comparisons of the zero-order and first-order advective models for ^{137}Cs in a tumulus-type disposal facility are presented in Figs. 5.2 and 5.3. Figure 5.2 is the fractional leach rate versus time, while Fig. 5.3 is the undecayed cumulative fraction leached versus time.

In Fig. 5.2, the leach rate exhibits a dramatic increase after about 100 years. This step increase is caused by the failure (i.e., cracking) of the lower layer of vaults. The opening of a flow path in a vault with essentially no resistance allows considerably more water to contact the waste almost immediately. This directly results in an increased advective leach rate. A second increase in the fractional leach rate is observed after about 175 years of leaching as the upper layer of vaults fail. Figure 5.2 depicts very little difference between the two advective models.

Figure 5.3 shows that the first-order model predicts a slightly lower undecayed cumulative fraction leached than does the zero-order model. From this figure, it is evident that the majority of the radionuclide leaching occurs after vault failure when advection is the dominant transport mechanism.

Undecayed cumulative fraction leached graphs for the other five radionuclides are presented in Appendix B (Figs. B.1 through B.5). The graphs for ^{14}C, ^{90}Sr, and ^{152}Eu are similar to those for ^{137}Cs. However, for ^{14}C the undecayed cumulative fraction leached

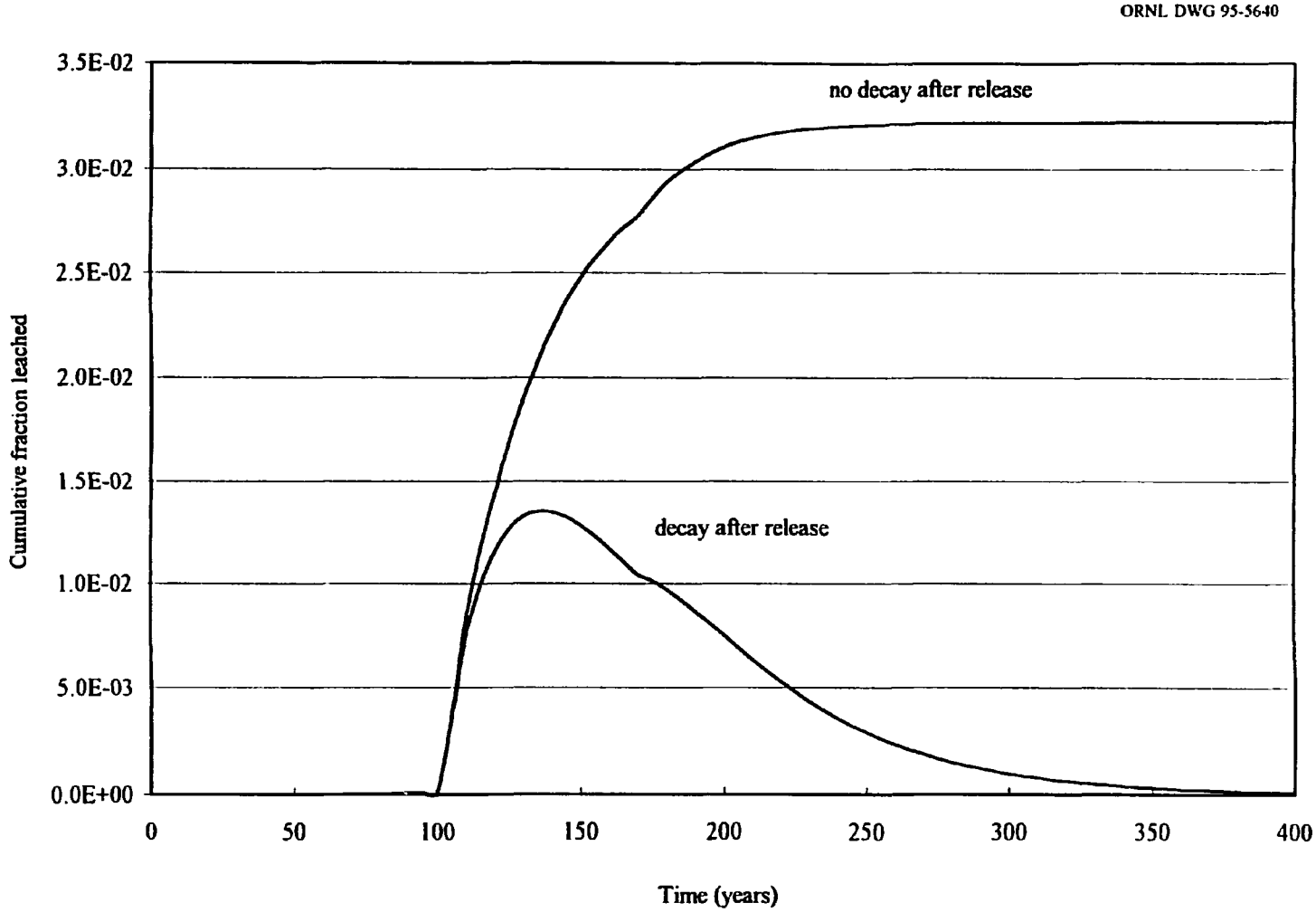

Fig. 5.1. Comparison of the cumulative fraction of ^{137}Cs leached from a tumulus (SOURCE1 with first-order advection model) with and without decay after release.

Table 5.2. Example of physicochemical parameters used in the SOURCE1 simulation of a tumulus-type waste disposal facility[a]

Waste trench area	4.66E+02 m^2
Groundwater total dissolved solids	3.49E+02 ppm
Groundwater temperature	1.50E+01 °C
Groundwater pH	6.75E+00
Saturated hydraulic conductivity:	
Recharge	5.80E-07 cm/s
Soil backfill	3.50E-03 cm/s
Concrete	1.50E-10 cm/s
Groundwater constituent concentrations:	
Ca^{2+}	2.10E-03 mol/L
Cl^-	2.04E-04 mol/L
CO_3^{2-}	1.00E-03 mol/L
Mg^{2+}	5.21E-04 mol/L
SO_4^{2-}	2.62E-04 mol/L
O_2	1.63E-04 mol/L
Constituent solubilities:	
$Ca(OH)_2$	2.00E-02 mol/L
CO_3^{2-}	1.20E-03 mol/L
Mg^{2+}	1.20E-03 mol/L
Concrete constituent concentrations:	
Calcium concentration in C-S-H system	1.75E+00 mol/L
Calcium concentration in pore fluid	2.00E-02 mol/L
CaO content in cement	2.11E+00 mol/L
Free Cl^-	1.00E-02 mol/L
Silica concentration in C-S-H system	7.10E-01 mol/L
Concrete design specifications:	
Compressive strength at 28 d	3.52E+02 kg/cm^2
Poisson's ratio of concrete	1.50E-01
Modulus of elasticity of steel	2.04E+06 kg/cm^2
Yield strength of steel	4.22E+03 kg/cm^2
Modulus of subgrade reaction	1.41E+02 kg/cm^2
Young's modulus of elasticity	2.04E+05 kg/cm^2
Concrete water/cement ratio	4.00E-01
Concrete density	2.40E+00 g/cm^3
Concrete porosity	1.50E-01

Table 5.2. (continued)

Concrete design specifications: (continued)	
Cement content	3.85E+02 kg/m^3
Initial pH	1.25E+01
Diffusion coefficients in concrete:	
NaOH, KOH	2.12E-11 m^2/s
$Ca(OH)_2$	1.82E-11 m^2/s
Cl^-	5.08E-11 m^2/s
CO_2	1.92E-10 m^2/s
O_2	2.10E-10 m^2/s
SO_4^{2-}	1.06E-11 m^2/s
Tumulus design specifications:	
Layers of vaults	2
Number of vaults wide	8
Number of vaults long	18
Vault dimensions:	
Vault width	1.52E+00 m
Vault length	2.13E+00 m
Vault height	1.65E+00 m
Concrete member thickness:	
Roof	1.78E+01 cm
Walls	1.78E+01 cm
Floor	1.78E+01 cm
Steel reinforcement radius:	
Roof	7.94E-01 cm
Walls	6.35E-01 cm
Floor	6.35E-01 cm
Spacing of steel reinforcement:	
Roof	2.54E+01 cm
Walls	3.05E+01 cm
Floor	3.05E+01 cm
Concrete cover thickness on tension face:	
Roof:	
X-direction	7.77E+00 cm
Y-direction	9.37E+00 cm

Table 5.2. (continued)

Walls:	
Horizontal direction	8.26E+00 cm
Vertical direction	9.52E+00 cm
[illegible]	
[illegible]	5.08E+00 cm
	6.35E+00 cm
Static load:	
Vault layer 1	3.65E-01 kg/cm^2
Vault layer 2	7.10E-01 kg/cm^2
Soil and waste properties:	
Earthen cover thickness	1.83E+00 m
Earthen cover density	1.76E+00 g/cm^3
Friction angle of waste backfill	4.00E+01 degree
Friction angle of soil backfill	3.00E+01 degree
Density of waste backfill	1.76E+00 g/cm^3
Density of soil backfill	1.76E+00 g/cm^3
Waste density	1.76E+00 g/cm^3
Average moisture content of waste	9.90E-01 vol. frac.
Concrete and waste package failure rates:	
Waste container:	
Start of failure	0.00E+00 years
Time to complete failure	6.00E+01 years
Epoxy coatings	
Start of failure	0.00E+00 years
Time to complete failure	2.00E+01 years

[a]Reference: D. W. Lee et al., *Performance Assessment for Continuing and Future Operations at Solid Waste Storage Area 6*, ORNL-6783, Martin Marietta Energy Systems, Inc., Oak Ridge National Laboratory, Oak Ridge, Tenn., February 1994.

Table 5.3. Monthly water infiltration values for a tumulus[a]

Year of simulation	Monthly water infiltration (cm)											
	Jan.	Feb.	Mar.	Apr.	May	Jun.	Jul.	Aug.	Sep.	Oct.	Nov.	Dec.
1 to 3	12.4	12.4	11.7	10.9	15.8	8.5	23.4	6.2	8	6.4	5.5	16
4	12.4	12.4	11.7	0	0	0	0	0	0	0	0	0
5	12.4	12.4	11.7	10.9	15.8	8.5	23.4	6.2	8	6.4	5.5	16
6	12.4	12.4	11.7	0.79	0.59	0.39	0.22	0.14	0.1	0.07	0.06	0.05
7 to 16	0.05	0.1	0.4	0.79	0.59	0.39	0.22	0.14	0.1	0.07	0.06	0.05
17	1.82	1.91	2.44	2.07	2.86	0.83	0.35	0.3	0.26	0.2	0.18	0.12
18	3.6	3.72	4.49	3.36	5.12	1.28	0.47	0.46	0.41	0.34	0.3	0.2
19	5.37	5.52	6.53	4.64	7.39	1.72	0.6	0.62	0.57	0.47	0.41	0.27
20	7.15	7.33	8.58	5.92	9.65	2.16	0.73	0.78	0.73	0.61	0.53	0.34
21	8.92	9.14	10.62	7.2	11.92	2.6	0.85	0.94	0.89	0.74	0.65	0.41
22	10.7	10.95	12.67	8.49	14.18	3.05	0.98	1.1	1.04	0.88	0.77	0.49
23	12.47	12.76	14.71	9.77	16.45	3.49	1.11	1.26	1.2	1.01	0.89	0.56
24	14.24	14.57	16.76	11.05	18.71	3.93	1.24	1.42	1.36	1.15	1.01	0.63
25	16.02	16.37	18.8	12.33	20.98	4.38	1.36	1.58	1.52	1.28	1.12	0.7
26	17.79	18.18	20.85	13.62	23.24	4.82	1.49	1.74	1.67	1.42	1.24	0.78
27 to 1000	19.57	19.99	22.89	14.9	25.51	5.26	1.62	1.9	1.83	1.55	1.36	0.85

[a]Reference: D. W. Lee et al., *Performance Assessment for Continuing and Future Operations at Solid Waste Storage Area 6*, ORNL-6783, Martin Marietta Energy Systems, Inc., Oak Ridge National Laboratory, Oak Ridge, Tenn., February 1994.

ORNL DWG 95-5641

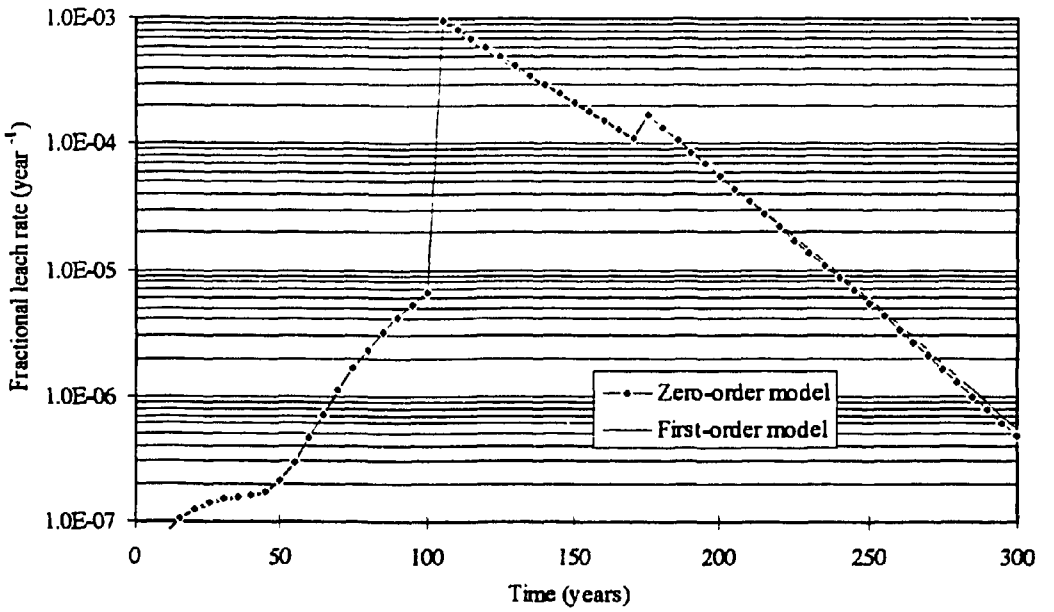

Fig. 5.2. Comparison of ^{137}Cs fractional leach rates from a tumulus (SOURCE1) using zero-order and first-order advection models.

ORNL DWG 95-5642

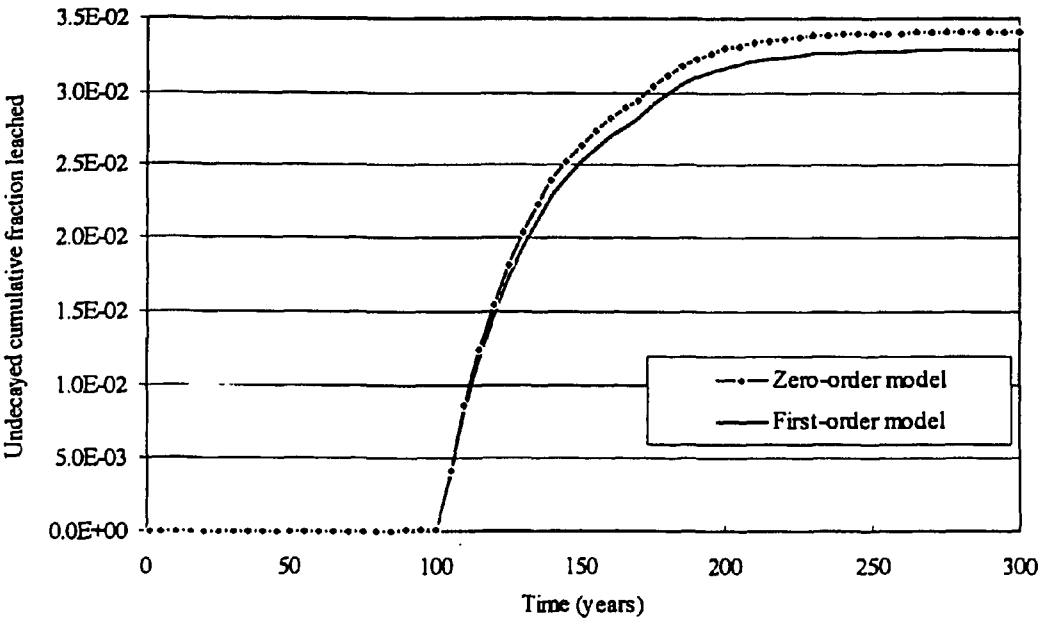

Fig. 5.3. Comparison of the undecayed cumulative fraction of ^{137}Cs leached from a tumulus (SOURCE1) using zero-order and first-order advection models.

predicted by both models ultimately reaches the same value since radioactive decay is not significant over the period (1000 years) of simulation. The graph for ^{238}U exhibits a linear increase in the undecayed cumulative fraction leached. This is a result of the ^{238}U leaching being limited by solubility; hence, the ^{238}U is released at a constant rate. Finally, no difference in the undecayed cumulative fraction leached predicted by the two models is observed for ^{3}H. Since ^{3}H has a relatively short half-life, high solubility, and a low K_d, its inventory undergoes a significant amount of decay and transport prior to vault failure when advection is the dominant transport mechanism.

5.1.2 Silo Type Disposal

The silo-disposal facility modeled consists of two concentric corrugated steel pipes placed in the ground. The annular space between the pipes is filled with grout. LLW is placed in the inner pipe, and any void space is filled with grout (see Fig. 3.2). The waste and the grout are assumed to be homogenously mixed within the volume of the silo. Physicochemical parameters used in modeling a silo are presented in Table 5.4. Table 5.5 provides the water infiltration rates used in the silo simulations.

The fractional leach rate and undecayed cumulative fraction leached for ^{137}Cs in a silo are presented in Figs. 5.4 and 5.5, respectively. Figure 5.4 shows that the silo failure is predicted to occur after about 240 years. The majority of the undecayed cumulative fraction leached occurs after the silo failure (Fig. 5.5). For ^{137}Cs, the zero-order model predicts a slightly higher undecayed cumulative fraction leached than does the first-order model.

Undecayed cumulative fraction leached graphs for the other five radionuclides are presented in Appendix B (Figs. B.6 through B.10). The responses of ^{90}Sr and ^{152}Eu are very similar to that of ^{137}Cs. The graphs for ^{14}C and ^{238}U shows that both advective models eventually predict the same undecayed cumulative fraction leached. Again, the short half-life coupled with high solubility and low K_d for ^{3}H leads to its elimination prior to silo failure. This results in no observed differences between the zero-order and first-order advective models for ^{3}H.

Table 5.4. Example of physicochemical parameters used in the SOURCE2 simulation of a silo-type waste disposal facility[a]

Waste trench area	1.00E+01 m^2
Groundwater total dissolved solids	3.49E+02 ppm
Groundwater temperature	1.50E+01 °C
Groundwater pH	6.75E+00
Saturated hydraulic conductivity:	
Recharge	5.80E-07 cm/s
Soil backfill	3.50E-03 cm/s
Concrete	1.00E-10 cm/s
Groundwater constituent concentrations:	
Ca^{2+}	2.10E-03 mol/L
Cl^-	2.04E-04 mol/L
CO_3^{2-}	1.00E-03 mol/L
Mg^{2+}	5.21E-04 mol/L
SO_4^{2-} (inside silo)	2.62E-04 mol/L
SO_4^{2-} (outside silo)	2.62E-04 mol/L
O_2	1.63E-04 mol/L
Constituent solubilities:	
$Ca(OH)_2$	2.00E-02 mol/L
CO_3^{2-}	1.20E-03 mol/L
Mg^{2+}	1.20E-03 mol/L
Concrete constituent concentrations:	
Calcium concentration in C-S-H system	1.75E+00 mol/L
Calcium concentration in pore fluid	2.00E-02 mol/L
CaO content in cement	2.11E+00 mol/L
Free Cl^-	1.00E-02 mol/L
Silica concentration in C-S-H system	7.10E-01 mol/L
Concrete design specifications	
Compressive strength at 28 d	3.52E+02 kg/cm^2
Poisson's ratio of concrete	1.50E-01
Modulus of elasticity of steel	2.04E+06 kg/cm^2
Yield strength of steel	4.22E+03 kg/cm^2
Modulus of subgrade reaction	2.11E+02 kg/cm^2
Young's modulus of elasticity	2.04E+05 kg/cm^2
Concrete water/cement ratio	4.00E-01
Concrete density	2.40E+00 g/cm^3

Table 5.4. (continued)

Concrete design specifications: (continued)	
Concrete porosity	1.50E-01
Cement content	3.85E+02 kg/m^3
Initial pH	1.26E+01
Diffusion coefficients in concrete:	
NaOH, KOH	2.12E-11 m^2/s
$Ca(OH)_2$	1.82E-11 m^2/s
Cl^-	5.08E-11 m^2/s
CO_2	1.92E-10 m^2/s
O_2	2.10E-10 m^2/s
SO_4^{2-}	1.06E-11 m^2/s
Silo design specifications:	
Silo dimensions:	
Silo radius	1.30E+00 m
Silo height	6.10E+00 m
Concrete member thickness:	
Roof	3.05E+01 cm
Walls	1.52E+01 cm
Floor	3.05E+01 cm
Steel reinforcement radius:	
Roof	4.76E-01 cm
Walls	0.00E+00 cm
Floor	4.76E-01 cm
Spacing of steel reinforcement:	
Roof	1.52E+01 cm
Walls	0.00E+00 cm
Floor	1.52E+00 cm
Corrugated steel thickness:	
Compression face	1.52E-01 cm
Tension face	1.52E-01 cm
Concrete cover thickness on tension face:	
Roof:	
X-direction	1.48E+01 cm

Table 5.4. (continued)

Concrete cover thickness on tension face: (continued)	
Y-direction	1.48E+01 cm
Walls:	
Horizontal direction	0.00E+00 cm
Vertical direction	0.00E+00 cm
Floor:	
X-direction	1.48E+01 cm
Y-direction	1.48E+01 cm
Static load	3.95E-01 kg/cm^2
Soil and waste properties	
Earthen cover thickness	1.83E+00 m
Earthen cover density	1.76E+00 g/cm
Friction angle of waste backfill	4.00E+01 degree
Friction angle of soil backfill	3.00E+01 degree
Density of waste backfill	1.76E+00 g/cm^3
Density of soil backfill	1.76E+00 g/cm^3
Waste density	1.76E+00 g/cm^3
Average moisture content of waste	9.90E-01 vol. frac.
Concrete and steel failure rates:	
Epoxy coating:	
Start of failure	0.00E+00 years
Time to complete failure	2.00E+01 years
Steel liner:	
Start of failure	0.00E+00 years
Time of complete failure	5.00E+01 years

[a]Reference: D. W. Lee et al., *Performance Assessment for Continuing and Future Operations at Solid Waste Storage Area 6*, ORNL-6783, Martin Marietta Energy Systems, Inc., Oak Ridge National Laboratory, Oak Ridge, Tenn., February 1994.

Table 5.5. Monthly water infiltration values for a silo[a]

Year of simulation	Monthly water infiltration (cm)											
	Jan.	Feb.	Mar.	Apr.	May	Jun.	Jul.	Aug.	Sep.	Oct.	Nov.	Dec.
1 to 8	41.95	44.98	47.28	40.75	58.43	22.2	55.74	37.73	9.83	18.28	7.97	46.18
9 to 48	0.05	0.1	0.4	0.79	0.59	0.39	0.22	0.14	0.1	0.07	0.06	0.05
49	3.69	3.83	4.65	3.46	5.33	1.22	0.35	0.34	0.29	0.2	0.18	0.12
50	7.32	7.56	8.9	6.12	10.07	2.05	0.49	0.53	0.48	0.34	0.3	0.2
51	10.96	11.29	13.15	8.79	14.81	2.88	0.62	0.73	0.67	0.47	0.41	0.27
52	14.59	15.01	17.4	11.46	19.55	3.72	0.75	0.93	0.87	0.61	0.53	0.34
53	18.23	18.74	21.65	14.12	24.29	4.55	0.89	1.12	1.06	0.74	0.65	0.41
54	21.86	22.47	25.89	16.79	29.03	5.38	1.02	1.32	1.25	0.88	0.77	0.49
55	25.5	26.2	30.14	19.46	33.77	6.21	1.16	1.52	1.44	1.01	0.89	0.56
56	29.14	29.93	34.39	22.12	38.51	7.04	1.29	1.71	1.63	1.15	1.01	0.63
57	32.77	33.66	38.64	24.79	43.25	7.87	1.42	1.91	1.82	1.28	1.12	0.7
58	36.41	37.39	42.89	27.46	47.99	8.71	1.56	2.11	2.01	1.42	1.24	0.78
59 to1000	40.04	41.11	47.14	30.12	52.73	9.54	1.69	2.3	2.21	1.55	1.36	0.85

[a]Reference: D. W. Lee et al., *Performance Assessment for Continuing and Future Operations at Solid Waste Storage Area 6*, ORNL-6783, Martin Marietta Energy Systems, Inc., Oak Ridge National Laboratory, Oak Ridge, Tenn., February 1994.

ORNL DWG 95-5643

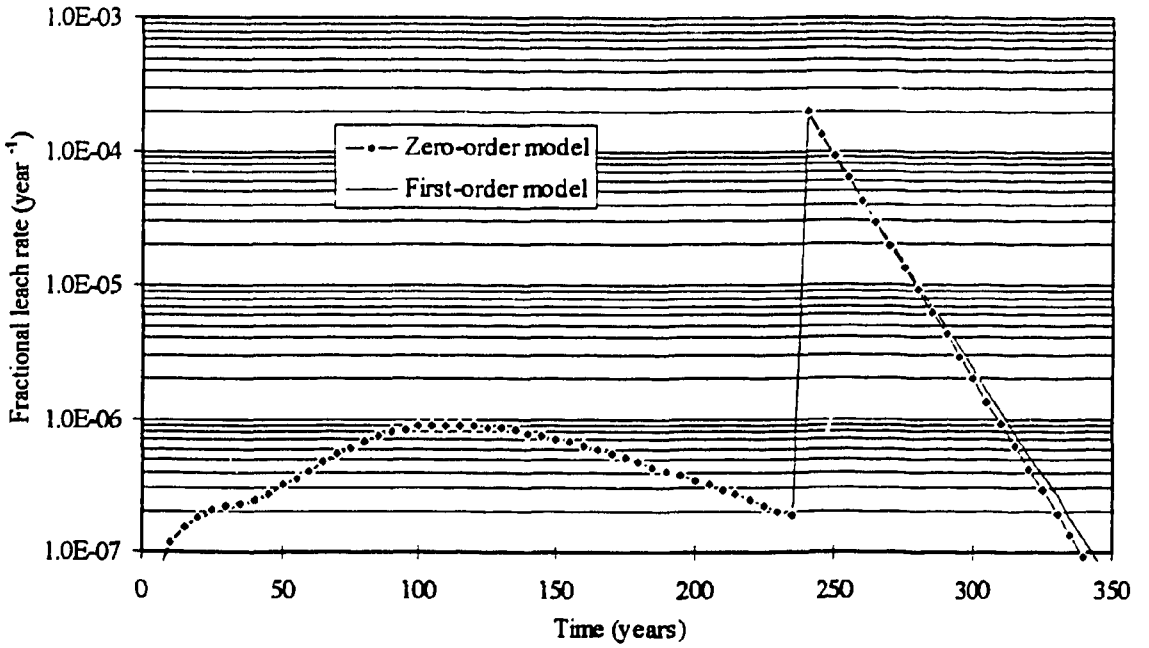

Fig. 5.4. Comparison of ^{137}Cs fractional leach rates from a silo (SOURCE2) using zero-order and first-order advection models.

ORNL DWG 95-5644

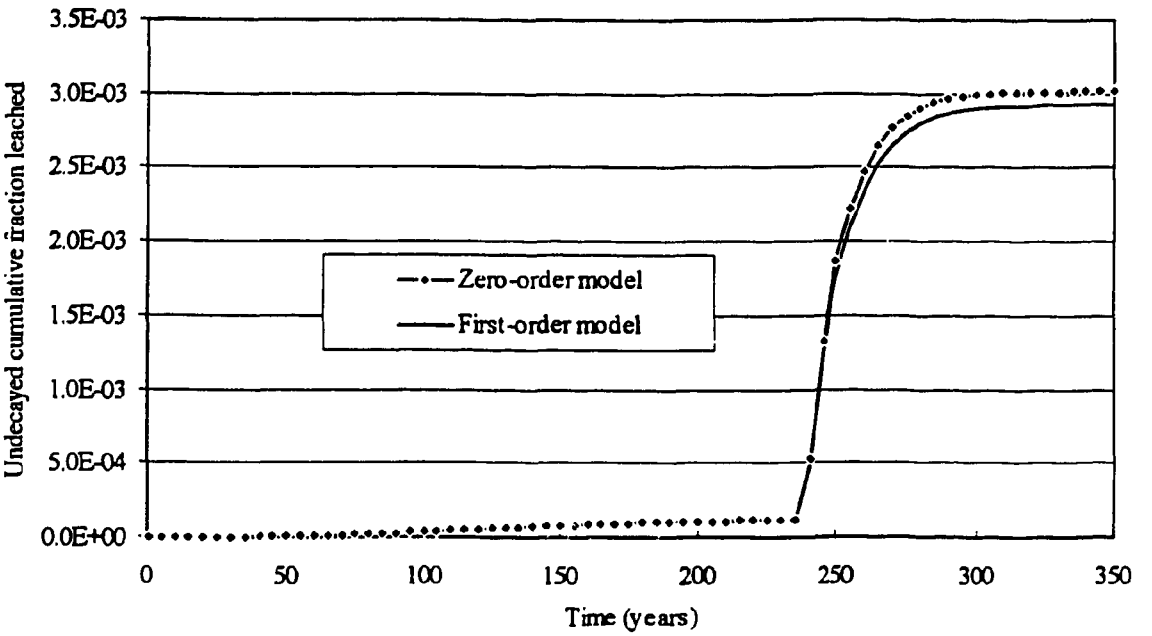

Fig. 5.5. Comparison of the undecayed cumulative fraction of ^{137}Cs leached from a silo (SOURCE2) using zero-order and first-order advection models.

5.4.3 Unlined Trench-Type Disposal

The unlined trench facility modeled consists of a below-grade trench which has no engineered barriers. This trench is filled with LLW and then is backfilled with natural soil. The waste and soil are assumed to be homogeneously mixed within the trench volume. Table 5.6 provides a summary of the physicochemical parameters used in modeling a trench. Water infiltration rates used in the trench simulations are presented in Table 5.7.

The fractional leach rate and undecayed cumulative fraction leached for ^{137}Cs in an unlined trench are presented in Figs. 5.6 and 5.7, respectively. Note that the fractional leach rate graph is significantly different from that for the tumulus or silo disposal technologies. This is a result of the absence of engineered barriers to leaching in an unlined trench; hence, advection is the dominant transport mechanism at time equal to zero. The fluctuations observed in the leach rate are a result of changes in the amount of water simulated to flow through the trench (see Table 5.7). For the first 8 years, the trench is assumed to remain uncovered (i.e., only natural soil covers the waste), resulting in a large amount of leaching. From the 9th through 48th year of leaching, an intact plastic cap is simulated to be in place on top of the trench. This accounts for the dramatic decrease in fractional leach rate. From the 49th to 59th year of leaching, the cap is modeled to fail linearly, directly resulting in increased leaching. Finally, at the 59th year of leaching, the cap has completely degraded, and the monthly rainfall values are fixed to the end of the simulation. This type of precipitation variation is used in all of the disposal technology simulations (e.g., Tables 5.3 and 5.5). However, large fluctuations in leaching are seen only for trenches because advection is the dominant transport mechanism at the beginning of the simulation. By contrast, large fluctuations are not seen for the tumulus and silo simulations because diffusion is the dominant mechanism during the period in which the precipitation is being varied.

Figure 5.7 shows that the zero-order advective model predicts a slightly higher undecayed cumulative fraction of ^{137}Cs leached than does the first-order model. Graphs of undecayed cumulative fraction leached for the other five radionuclides are presented in

Table 5.6. Example of physicochemical parameters used in the SOURCE2 simulation of a trench-type waste disposal facility[a,b]

Waste trench area	4.70E+01 m^2
Groundwater total dissolved solids	3.49E+02 ppm
Groundwater temperature	1.50E+01 °C
Groundwater pH	6.75E+00
Saturated hydraulic conductivity:	
Recharge	5.80E-07 cm/s
Soil backfill	3.50E-03 cm/s
Concrete	3.50E-03 cm/s
Groundwater constituent concentrations:	
Ca^{2+}	2.10E-03 mol/L
Cl^-	2.04E-04 mol/L
CO_3^{2-}	1.00E-03 mol/L
Mg^{2+}	5.21E-04 mol/L
SO_4^{2-} (inside trench)	2.62E-04 mol/L
SO_4^{2-} (outside trench)	2.62E-04 mol/L
O_2	1.63E-04 mol/L
Constituent solubilities:	
$Ca(OH)_2$	2.00E-02 mol/L
CO_3^{2-}	1.20E-03 mol/L
Mg^{2+}	1.20E-03 mol/L
Concrete constituent concentrations:	
Calcium concentration in C-S-H system	1.75E+00 mol/L
Calcium concentration in pore fluid	2.00E-02 mol/L
CaO content in cement	2.11E+00 mol/L
Free Cl^-	1.00E-02 mol/L
Silica concentration in C-S-H system	7.10E-01 mol/L
Concrete design specifications:	
Compressive strength at 28 d	3.52E+02 kg/cm^2
Poisson's ratio of concrete	1.50E-01
Modulus of elasticity of steel	0.00E+00 kg/cm^2
Yield strength of steel	0.00E+00 kg/cm^2
Modulus of subgrade reaction	2.11E+01 kg/cm^2
Young's modulus of elasticity	0.00E+00 kg/cm^2
Concrete water/cement ratio	4.00E-01
Concrete density	2.40E+00 g/cm^3

Table 5.6. (continued)

Concrete design specifications: (continued)	
Concrete porosity	1.50E-01
Cement content	3.85E+02 kg/m^3
Initial pH	1.25E+01
Diffusion coefficients in concrete:	
NaOH, KOH	2.12E-11 m^2/s
$Ca(OH)_2$	1.82E-11 m^2/s
Cl^-	5.08E-11 m^2/s
CO_2	1.92E-10 m^2/s
O_2	2.10E-10 m^2/s
SO_4^{2-}	1.06E-11 m^2/s
Silo design specifications:[a]	
Silo dimensions:	
Silo radius	4.98E+00 m
Silo height	5.20E+00 m
Concrete member thickness:	
Roof	3.05E+01 cm
Walls	1.52E+01 cm
Floor	3.05E+01 cm
Steel reinforcement radius:	
Roof	0.00E+00 cm
Walls	0.00E+00 cm
Floor	0.00E+00 cm
Spacing of steel reinforcement:	
Roof	0.00E+00 cm
Walls	0.00E+00 cm
Floor	0.00E+00 cm
Corrugated steel thickness:	
Compression face	0.00E+00 cm
Tension face	0.00E+00 cm
Concrete cover thickness on tension face:	
Roof:	
X-direction	1.48E+01 cm
Y-direction	1.48E+01 cm

Table 5.6. (continued)

Concrete cover thickness on tension face: (continued)	
Walls:	
Horizontal direction	0.00E+00 cm
Vertical direction	0.00E+00 cm
Floor:	
X-direction	1.48E+01 cm
Y-direction	1.48E+01 cm
Static load	3.95E-01 kg/cm^2
Soil and waste properties:	
Earthen cover thickness	1.83E+00 m
Earthen cover density	1.76E+00 g/cm^3
Friction angle of waste backfill	4.00E+01 degree
Friction angle of soil backfill	3.00E+01 degree
Density of waste backfill	1.76E+00 g/cm^3
Density of soil backfill	1.76E+00 g/cm^3
Waste density	1.76E+00 g/cm^3
Average moisture content of waste	9.90E-01 vol. frac.
Concrete and waste package failure rates:	
Epoxy coating:	
Start of failure	0.00E+00 years
Time to complete failure	0.00E+00 years
Steel liner:	
Start of failure	0.00E+00 years
Time of complete failure	0.00E+00 years

[a]Trench modeled as a right circular cylinder with equivalent surface area. Cement and reinforcement parameters selected so that the walls of the "cylinder" fail (i.e., crack) at the beginning of the simulation (i.e., time zero).

[b]Reference: D. W. Lee et al., *Performance Assessment for Continuing and Future Operations at Solid Waste Storage Area 6*, ORNL-6783, Martin Marietta Energy Systems, Inc., Oak Ridge National Laboratory, Oak Ridge, Tenn., February 1994.

Table 5.7. Monthly water infiltration values for an unlined trench[a]

Year of simulation	Monthly water infiltration (cm)											
	Jan.	Feb.	Mar.	Apr.	May	Jun.	Jul.	Aug.	Sep.	Oct.	Nov.	Dec.
1 to 8	70.6	76.37	79.62	69.85	83.81	22.21	62.31	20.05	11.5	13.01	2.35	45.97
9 to 48	0.05	0.1	0.4	0.79	0.59	0.39	0.22	0.14	0.1	0.07	0.06	0.05
49	6.14	6.36	7.56	5.28	8.6	1.73	0.36	0.38	0.34	0.2	0.18	0.12
50	12.24	12.63	14.72	9.78	16.6	3.08	0.51	0.63	0.57	0.34	0.3	0.2
51	18.33	18.89	21.88	14.27	24.61	4.42	0.65	0.87	0.81	0.47	0.41	0.27
52	24.42	25.15	29.04	18.76	32.62	5.77	0.79	1.12	1.05	0.61	0.53	0.34
53	30.51	31.42	36.2	23.26	40.63	7.11	0.93	1.36	1.28	0.74	0.65	0.41
54	36.61	37.68	43.35	27.75	48.63	8.46	1.08	1.61	1.52	0.88	0.77	0.49
55	42.7	43.95	50.51	32.25	56.64	9.8	1.22	1.85	1.75	1.01	0.89	0.56
56	48.79	50.21	57.67	36.74	64.65	11.15	1.36	2.1	1.99	1.15	1.01	0.63
57	54.88	56.47	64.83	41.23	72.66	12.49	1.5	2.34	2.23	1.28	1.12	0.7
58	60.98	62.74	71.99	45.73	80.66	13.84	1.65	2.59	2.46	1.42	1.24	0.78
59 to1000	67.07	69	79.15	50.22	88.67	15.18	1.79	2.83	2.7	1.55	1.36	0.85

[a]Reference: D. W. Lee et al., *Performance Assessment for Continuing and Future Operations at Solid Waste Storage Area 6*, ORNL-6783, Martin Marietta Energy Systems, Inc., Oak Ridge National Laboratory, Oak Ridge, Tenn., February 1994.

ORNL DWG 95-5645

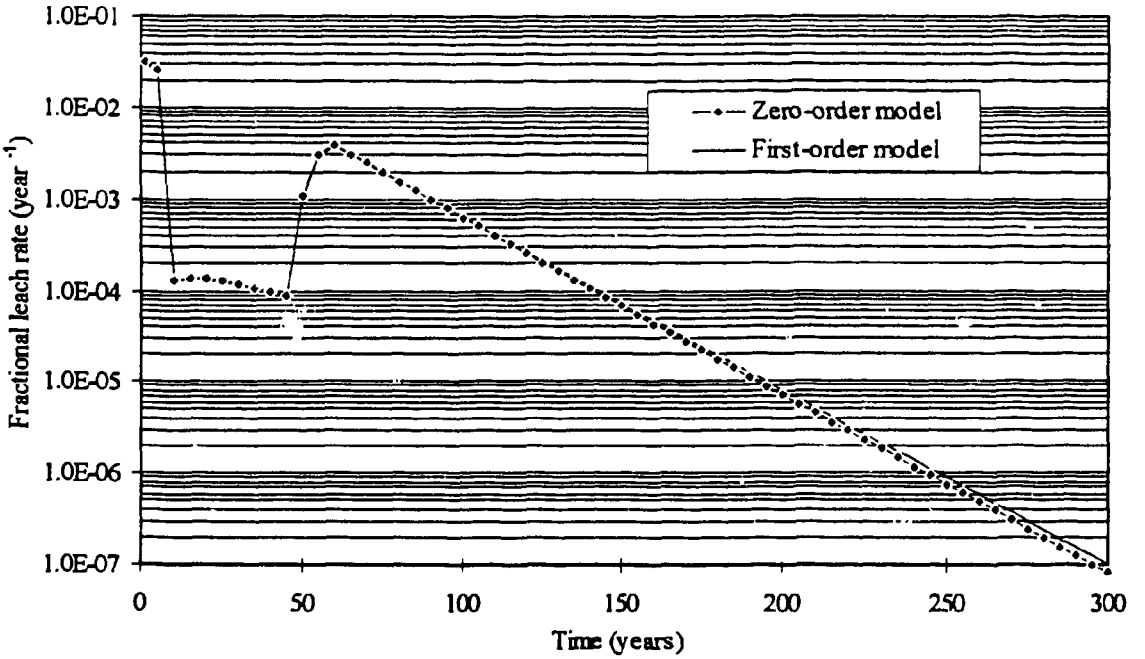

Fig. 5.6. Comparison of ^{137}Cs fractional leach rates from an unlined trench (SOURCE2) using zero-order and first-order advection models.

ORNL DWG 95-5646

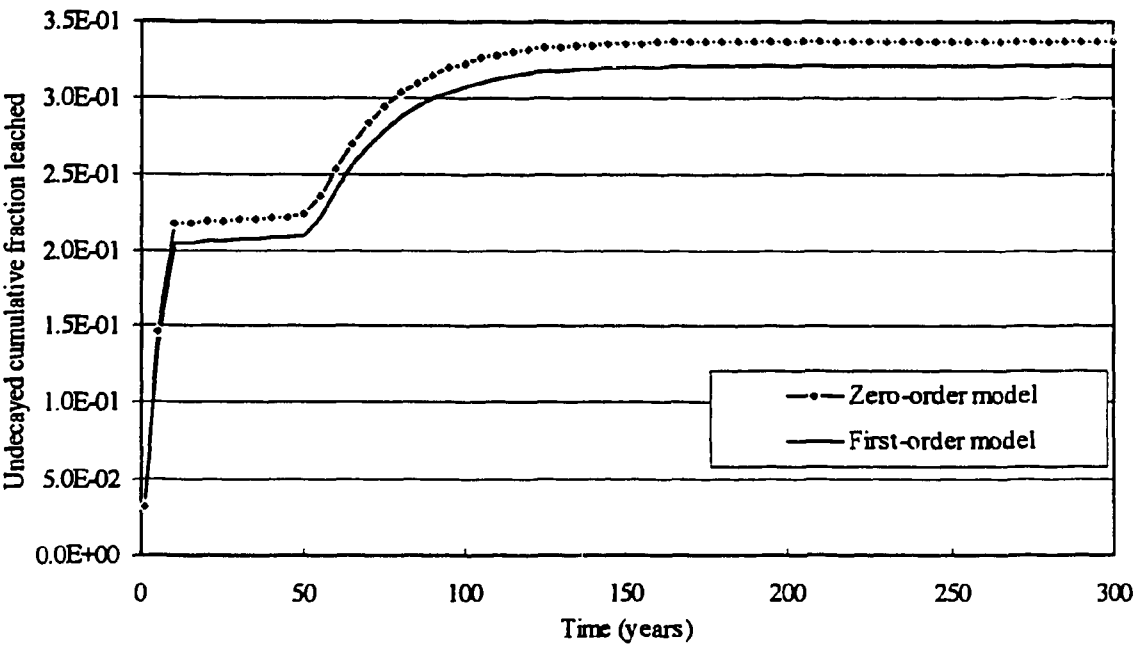

Fig. 5.7. Comparison of the undecayed cumulative fraction of ^{137}Cs leached from an unlined trench (SOURCE2) using zero-order and first-order advection models.

Appendix B (Figs. B.11 through B.15). The graphs for each of these radionuclides is similar to that for ^{137}Cs. The graphs for the two longer-lived radionuclides, ^{14}C and ^{238}U, show that the zero-order and first-order models both eventually reach the same undecayed cumulative fraction leached.

5.5 HALF-LIFE EFFECTS ON ADVECTIVE MODELS

In Sect. 5.4, several comparisons were made between the zero-order and first-order advective models for both short-lived and long-lived nuclides. However, to explicitly examine the effect of half-life on the two models, two radioisotopes of one element were selected for model comparisons. To accomplish this, all properties, except half-life, for the two radionuclides under consideration were set to the same value. Hence, any model differences can be attributed to differences in half-life.

The radionuclides selected for comparison were ^{135}Cs (2.3×10^6 years) and ^{137}Cs (30.17 years). The other parameters used for both of these radionuclides are the same as those presented for ^{137}Cs in Table 5.1. Graphs of undecayed cumulative fraction ^{135}Cs leached for tumulus, silo, and trench disposal technologies are presented in Figs. 5.8, 5.9, and 5.10, respectively. Similar graphs for ^{137}Cs are presented in Figs. 5.3, 5.5, and 5.7.

The most obvious difference between the two radionuclides is that for ^{135}Cs the undecayed cumulative fraction leached eventually reaches a value of 1.0 for all three disposal technologies. For ^{137}Cs some fraction less than 1.0 is reached as a result of radioactive decay. Additionally, as noted earlier, for ^{137}Cs the zero-order model predicts a higher undecayed cumulative fraction released than does the first-order model.

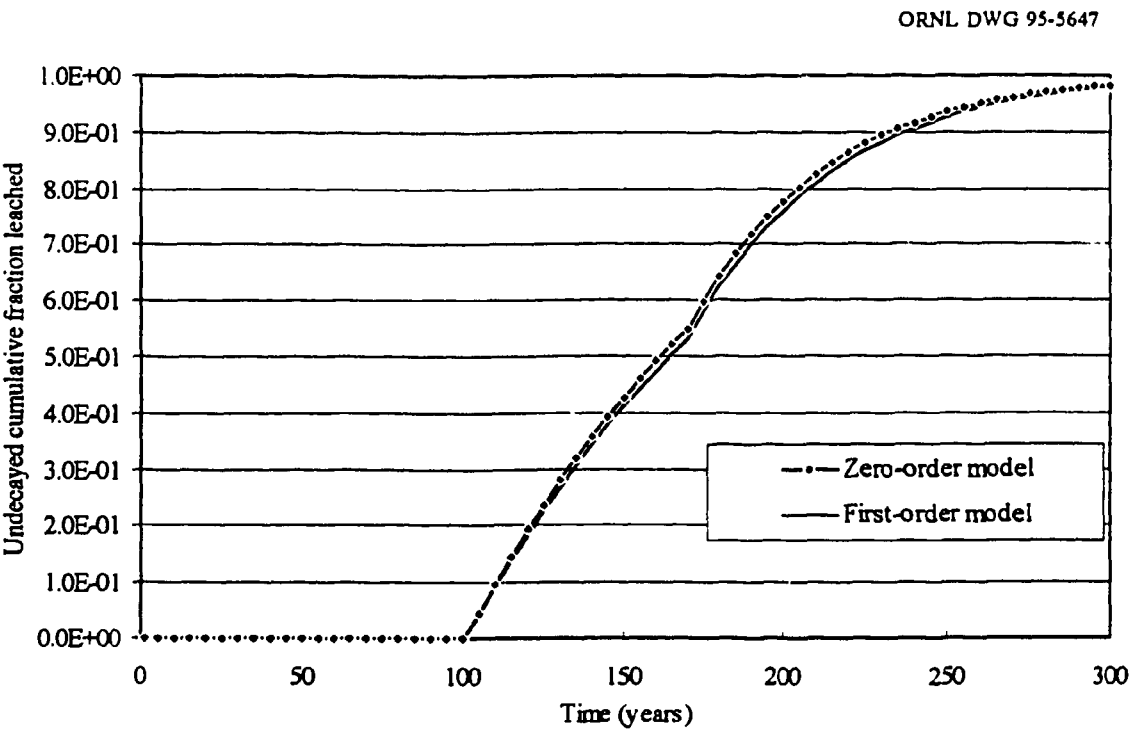

Fig. 5.8. Comparison of the undecayed cumulative fraction of ^{135}Cs leached from a tumulus (SOURCE1) using zero-order and first-order advection models.

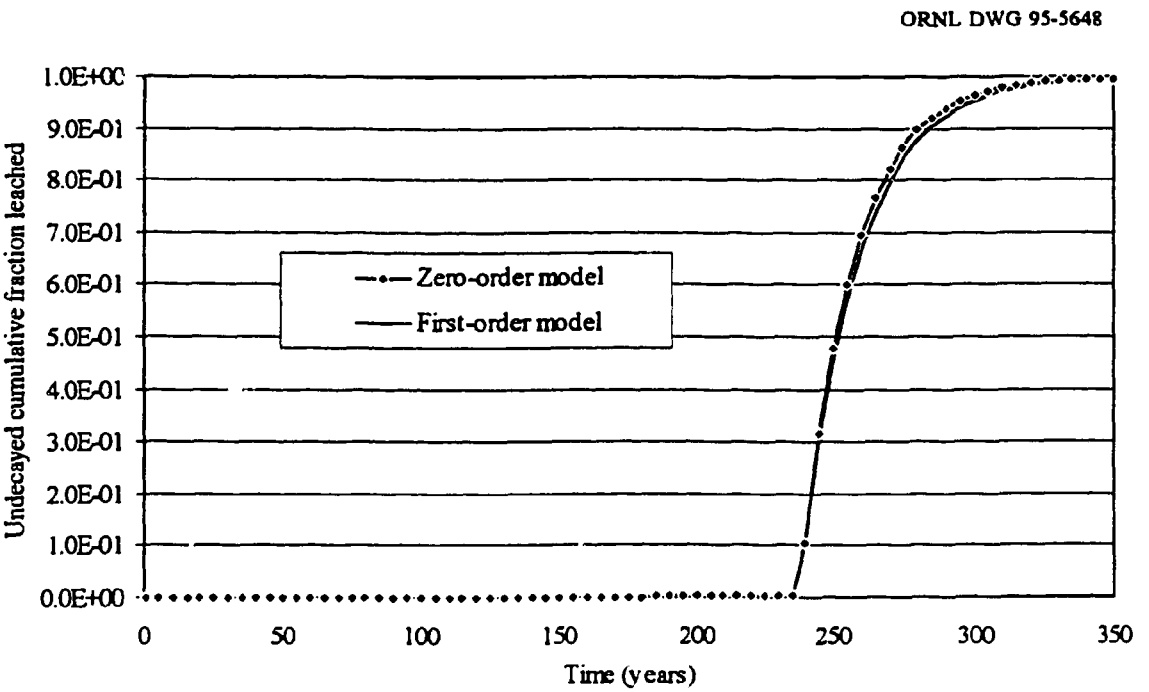

Fig. 5.9. Comparison of the undecayed cumulative fraction of ^{135}Cs leached from a silo (SOURCE2) using zero-order and first-order advection models.

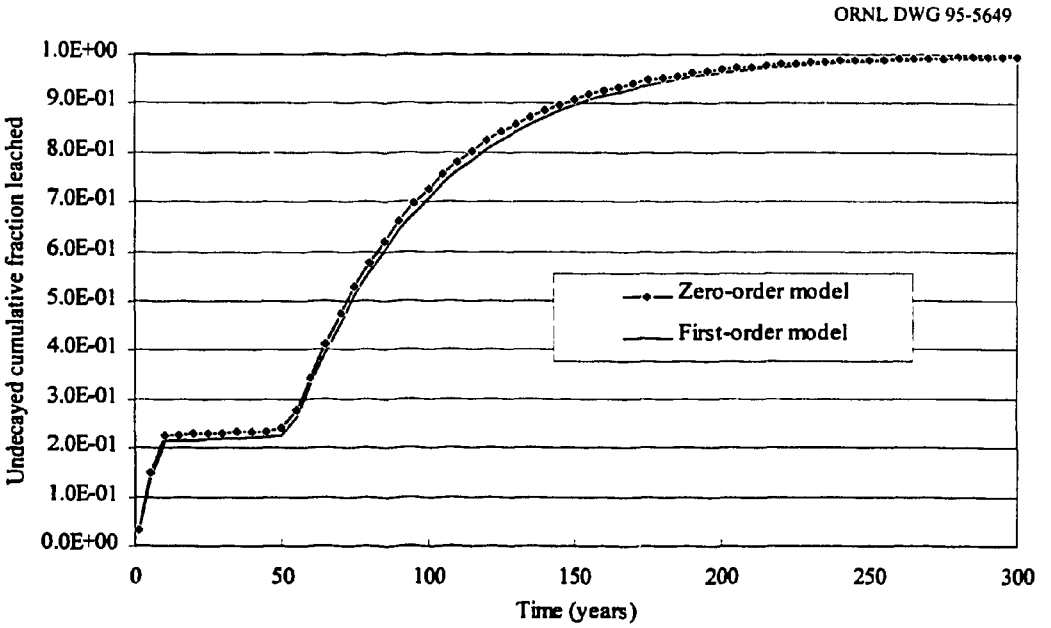

Fig. 5.10. Comparison of the undecayed cumulative fraction of ^{135}Cs leached from an unlined trench (SOURCE2) using zero-order and first-order advection models.

5.6 DISTRIBUTION COEFFICIENT EFFECTS ON ADVECTIVE MODELS

To examine the effect of the distribution coefficient on the two advective models, several simulations were performed for ^{137}Cs and three values of K_d. For the types of facilities modeled, the value of K_d for ^{137}Cs was assumed to range from 1.99 to 199 mL/g, with 19.9 mL/g being the most probable value. The three values of K_d selected were 1.99, 19.9, and 199 mL/g.[27] Each of these values was applied for simulations of ^{137}Cs in tumulus, silo, and unlined trench-type disposal facilities. The initial inventory of ^{137}Cs in each of these facilities is given in Table 5.1. Physicochemical parameters and water infiltration rates for these facilities are provided in Tables 5.2 through 5.7.

Recall that the retarded diffusion coefficient is a function of the distribution coefficient [Eq. (4.63)]. Thus, when K_d is changed, the retarded diffusion coefficient must also be changed. The value of the retarded diffusion coefficient is calculated using

[Eq. (4.63)]. Values of the distribution coefficients and diffusion coefficients used in these simulations are presented in Table 5.8.

Simulation results for the tumulus disposal technology are presented in Figs. 5.3, 5.11, and 5.12. Figures 5.5, 5.13, and 5.14 depict simulations for the silo disposal technology. Results for unlined trenches are shown in Figs. 5.7, 5.15, and 5.16. In addition, the maximum undecayed cumulative fraction leached value for each disposal technology and K_d value is presented in Table 5.9. The *percentage difference* in Table 5.9 is defined as the difference between the zero-order and first-order values divided by the zero-order value.

Table 5.9 shows that there is a small difference between the two advective models as K_d is varied. The percent differences for the simulations performed range from 0.00 to 6.73%. As expected, the undecayed cumulative amount leached calculated by each model decreases with increasing K_d.

For the tumulus and silo, both advective models predict nearly the same maximum undecayed fraction leached for low K_d values. The percent differences between the two models increase with K_d for these technologies. Both the tumulus and silo have a period dominated by diffusive transport (i.e., the time prior to disposal facility cracking). For low values of K_d, simulations using the different advective models result in nearly identical undecayed cumulative fraction leached values since most of the radionuclide transport is due to diffusion. However, as K_d increases, the total radionuclide transport decreases. Hence, any difference between the two advective models appears larger when presented as a percentage difference.

Radionuclide transport from an unlined trench is dominated by advection during the entire simulation. Therefore, this disposal technology provides the best insight into any differences between the advective models. Note that the percent difference between the models decreases with increasing K_d for the trench. Recall that the leach rate constant, λ_L

Table 5.8. Distribution coefficients and diffusion coefficients for cesium used in the analysis of the effect of K_d on the first-order and zero-order advective models[a]

Waste				Concrete			
K_d (mL/g)[b]	K (dimensionless)[c]	G (dimensionless)[b]	D (m^2/s)[d]	K_d(mL/g)[b]	K (dimensionless)[c]	G (dimensionless)[b]	D (m^2/s)[d]
1.99	10	3	6.24×10^{-11}	1.3	20	20	4.9×10^{-12}
19.9	100	3	6.80×10^{-12}	13	200	20	5.12×10^{-13}
199	1000	3	6.86×10^{-13}	130	2000	20	5.15×10^{-14}

[a]The self-diffusion coefficient, D_s, for cesium is 2.06×10^{-9} m^2/s.

[b]Reference: D. W. Lee et al., *Performance Assessment for Continuing and Future Operations at Solid Waste Storage Area 6*, ORNL-6783, Martin Marietta Energy Systems, Inc., Oak Ridge National Laboratory, Oak Ridge, Tenn., February 1994.

[c]$K = K_d (\rho_b/n)$. Waste: $\rho_b = 1.76$ g/cm^3, $n = 0.35$; concrete: $\rho_b = 2.40$ g/cm^3, $n = 0.15$.

[d]The diffusion coefficient is calculated with the expression $D = D_s/[G(1 + K)H^{-1}]$. $H = 1$.

ORNL DWG 95-5650

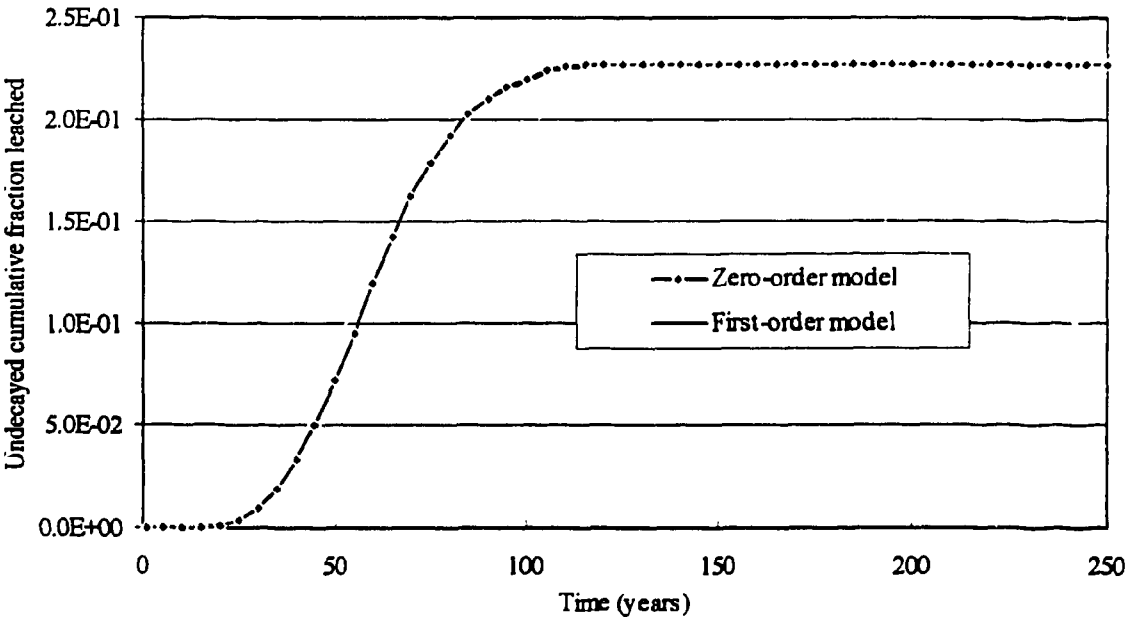

Fig. 5.11. Comparison of the undecayed cumulative fraction of ^{137}Cs leached from a tumulus (SOURCE1) using zero-order and first-order advection models for K_d = 1.99.

ORNL DWG 95-5651

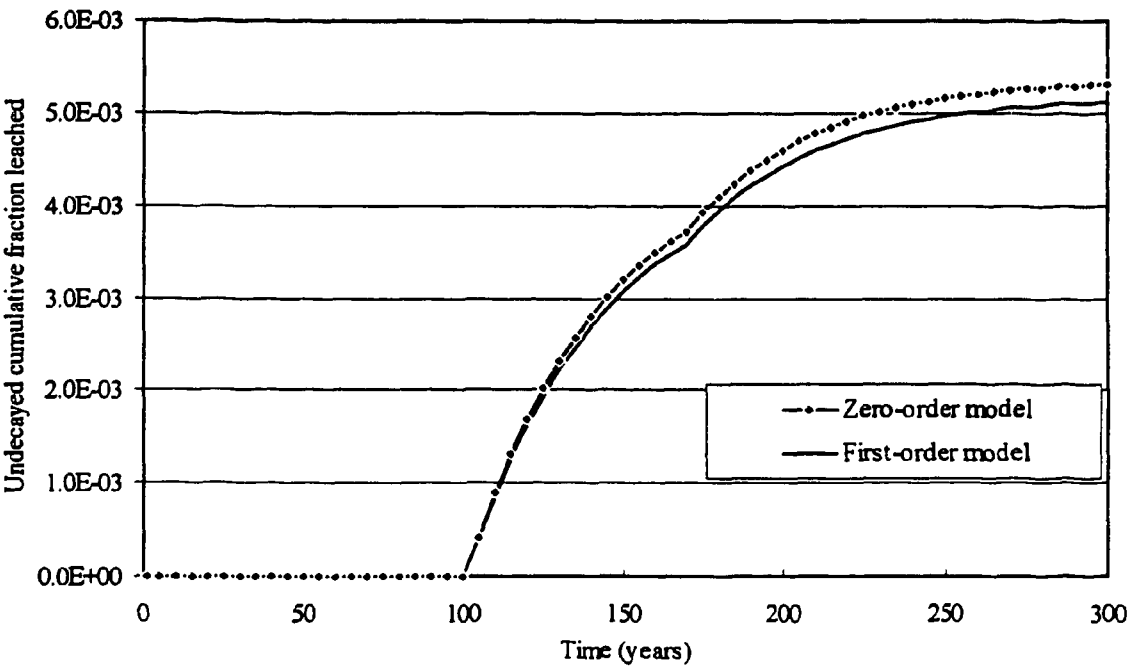

Fig. 5.12. Comparison of the undecayed cumulative fraction of ^{137}Cs leached from a tumulus (SOURCE1) using zero-order and first-order advection models for K_d = 199.

ORNL DWG 95-5652

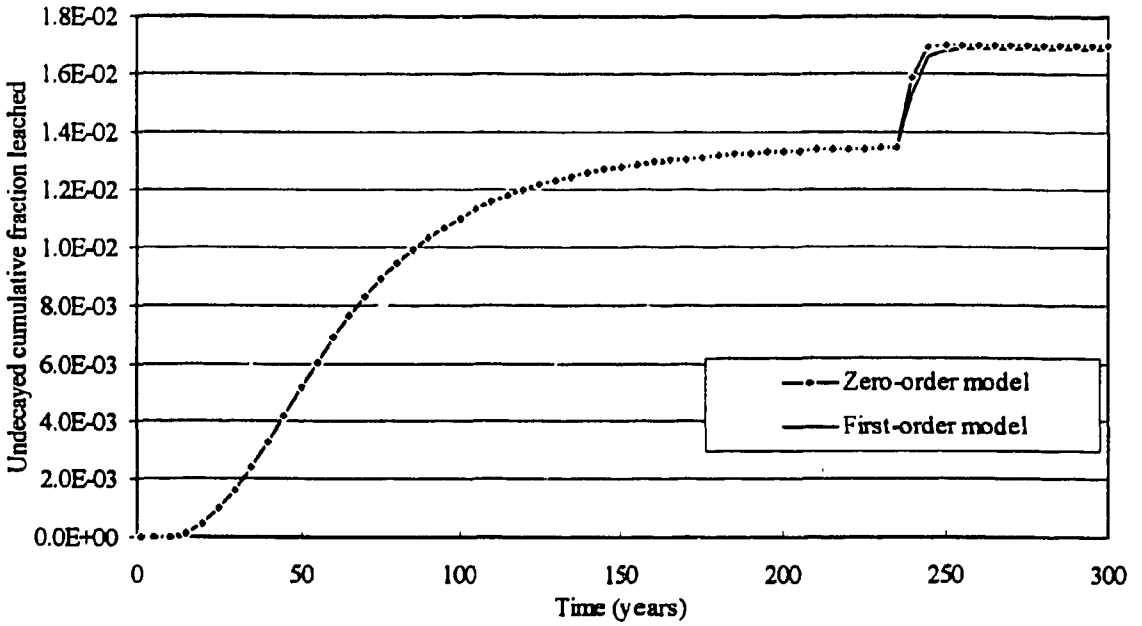

Fig. 5.13. Comparison of the undecayed cumulative fraction of ^{137}Cs leached from a silo (SOURCE2) using zero-order and first-order advection models for K_d = 1.99.

ORNL DWG 95-5653

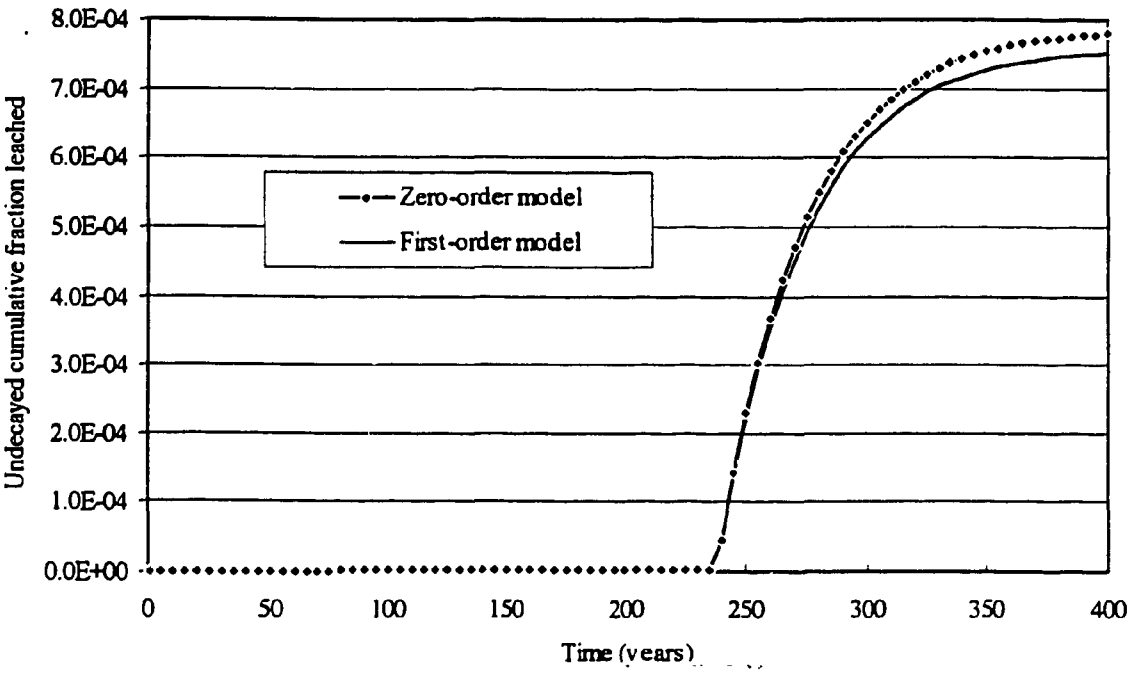

Fig. 5.14. Comparison of the undecayed cumulative fraction of ^{137}Cs leached from a silo (SOURCE2) using zero-order and first-order advection models for K_d = 199.

ORNL DWG 95-5654

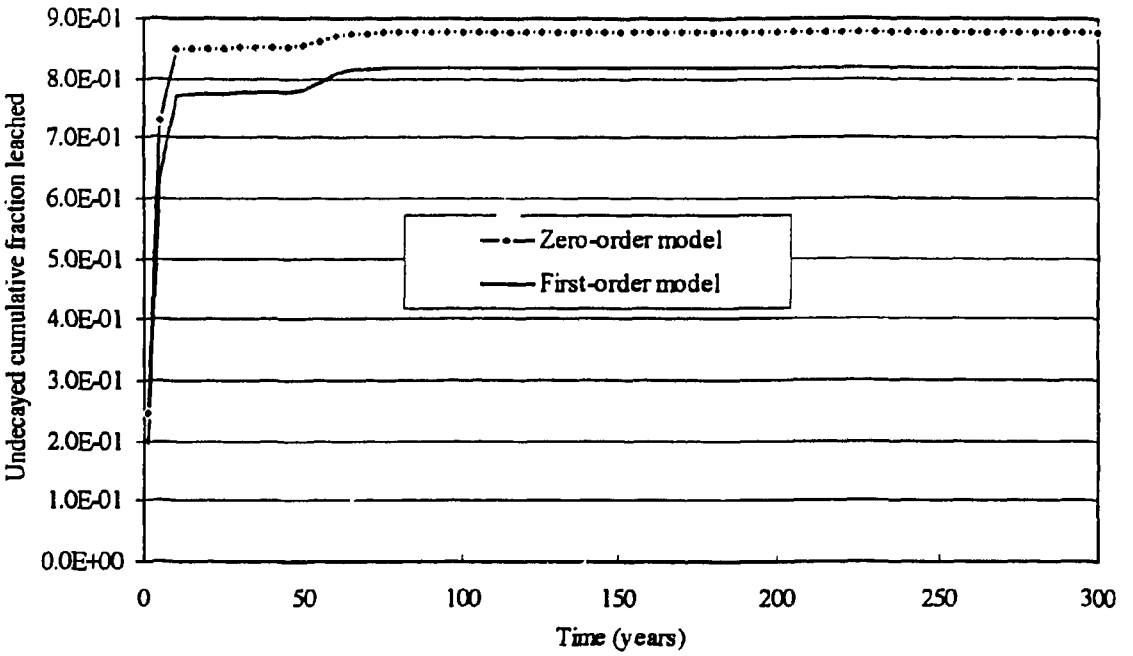

Fig. 5.15. Comparison of the undecayed cumulative fraction of ^{137}Cs leached from an unlined trench (SOURCE2) using zero-order and first-order advection models for K_d = 1.99.

ORNL DWG 95-5655

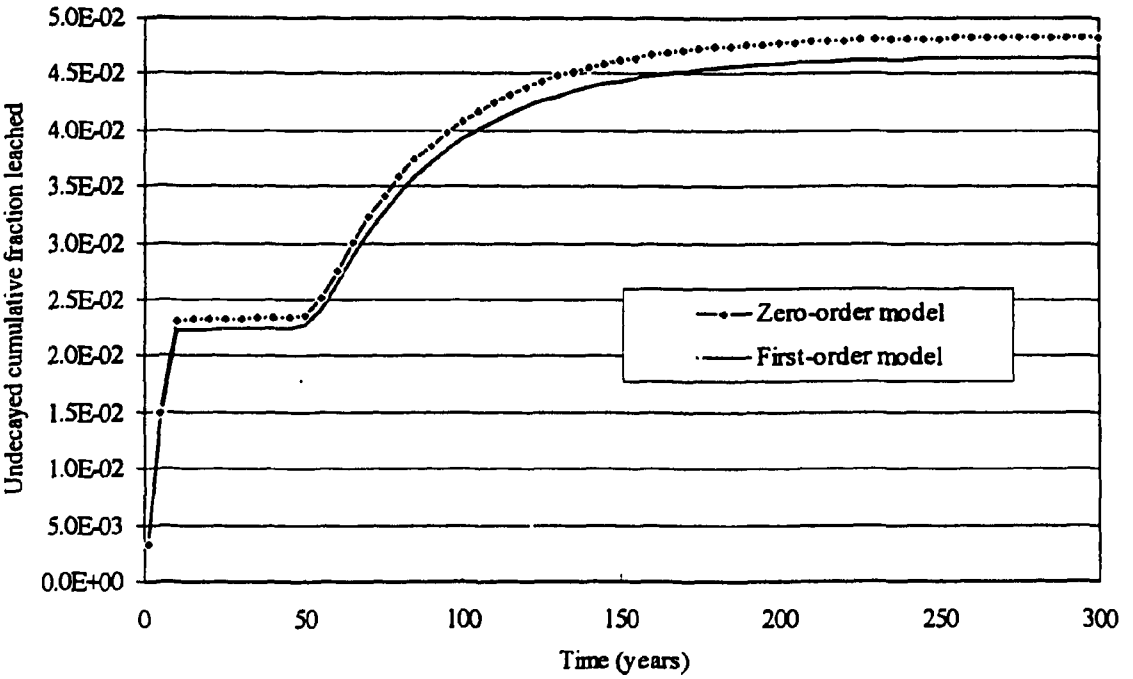

Fig. 5.16. Comparison of the undecayed cumulative fraction of ^{137}Cs leached from an unlined trench (SOURCE2) using zero-order and first-order advection models for K_d = 199.

Table 5.9. Comparison of maximum undecayed cumulative fraction leached values for ^{137}Cs using two advective models

K_d (mL/g)	Maximum undecayed cumulative fraction leached		Percent difference
	Zero-order model	First-order model	
		Tumulus	
1.99	2.27×10^{-1}	2.27×10^{-1}	0.00
19.9	3.41×10^{-2}	3.29×10^{-2}	3.52
199	5.37×10^{-3}	5.18×10^{-3}	3.54
		Silo	
1.99	1.70×10^{-2}	1.69×10^{-2}	0.59
19.9	3.02×10^{-3}	2.93×10^{-3}	2.98
199	7.87×10^{-4}	7.59×10^{-4}	3.56
		Trench	
1.99	8.77×10^{-1}	8.18×10^{-1}	6.73
19.9	3.37×10^{-1}	3.22×10^{-1}	4.45
199	4.84×10^{-2}	4.65×10^{-2}	3.93

[Eq. (4.35)], decreases with increasing K_d. Comparison of Eqs. (4.54) and (4.59) shows that, as λ_L becomes smaller (as compared to λ_d), Eq. (4.54) reduces to Eq. (4.59). Hence, the leach rate predicted by the first-order model approaches that predicted by the zero-order model as K_d increases. Additionally, from examination of Eqs. (4.54) and (4.59), it is also noted that the zero-order model solution approaches that of the first-order model as the length of time steps is reduced.

5.7 SUMMARY OF RESULTS

In this chapter, the zero-order and first-order advection models were compared by using a range of radionuclides which represented a wide variety of solubilities, distribution coefficients, and half-lifes. In general, the results from the two advective models were very similar. For the short-lived radionulcides, the zero-order model

consistently predicted a slightly higher undecayed cumulative fraction leached than did the first-order model. However, the first-order model ultimately predicts the same undecayed cumulative fraction leached as the zero-order model for long-lived radionuclides. The value of K_d was shown to produce small differences between the two models.

The first-order advection model presented gives a different time-response equation for calculating the contaminant release caused by advection from a disposal facility. This model allows for continuous update of the inventory during a time step. The zero-order model updates the inventory only at the end of a time step. From the simulations examined, it is evident that the zero-order model is conservative (i.e., predicts equal or larger amounts leached) as compared to the first-order model. Because both models yield similar results, the first-order model can serve as verification of the results for advective transport obtained with the zero-order model in Version 1.0 of the SOURCE codes.

6. APPLICATION OF THE SOURCE1 CODE TO THE DEVELOPMENT OF AN INTRUDER SCENARIO

6.1 INTRODUCTION

One concern addressed by performance assessments of LLW disposal facilities is the release of radionuclides from the waste and their transport from the disposal site into the biosphere; in particular, into the groundwater. The concern is that these radionuclides, as they move through the environment, may lead to an off-site individual receiving an unacceptable radiation dose from exposure to contamination. An additional concern is the potential on-site dose to an individual who accidently, or inadvertently, enters a disposal facility. This individual is referred to as an *inadvertent intruder*. The model conditions (i.e., timing) under which this intruder is assumed to enter the disposal facility is called the *intruder scenario*. Timing includes the time after facility closure, the length of stay, the number of intrusions, etc. Obviously, there are a large number of possible scenarios that may be considered to calculate potential doses to an intruder. Some scenarios that have been used in performance assessments are described in Ref. 27.

Clearly, the choice of an intruder scenario has a major impact on the calculated dose to an individual. Scenarios that assume early entry into a disposal facility will yield larger calculated intruder doses than those that assume later entry. The choice of a specific intruder scenario is necessarily subjective because the actions of a human are being predicted rather than the responses of a physical system. Such a choice of a scenario should be made only after careful consideration of the potential performance of the disposal facility as a barrier to human intrusion.

The dose that an inadvertent intruder receives is directly proportional to the radionuclide inventory remaining in the disposal facility at the time of intrusion. The inventory remaining is, in turn, a function of the time of intrusion and the amount of radionuclide leaching that has occurred prior to the intrusion. These two factors, time of intrusion and the amount of leaching from the disposal facility, together form the basis

for an intruder scenario. Several possible variations and combinations of these factors are discussed in the following paragraphs.

The time of intrusion into the waste may be arbitrarily established by a regulation or DOE Order. Alternatively, the preparers of a performance assessment may select a time of intrusion which will have to be defended. Several factors may influence the selection of the time of intrusion including: expected time of disposal-facility closure, expected length of time of site control after disposal-facility closure, potential future use of the site, and degradation of engineered barriers. The first three factors are very subjective and difficult to estimate. On the other hand, it is possible, using existing computer models, to estimate the degradation of engineered barriers. This estimate can be used to establish a reasonable time at which inadvertent intrusion could occur. A method, for establishing a time of intrusion, based on disposal facility degradation, is described in this chapter.

Once a time of intrusion is established, the radionuclide inventory remaining in the waste can be evaluated using several methods. One approach is to use the same computer models and physicochemical parameters that were formerly used to calculate the source term for radionuclide transport through the environment. However, in general, the parameters used in these models are conservative so that the amount of leaching from a facility will be overestimated. Hence, using conservative leaching parameters for an environmental transport source term determination will result in a nonconservative estimate of the inventory remaining at any given time. The calculated intruder dose would then be potentially underestimated.

Another approach to evaluate the remaining inventory at the time of intrusion is to take no credit for the radionuclide leaching. In this case, the only adjustment to the radionuclide inventory would be caused by radioactive decay. This approach results in a very conservative estimate of the radionuclide inventory, and the calculated intruder dose would potentially be overestimated.

A third alternative is to estimate the remaining radionuclide inventory somewhere between that of the two previously discussed approaches. This estimate could be accomplished by selecting reasonable leaching parameters for the source term model

which minimize the amount of leaching from the facility. Some credit could then be taken for radionuclide leaching in the intruder-dose estimation. A methodology for implementing this third approach is described in the following sections.

The intruder scenario developed consists of predicting both the time of intrusion and the remaining radionuclide inventory at the time of intrusion. Therefore, a method is needed that will provide a reasonable but conservative estimate of these two variables. The approach chosen consists of applying sensitivity and uncertainty analyses to the SOURCE1 code (with the first-order advection model). A tumulus-type disposal facility is used to present the proposed method. The properties of the facility are described in Table 5.2 of Chapter 5. The radionuclide inventory is assumed to consist of ^{137}Cs with the initial inventory and physical properties described in Table 5.1 of Chapter 5. To develop an intruder scenario, a sensitivity analysis is performed on SOURCE1 to identify the sensitive input parameters. Then, a range of uncertainty for each of these parameters is established. Using this range of parameters, an uncertainty analysis is used to calculate a potential year of intrusion. Finally, the uncertainty analysis is performed a second time to calculate the remaining inventory at the potential year of intrusion. One should note that this method is demonstrated only for SOURCE1 and one radionuclide. However, it is equally applicable to SOURCE2, other source term codes, and other radionuclides.

6.2 SENSITIVITY AND UNCERTAINTY ANALYSES

A large number of input parameters are normally required for complex source term models. Each of these parameters may have some uncertainty associated with it; hence, each will impact the uncertainty in the model solution. Thus, a method is needed to evaluate the influence of individual parameters on model predictions. A parameter that has a large influence on the model solution may warrant extensive investigation and experimentation to reduce the uncertainty in its value. Other parameters may be determined only within a relatively large range of uncertainty and have no effect on the model prediction.

Monte Carlo random sampling methods have been used to vary model parameters over a range of values with specified frequency distributions and to generate corresponding sets of model predictions.[49-51] An analysis of these parameter sets and the model results can be used to identify the effects of parameter perturbations on model prediction and is termed a *sensitivity analysis*. Variation of model parameters within a known range to determine the variability of the model predictions is referred to as an *uncertainty analysis*. To perform sensitivity and uncertainty analyses, a more efficient, systematic random sampling method, Latin Hypercube sampling,[52] has been shown to require the minimum number of samples necessary to represent adequately the probability distribution of each parameter.[49] The range of possible parameter values is divided into equal probability class intervals, and samples are randomly selected from each interval. This procedure ensures that the range of each parameter will be evenly sampled and that the distribution of each parameter will be better represented with fewer samples.

Sensitivity and uncertainty analyses were performed on SOURCE1 using the Latin Hypercube method. The PRISM code[50] was used to implement this random sampling technique. Of the slightly more than 100 input parameters required for a SOURCE1 simulation, 46 were selected for the sensitivity analysis.[27] Input data sets were generated for a selected number (200) of equal probability class intervals. Each parameter was assigned a normal distribution with a standard deviation equal to 1% of its mean value. A statistical summary of the model results produced indices of sensitivity that related the effects of heterogeneity of input variables to model predictions. This summary was used to identify the sensitive parameters, which were defined to be those input parameters that contributed at least 5% of the variability in the leach-rate calculation at any time during the simulation. This analysis resulted in the identification of 13 parameters having the most influence on SOURCE1 predictions.

Once the sensitive input parameters were identified, a range of uncertainty was established for each. In addition, a probability distribution (e.g., normal, triangular, uniform, etc.) was assigned to each variable along with the statistical values (e.g., mean,

standard deviation, minimum and maximum) required to characterize the distribution. The 13 sensitive parameters and the statistical information used in the uncertainty analyses are presented in Table 6.1. The uncertainty analysis is used to determine the potential time of intrusion and the remaining radionuclide inventory as described in the following sections.

6.3 EVALUATION OF TIME OF INTRUSION

The time at which an intruder enters a disposal facility cannot be assigned with unassailable certainty. However, using a knowledge of the engineered barriers present, it is possible to estimate a reasonable time at which an individual could inadvertently penetrate the disposal facility. One such potential time is when the concrete is no longer a credible barrier and it can not be readily distinguished from the natural soil. This is based on the assumption that an intact concrete barrier would discourage an individual from inadvertently entering the disposal facility. Hence, if the time at which the concrete degrades to a state indistinguishable from natural soil can be evaluated, then it should be reasonable to expect that this would be the earliest time that inadvertent intrusion might occur. This time can then be established as a reasonable time of intrusion for the intruder scenario.

The SOURCE1 code contains routines which calculate the degradation of the vaults in a tumulus-type disposal facility. These routines can be used to estimate the time of intrusion by calculating when the vault-wall thickness reaches some established value. A value of zero is chosen to demonstrate this method. However, the wall thickness value could vary based on knowledge of the disposal system and expectations regarding inadvertent intrusion. Clearly, when the vault-wall thickness is reduced to 0.0 m, the vaults are no longer a credible barrier and they should be indistinguishable from natural soil.

The SOURCE1 code can be used to calculate the predicted time at which the vault wall is no longer credited as having any thickness (i.e., equals 0.0 m in this case). However, a calculation using a single set of input parameters may not provide a

Table 6.1. SOURCE1 code sensitive parameters and range of uncertainty[a]

Parameter	Distribution	Mean	Standard deviation	Minimum	Maximum
Density of earthen cover (g/cm^3)	Triangular	1.76		1.60	2.20
Density of waste (g/cm^3)	Triangular	1.76		1.00	2.60
Moisture content of waste (unitless)	Triangular	0.99		0.15	1.00
Sulfate diffusion coefficient in concrete (m^2/s)	Triangular	1.06×10^{-11}		9.54×10^{-12}	1.17×10^{-11}
Time for complete corrosion of metal waste containers (year)	Triangular	60		25	100
Time for complete failure of epoxy coating on reinforcing steel (year)	Triangular	20		10	50
Saturated hydraulic conductivity of the soil under the tumulus (cm/s)	Log-normal	5.8×10^{-7}	2.31×10^{-6}	2.31×10^{-11}	1.16×10^{-3}
Saturated hydraulic conductivity of concrete (cm/s)	Triangular	1.0×10^{-10}		1.0×10^{-11}	1.0×10^{-9}
Saturated hydraulic conductivity of concrete (cm/s)	Triangular	1.0×10^{-10}		1.0×10^{-11}	1.0×10^{-9}

Table 6.1. (continued)

Parameter	Distribution	Mean	Standard deviation	Minimum	Maximum
Radionuclide distribution coefficient in waste[b] (mL/g)	Triangular	19.9		1.99	199
Radionuclide inventory[b] (g/vault)	Not applicable[c]	5.81×10^{-4}			
Radionuclide diffusion coefficient in concrete[b] (m^2/s)	Triangular	5.12×10^{-13}		1.02×10^{-13}	1.02×10^{-12}
Concentration of sulfate inside vault (mol/L)	Triangular	2.62×10^{-4}		2.49×10^{-4}	2.75×10^{-4}
Concentration of sulfate in groundwater (mol/L)	Triangular	2.62×10^{-4}		2.49×10^{-4}	2.75×10^{-4}

[a]Except for the sulfate concentrations, parameter values and distributions were taken from D. W. Lee et. al., *Performance Assessment for Continuing and Future Operations at Solid Waste Storage Area 6*, ORNL-6783, Martin Marietta Energy Systems, Inc., Oak Ridge National Laboratory, Oak Ridge, Tennessee, February 1994. Sulfate concentrations were based on more recent work at ORNL.

[b]Radionuclide assumed to be ^{137}Cs. This radionuclide was chosen because (1) the transport parameters (e.g., distribution and diffusion coefficients) have been widely studied, (2) to avoid solubility constrained leaching, and (3) it is expected that there would be very little cesium naturally present to isotopically dilute the ^{137}Cs in the waste.

[c]The initial radionuclide inventory was the same for each simulation because the final radionuclide inventory was a desired output. This approach avoided artificially perturbating the final inventory result.

conservative (i.e., the earliest time) result. To identify a conservative time, an uncertainty analysis can be performed on SOURCE1. This analysis integrates the effects of the sensitive parameters on model predictions and results in a distribution of times at which the vault-wall thickness is reduced to 0.0 m. The uncertainty analysis was conducted with the parameters presented in Table 6.1. Two-hundred input data files were randomly generated using PRISM. These data files were then executed as SOURCE1 simulations, and the time at which wall thickness degraded to 0.0 m in each simulation was identified. The results of these simulations is presented as a relative frequency distribution in Fig. 6.1. *Relative frequency* is defined as the number of occurrences of a given event divided by the total number of events.

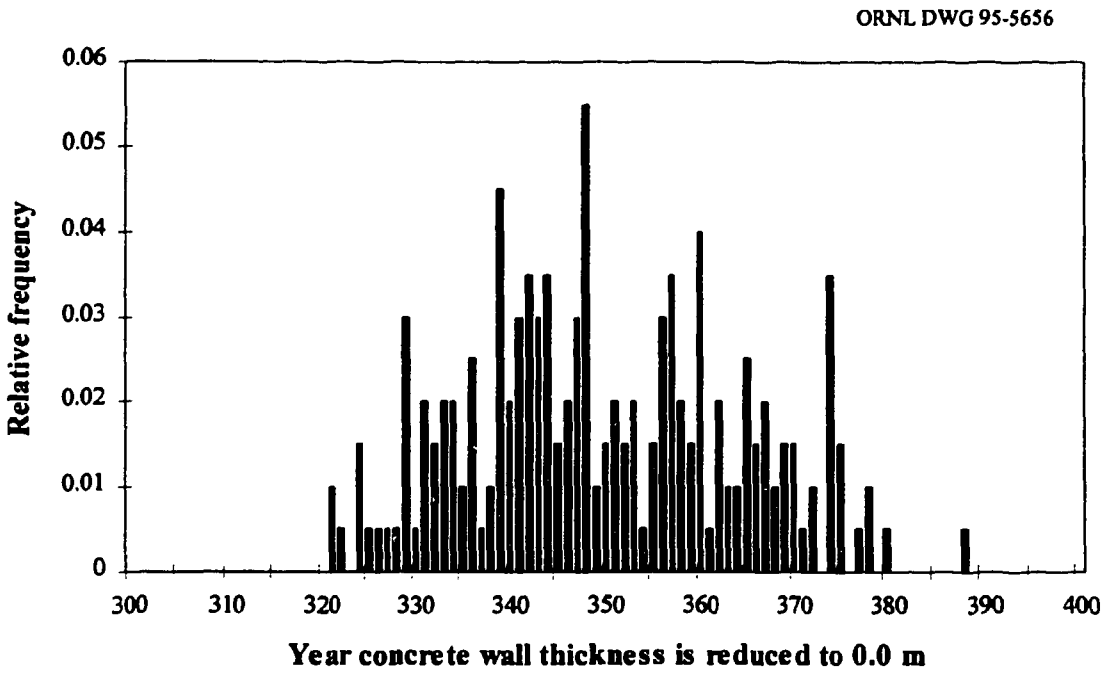

Fig. 6.1. Relative frequency of vault-wall thickness reaching 0.0 m for a tumulus-type disposal facility.

Figure 6.1 shows that the predicted year that the vault-wall thickness degrades to 0.0-m varies from 322 to 388 years. To be conservative, the earliest year for reaching a 0.0 m wall thickness would be selected. Hence, the time of intrusion was established as 322 years after facility closure. The projected radionuclide inventory at this time can then be evaluated to estimate the potential dose to an intruder.

6.4 EVALUATION OF REMAINING INVENTORY AT TIME OF INTRUSION

Once a reasonable time of intrusion has been established, the inventory remaining in the disposal facility can be estimated. During the period preceding intrusion, the radionuclide inventory decreases because of radioactive decay and leaching. An uncertainty analysis was used again to provide a conservative estimate of this inventory. This analysis resulted in a distribution of inventory values at the year of intrusion.

For this example, the inventory remaining was evaluated at 322 years. The results of the uncertainty analysis are presented as a relative frequency distribution in Fig. 6.2. Because inventory values covered a wide range, a logarithmic scale was used for the x-axis. The values of inventory remaining vary from 1.78×10^{-9} g to 6.42×10^{-5} g. Thus, for a conservative calculation of dose to an intruder at 322 years, the highest value, 6.42×10^{-5} g of ^{137}Cs, was chosen. This inventory could then be used to estimate the potential dose to an intruder.

6.5 SUMMARY OF METHOD

In this chapter, a method for developing an intruder scenario was presented. This method is based on the assumption that an individual would inadvertently intrude into a facility only after concrete is no longer a credible barrier and is indistinguishable from the native soil for all practical purposes. The example presented was for a case where wall thickness for a tumulus vault degraded to 0.0 m. Sensitivity and uncertainty analyses were performed on SOURCE1 to evaluate the potential time of intrusion and remaining

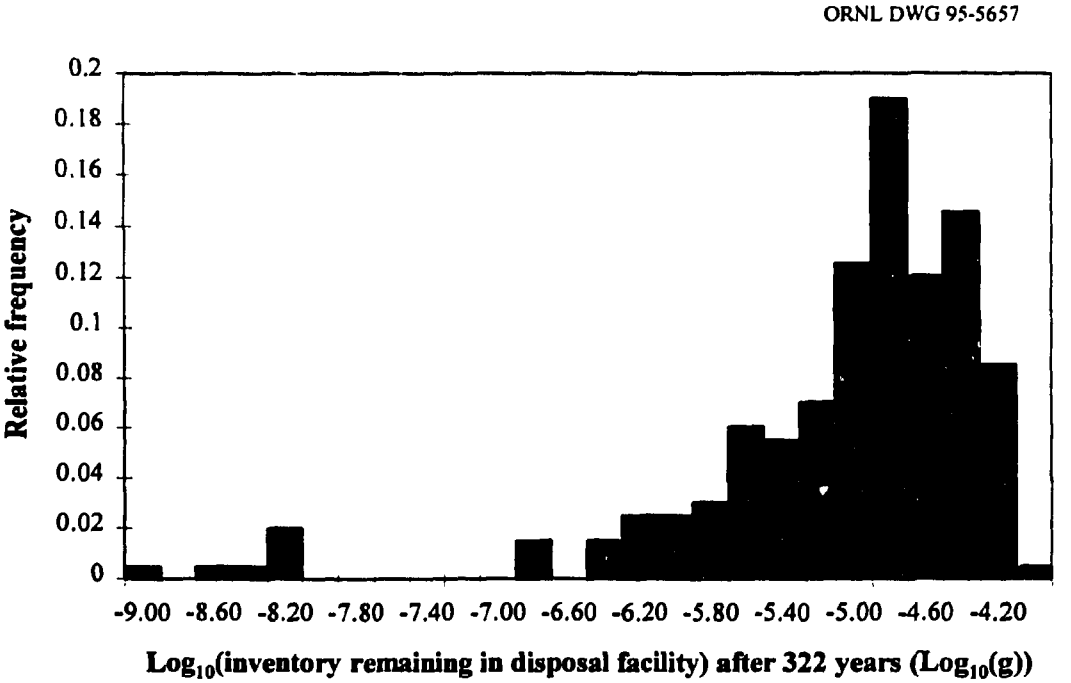

Fig. 6.2. Relative frequency of ^{137}Cs inventory remaining after 322 years for a tumulus-type disposal facility.

radionuclide inventory at that time. These analyses integrate the effects of the sensitive model parameters into the intruder scenario selection. For this example, only ^{137}Cs in a tumulus-type disposal facility was used. However, this method can be applied to any other radionuclide. Additionally, the method can be applied to SOURCE2 and other source term codes.

7. CONCLUSIONS

From this analysis of source term modeling for LLW performance assessments, the following conclusions have been reached:

1. The zero-order and first-order advection models used give results that are essentially the same. In every case studied, as presented in the graphs of undecayed cumulative fraction leached, the zero-order model predicts equal or slightly higher amounts leached than does the first-order model.

2. For short-lived radionuclides, the zero-order model predicted slightly higher undecayed cumulative fraction leached than did the first-order model. However, for long-lived radionuclides, both models eventually approach the same value of undecayed cumulative fraction leached.

3. Variation of the distribution coefficient, K_d, produces very little difference between the response of the zero-order and first-order models. In general, as the value of K_d is increased, the equation that describes the zero-order model approaches the equation that describes the first-order model.

4. The response of the zero-order model approaches that of the first-order model as the length of time steps is reduced.

5. Advection is the dominant radionuclide transport mechanism after a disposal facility fails (i.e., cracks), as made clear by examination of the fractional leach rate graphs for each disposal technology.

6. The close agreement between the two advection models indicates that the more rigorous first-order solution verifies the less rigorous zero-order solution.

7. The commonly applied concept of a leach rate constant is useful in that it allows advective transport to be expressed as a linear first-order differential equation and to be readily combined with other first-order or pseudo-first-order mechanisms.

8. With the leach rate constant represented as the reciprocal of the mean residence time, T_R, it is interpreted to mean that the contaminant concentrations at two points, separated by a distance W, differ by a factor of e in a time span T_R.

9. The first-order advective model continuously updates the contaminant inventory as a result of contaminant leaching. By contrast, the zero-order model updates the inventory as a result of leaching only at the end of a time step.

10. The extension of sensitivity and uncertainty analyses to develop an intruder scenario offers an unequivocal method to estimate a time of intrusion and the inventory at intrusion. Note that the calculational method is unequivocal, not necessarily the predicted results.

11. The method presented for intruder scenario development can be applied to source term codes other than SOURCE1 and also to other radionuclides.

12. The sensitivity analysis performed on SOURCE1 identified 13 sensitive parameters. Because more than 100 input parameters are required for a SOURCE1 simulation, the sensitivity analysis provides insight into which parameters should be most thoroughly investigated.

13. A wide variety of source term codes are available, and each has its limitations. Among these codes, SOURCE1 and SOURCE2 (along with their predecessor,

BARRIER) are state of the art with regard to coupling the calculation of engineered barrier degradation with the calculation of radionuclide release.

14. Source term codes are an important element in the performance assessment process. Through this process, the results from source term codes have a large impact on disposal limits and operations at waste disposal facilities

15. It is evident from this work that source term modeling for performance assessments is a very broad area. Several additional areas of potential investigation are described in Chapter 8, "Recommendations." The work in this study and continued work in the recommended areas will continue to improve the understanding and modeling of LLW disposal facility source terms.

8. RECOMMENDATIONS

8.1 INTRODUCTION

A number of limitations and areas for improvement in source term modeling were identified during the preparation of this report. These are summarized as recommendations in this chapter. The first five recommendations are improvements that might be made in the SOURCE codes. Although, in the context of this report, these five recommendations are specific to SOURCE1 and SOURCE2, they may be equally applicable to other source term codes. The next two (6th and 7th) recommendations involve the application of sensitivity and uncertainty analyses to source term codes. This discussion focuses on the relationship between the distribution and diffusion coefficients that are used as code input parameters. In addition, an area of potential further development of the intruder scenario presented in Chapter 6 is discussed. Finally, a recommendation (the 8th) concerning the use of source term codes as a design tool is outlined.

8.2 RECOMMENDATION 1: ALTERNATIVE SOLUTION OF THE ADVECTION-DIFFUSION EQUATION

The advection-diffusion equation developed in Chapter 4 was solved semianalytically to describe the transport of radionuclides from a waste disposal facility. The solution was based on the assumption that either advection or diffusion was the dominant transport mechanism; thus allowing each mechanism to be solved separately. This assumption, which obviously simplifies the problem solution, may limit the applicability of the model developed. To evaluate this potential limitation, a numerical solution could be performed on the advection-diffusion equation. This type of solution gives a more rigorous coupling of the contributions from each of the transport mechanisms. Additionally, this approach could be extended even further by dividing the waste form into regions (e.g., a waste region surrounded by a concrete region) and performing a numerical solution for each region. The derivation of transport equations for this situation would couple a region to

its adjacent regions. This type of approach (similar to that used in FLOTHRU) allows for the modeling of a heterogeneous system which has different transport parameters in each region.

8.3 RECOMMENDATION 2: ACCOUNTING FOR RADIOACTIVE DAUGHTERS

The SOURCE computer codes calculate the transport and decay of radioactive contaminants. Once a contaminant decays, its progenies are not considered. However, the daughter or daughters of this decay may be other radioisotopes of the same nuclide or different radionuclides, which could be of concern for dose estimations in a performance assessment. Radioactive daughters are sometimes accounted for by assuming that they are in equilibrium with the parent. This assumption means, by default, that each radionuclide in the decay chain has the same transport parameters (e.g., diffusion coefficient, distribution coefficient, solubility, etc.). Another approach to accounting for radioactive daughters would be to incorporate radionuclide ingrowth into the SOURCE codes. If daughters are tracked, then different transport parameters could be assigned to each.

8.4 RECOMMENDATION 3: CONCRETE-DEGRADATION MECHANISMS

Currently, three concrete-degradation mechanisms are modeled in the SOURCE codes: sulfate attack, calcium hydroxide leaching, and steel reinforcement corrosion. However, other mechanisms can cause the deterioration of concrete barriers used in LLW disposal (e.g., freeze-thaw cycling, alkali-aggregate reaction, and carbonation). Reference 53 outlines a number of degradation mechanisms and identifies computer models that are either currently in use or under development for each. These models should be explored for applicability to the SOURCE codes. If applicable, models could be incorporated into the SOURCE codes to expand the number of degradation options

available. This would make the SOURCE codes more generic and flexible in their applications to different disposal environments.

8.5 RECOMMENDATION 4: CORROSION MODELS OF METAL BARRIERS

The current version of the SOURCE codes uses a simple, linear corrosion model to simulate the deterioration of metal barriers. A great deal of research could be done in this area to improve the corrosion model. For example, theoretical and empirical models could be identified for incorporation into the SOURCE codes. Improved corrosion models, coupled with added concrete-degradation models (Sect. 8.4) would enhance the ability of the source codes to predict engineered barrier degradation. This prediction not only influences release and transport from a disposal facility, but also influences the selection of an intruder scenario (Chapter 6).

8.6 RECOMMENDATION 5: EVALUATION OF THE RELATIONSHIP BETWEEN MOBILE AND IMMOBILE CONTAMINANTS

The derivation of the advection-diffusion equation [Eq. (4.23)] assumed that the relationship between mobile and immobile contaminants could be represented by a linear isotherm (i.e., by using a distribution coefficient). Specifically, a Freundlich isotherm [with $N = 1$ and $k = K_d$ in Eq. (4.12)] was used. However, other isotherms are available. Isotherm models that are also frequently used in the modeling of contaminant transport include the Langmuir and Dubinin-Radushkevich models.[30]

Other methods to describe the relationship between mobile and immobile contaminants in addition to isotherm models are presented in Ref. 30. These methods include: parametric K_d models, mass-action adsorption models, and surface complexation models. Each of these models has limits on its applicability to a specific waste disposal situation. Each model (and any others that are identified) could be evaluated and, if appropriate, incorporated into the SOURCE codes. Again, this would

increase the general applicability and flexibility of the SOURCE codes for modeling different disposal environments.

8.7 RECOMMENDATION 6: VARIATION OF DIFFUSION COEFFICIENTS AND DISTRIBUTION COEFFICIENTS FOR SENSITIVITY AND UNCERTAINTY ANALYSES

In Chapter 4, distribution coefficients are used to calculate retarded diffusion coefficients [e.g., Eq. (4.63)]. In Chapter 5, when distribution coefficients were varied, the diffusion coefficients were adjusted to reflect this variation (e.g., see Sect. 5.6). However, as described in Chapter 6, when performing the sensitivity and uncertainty analyses, the diffusion coefficients were varied independently of the distribution coefficients. This analysis did not take into account that variation of the distribution coefficient changes the diffusion coefficient; in other words, they are not independent parameters. Hence, to improve the sensitivity and uncertainty analyses, a method should be developed to link the diffusion and distribution coefficients developed as input parameters for these analyses.

8.8 RECOMMENDATION 7: UNCERTAINTY IN SOURCE TERM MODELS USED IN INTRUDER SCENARIO DEVELOPMENT

In Chapter 6, a method for developing an intruder scenario was presented. This method, based on sensitivity and uncertainty analyses, evaluated the time at which concrete is no longer considered a credible barrier and the remaining radionuclide inventory at that time. Note that consideration was given to uncertainty in the input parameters to the source term model, but not uncertainty in the model itself (i.e., how well the computer model represents the actual system). If the probability that the model represents the system is less than 1, the analysis for the intruder scenario would be modified to reflect this. A method to determine model uncertainty is outlined in Ref. 54.

Therefore, to further develop the intruder scenario, model uncertainty should be considered and incorporated into the methodology presented in Chapter 6.

8.9 RECOMMENDATION 8: SOURCE TERM CODES AS DESIGN TOOLS

Source term codes can be useful tools in the design of waste disposal facilities if the codes have been shown to be reliable for such systems. In the design phase of a facility, different types of disposal technologies might be simulated to identify the technology that should yield optimum performance for a particular disposal environment. In addition, different types and combinations of materials (e.g., various concrete mixtures, asphalt formulations, metals, etc.) could be simulated to evaluate their impacts on facility performance. These types of evaluations can be both an economic benefit and a time savings to disposal facility designers.

In Chapter 5, three different disposal technologies were examined. Although the simulations performed were not explicitly designed for disposal technology comparisons, some relative measure of the performance of each technology could be inferred. For example, simulations could be performed such that more meaningful comparisons of disposal technologies could be made. Ideally, these simulations would keep common factors the same (e.g., initial radionuclide inventory, rainfall rate, etc.) so that any observed differences could be attributed to disposal facility design. In addition, different concrete mixtures and metal barriers could be simulated in a given facility to evaluate how performance of the facility varies. This type of study, using the SOURCE codes, would be extremely helpful in making decisions concerning LLW disposal. Refinements in the SOURCE codes, such as those suggested in Sects. 8.2 through 8.6, should enhance the usefulness of the SOURCE codes as design tools.

REFERENCES

1. U.S. Department of Energy, *Use of Engineered Soils and Other Site Modifications for Low-Level Radioactive Waste Disposal*, DOE/LLW-207, IT Corporation, Albuquerque, N.M., August 1994.

2. A. S. Rood, *GWSCREEN: A Semi-Analytical Model for Assessment of the Groundwater Pathway from Surface or Buried Contamination: Theory and User's Manual*, EGG-GEO-10158, Idaho National Engineering Laboratory, Idaho Falls, Idaho, March 1992.

3. C. J. Suen and T. M. Sullivan, *Sensitivity Analysis and Benchmarking of the BLT Low-Level Waste Source Term Code*, NUREG/CR-5943, BNL-NUREG-52346, Brookhaven National Laboratory, Upton, N.Y., July 1993.

4. T. M. Sullivan, *Disposal Unit Source Term (DUST) Data Input Guide*, NUREG/CR-6041, BNL-NUREG-52375, U.S. Nuclear Regulatory Commission, Brookhaven National Laboratory, Upton, N.Y., May 1993.

5. R. Shuman, et. al., *The BARRIER Code, A Tool for Estimating the Long-Term Performance of Low-Level Radioactive Waste Disposal Facilities, User's Manual*, EPRI NP-6218-CCML, Rogers and Associates Engineering Corporation, Salt Lake City, Utah, February 1989.

6. R. Shuman, N. Chau, and E. A. Jennrich, *The SOURCE Computer Codes: Models for Evaluating the Long-Term Performance of SWSA 6 Disposal Units, Version 1.0: User's Manual*, RAE-9005/8-1, Rogers and Associates Engineering Corporation, Salt Lake City, Utah, April 1992.

7. G. T. Yeh, *FEMWATER: A Finite Element Model of Water Flow Through Saturated-Unsaturated Porous Media—First Revision*, ORNL-55671R1, Martin Marietta Energy Systems, Inc., Oak Ridge National Laboratory, Oak Ridge, Tenn., 1987.

8. J. C. Walton, L. E. Plansky, R. W. Smith, *Models for Estimation of Service Life of Concrete Barriers in Low-Level Radioactive Waste Disposal*, NUREG/CR-5542, EGG-2597, U.S. Nuclear Regulatory Commission, Washington, D.C., September 1990.

9. U.S. Department of Energy Order 5820.2A, "Radioactive Waste Management," Washington, D.C., September 1988.

10. J. G. Moore, et al., *Development of Cementitious Grouts for the Incorporation of Radioactive Wastes. Part I: Leach Studies*, ORNL-4962, Union Carbide Corporation, Oak Ridge National Laboratory, Oak Ridge, Tenn., April 1975.

11. J. G. Moore, *Development of Cementitious Grouts for the Incorporation of Radioactive Wastes. Part 2: Continuation of Cesium and Strontium Leach Studies*, ORNL-5142, Union Carbide Corporation, Oak Ridge National Laboratory, Oak Ridge, Tenn., Sept. 1976.

12. W. D. Bostick, et al., *Blast Furnace Slag-Cement Blends for the Immobilization of Technetium-Containing Wastes*, K/QT-203, Martin Marietta Energy Systems, Inc., Oak Ridge National Laboratory, Oak Ridge, Tenn., November 1988.

13. J. E. Till and H. R. Meyer, eds, *Radiological Assessment, A Textbook on Environmental Dose Analysis*, NUREG/CR-3332, U.S. Nuclear Regulatory Commission, Washington, D.C., September 1983.

14. J. W. Poston, "Reference Man: A System for Internal Dose Calculations," *Radiological Assessment, A Textbook on Environmental Dose Analysis*, pp. 6.1–6.31 in NUREG/CR-3332, eds. J. E. Till and H. R. Meyer, U.S. Nuclear Regulatory Commission, Washington, D.C., September 1983.

15. D. C. Kocher, "External Dosimetry," pp. 8.1–8.52 in *Radiological Assessment, A Textbook on Environmental Dose Analysis*, NUREG/CR-3332, ed. J. E. Till and H. R. Meyer, U.S. Nuclear Regulatory Commission, Washington, D.C., September 1983.

16. J. M. Pommersheim and J. R. Clifton, *Models of Transport Processes in Concrete*, NUREG/CR-4269, U.S. Nuclear Regulatory Commission, National Institute of Standards and Technology, Gaithersburg, Maryland, January 1991.

17. J. C. Walton, *Performance of Intact and Partially Degraded Concrete Barriers in Limiting Mass Transport*, NUREG/CR-5445, EGG-2662, Idaho National Engineering Laboratory, Idaho Falls, Idaho, June 1992.

18. R. D. Rogers, M. A. Hamilton, and J. W. McConnell, Jr., *Microbial-Influenced Cement Degradation—Literature Review*, NUREG/CR-5987, EGG-2695, Idaho National Engineering Laboratory, Idaho Falls, Idaho, March 1993.

19. A. Atkinson and J. A. Hearne, "Mechanistic Model for the Durability of Concrete Barriers Exposed to Sulphate-Bearing Groundwaters," pp. 149–56 in *Materials Research Society Symposium Proceedings*, **176**, 1990.

20. W. F. Langelier, "The Analytical Control of Anti-Corrosion Water Treatment," *Journal of American Water Works Association* **28**(10), 1500–21 (1936).

21. A. Atkinson, *The Time Dependence of pH Within a Repository for Radioactive Waste Disposal*, AERE-R11777, Harwell Laboratory, Didcot, United Kingdom, April 1985.

22. S. A. Greenburg and T. N. Chang, "Investigation of the Colloidal Hydrated Calcium Silicates. II. Solubility Relationships in the Calcium Oxide-Silica-Water System at 25 D," *Journal of Physical Chemistry* **69**, 182 (1965).

23. F. M. Lea, *The Chemistry of Cement and Concrete*, 3rd ed., Edward Arnold, Ltd., London, 1970.

24. K. Tuutti, *Corrosion of Steel in Concrete*, Swedish Cement and Concrete Research Institute, Stockholm, 1982.

25. D. A. Hausmann, "Steel Corrosion in Concrete: How Does It Occur?" *Materials Protection*, pp. 19–23, November 1967.

26. A Fick, *Annln Phys.*, **170**, 59 (1855).

27. D. W. Lee, et al., *Performance Assessment for Continuing and Future Operations at Solid Waste Storage Area 6*, ORNL-6783, Martin Marietta Energy Systems, Inc., Oak Ridge National Laboratory, Oak Ridge, Tenn., February 1994.

28. J. Bear, *Dynamics of Fluids in Porous Media*, Dover Publications, Inc., New York, 1972.

29. G. L. Moltyaner and D. R. Champ, *Mass Transport in Saturated Porous Media: Estimation of Transport Parameters*, AECL-9610, Chalk River Nuclear Laboratories, Chalk River, Ontario, November 1987.

30. R. J. Serne, *Conceptual Adsorption Models and Open Issues Pertaining to Performance Assessment*, PNL-SA-20045, Pacific Northwest Laboratory, Richland, Wash., October 1991.

31. P. F. Salter, L. L. Ames, and J. E. McGarrah, *Sorption of Selected Radionuclides on Secondary Minerals Associated with the Columbia River Basalts*, RHO-BWI-LD-43, Rockwell Hanford Operations, Richland, Wash., April 1981.

32. L. L. Rogers, *Nonlinear Optimal Remediation of Contaminated Aquifers Incorporating Linear Sorption; Principles and Case History*, UCRL-102152, DE90011469, Lawrence Livermore National Laboratory, Livermore, Calif., May 1990.

33. J. Bear, *Modeling and Applications of Transport Phenomena in Porous Media*, von Karman Institute for Fluid Dynamics Lecture Series, 1990-01, Vol. 1, Rhode Saint Genese, Belgium, February 1990.

34. D. O. Lomen, A. Islas, and A. W. Warrick, "A Perturbation Solution for Transport and Diffusion of a Single Reactive Chemical with Nonlinear Rate Loss," pp. 281–88 in *Field-Scale Water and Solute Flux in Soils*, ed. K. Roth, et al. Birkhäuser Verlag, Boston, 1990.

35. P. S. Huyakorn, J. B. Kool, Y. S. Wu, *VAM2D-Variably Saturated Analysis Model in Two Dimensions Version 5.2 with Hysteresis and Chained Decay Transport—Documentation and User's Guide*, NUREG/CR-5352, Rev. 1, U.S. Nuclear Regulatory Commission, Washington, D.C., October 1991.

36. R. S. Rundberg, "A Suggested Approach Toward Measuring Sorption and Applying Sorption Data to Repository Performance Assessment," pp. 187–215, *Proc. Radionuclide Sorption from the Safety Evaluation Perspective, Interlaken, Switzerland, October 16-18 1991*, Nuclear Energy Agency Organization for Economic Cooperation and Development, Paris, 1992.

37. T. T. Vandergraaf, K. V. Ticknor, and T. W. Melnyk, "The Selection and Use of a Sorption Database for the Geosphere Model in the Canadian Nuclear Fuel Waste Management Program," pp. 81–120, *Proc. Radionuclide Sorption from the Safety Evaluation Perspective, Interlaken, Switzerland, October 16-18, 1991*, Nuclear Energy Agency Organization for Economic Cooperation and Development, Paris, 1992.

38. C. F. Baes and R. D. Sharp, "A Proposal for Estimation of Soil Leaching and Leaching Constants for use in Assessment Models," *J. Environ. Qual.*, **12**(1) 17-28 (1983).

39. R. C. Routson and R. J. Serne, *One-Dimensional Model of the Movement of Trace Radioactive Solute Through Soil Columns: The PERCOL Model*, Battelle Pacific Northwest Laboratories, Richland, Wash., 1972.

40. G. H. Jirka, A. N. Findikakis, Y. Onishi, and P. J. Ryan, "Transport of Radionuclides in Surface Waters," pp. 3.1–3.58, *Radiological Assessment, A*

Textbook on Environmental Dose Analysis, NUREG/CR-3332, ed. J. E. Till and H. R. Meyer, U.S. Nuclear Regulatory Commission, Washington, D.C., September 1983.

41. J. Weaver and C. G. Enfield, *Predicting Subsurface Contaminant Transport and Transformation: Considerations for Model Selection and Field Validation*, EPA/600/2-89/045, Robert S. Kerr Environmental Research Laboratory, U.S. Environmental Protection Agency, Ada, Okla., August 1989.

42. H. Matsuzuru and A. Suzuki, "Modeling of Release of Radionuclides from an Engineered Disposal Facility for Shallow Land Disposal of Low-Level Radioactive Waste, *Waste Management*, 9, (1) 45–56 (1989).

43. T. L. Gilbert, et al., *A Manual for Implementing Residual Radioactive Material Guidelines*, ANL/ES-160, DOE/CH/8901, Argonne National Laboratory, Argonne, Ill., June 1989.

44. R. Khaleel and T. LeGore, *Effects of Varying Recharge on Radionuclide Flux Rates to the Water Table at a Low-Level Solid Waste Burial Site*, Westinghouse Hanford Company, Richland, Wash.

45. E. L. Cussler, *Diffusion, Mass Transfer in Fluid Systems*, Cambridge University Press, New York, 1984.

46. M. G. Cowgil, T. M. Sullivan, *Source Term Evaluation for Radioactive Low-Level Waste Disposal Performance Assessment*, NUREG/CR-5911, BNL-NUREG-52334, U.S. Nuclear Regulatory Commission, Washington, D.C., January 1993.

47. G. W. Roles, *Characteristics of Low-Level Radioactive Waste Disposal During 1987 Through 1989*, NUREG-1418, U.S. Nuclear Regulatory Commission, Washington, D.C., December 1990.

48. U.S. Department of Energy, *Spent Fuel and Radioactive Waste Inventories, Projections, and Characteristics*, DOE/RW-0006, Rev. 9, Martin Marietta Energy Systems, Inc., Oak Ridge National Laboratory, Oak Ridge, Tenn., March 1994.

49. R. L. Iman and J. C. Helton, *A Comparison of Uncertainty and Sensitivity Analysis Techniques for Computer Models*, NUREG/CR-3904, SAND84-1461, Sandia National Laboratory, Albuquerque, N.M., 1985.

50. R. H. Gardner, B. Rojder, and U. Bergstrom, *PRISM: A Systematic Method for Determining the Effect of Parameter Uncertainties on Model Predictions*, Studsvik Energiteknik AB report, NW-83/555, Nykoping, Sweden, 1983.

51. K. A. Rose, et al., "Parameter Sensitivities, Monte Carlo Filtering, and Model Forecasting Under Uncertainty," *Journal of Forecasting*, **10**, 117–33 (1991).

52. R. L. Inman and M. J. Shortencarier, *A Fortran 77 Program and User's Guide for the Generation of Latin Hypercube and Random Samples for Use with Computer Models*, NUREG/CR-3624, SAND83-2365, Sandia National Laboratory, Albuquerque, N.M., March 1984.

53. L. E. Plansky and R. R. Seitz, *User's Guide for Simplified Computer Models for the Estimation of Long-Term Performance of Cement-Based Materials*, NUREG/CR-6138, EGG-2719, Idaho National Engineering Laboratory, Idaho Falls, Idaho, February 1994.

54. D. W. Lee, M. W. Yambert, and D. C. Kocher, "Uncertainty Analysis for Low-Level Radioactive Waste Disposal Performance Assessment at Oak Ridge National Laboratory," pp. 1534–38 in *Proc. International Topical Meeting on Nuclear Waste and Hazardous Waste Management, Spectrum '94, Aug. 14-18, 1994, Atlanta, Ga.*, Vol. 2, American Nuclear Society, Inc., LaGrange Park, Ill., 1994.

Appendix A

RELATIONSHIP OF THE DIMENSIONLESS DISTRIBUTION COEFFICIENT TO OTHER COMMONLY MEASURED DISTRIBUTION COEFFICIENTS

Table A.1. Relationship of the dimensionless distribution coefficient (K) to some other commonly measured distribution coefficients[a]

Type of distribution coefficient	Units of distribution coefficient	Relationship to K
Mixed,[b] K_{MP}	$\frac{\text{amount of species/mass of pore-free solid}}{\text{amount of species/volume of liquid}}$	$K = \rho_p \left(\frac{1 - \epsilon}{\epsilon} \right) K_{MP}$
Mixed,[c] K_{MB}	$\frac{\text{amount of species/mass of porous body}}{\text{amount of species/volume of liquid}}$	$K = \rho_b \left(\frac{1}{\epsilon} \right) K_{MB}$
Volume, K_{VV}	$\frac{\text{amount of species/volume of pore-free solid}}{\text{amount of species/volume of liquid}}$	$K = \left(\frac{1 - \epsilon}{\epsilon} \right) K_{VV}$
Geometry, K_{GV}	$\frac{\text{amount of species/volume of porous body}}{\text{amount of species/volume of liquid}}$	$K = \left(\frac{1}{\epsilon} \right) K_{GV}$

[a]Reference: H. W. Godbee, et al., "Waste Confinement Systems and Waste-Form Durability," pp 125–41, *Effective and Safe Waste Management: Interfacing Sciences and Engineering with Monitoring and Risk Analysis*, ed. R. L. Jolley and R. G. M. Wang, Lewis Publishers, Boca Raton, Florida, 1993.

[b]ρ_p is the density of the pore-free solid (i.e., mass of pore-free solid/volume of pore-free solid). ϵ is the void fraction (i.e., volume of pores/volume of porous body).

[c]ρ_b is the density of the porous body (mass of porous body/volume of porous body).

Appendix B

GRAPHS OF ADVECTIVE MODEL COMPARISONS

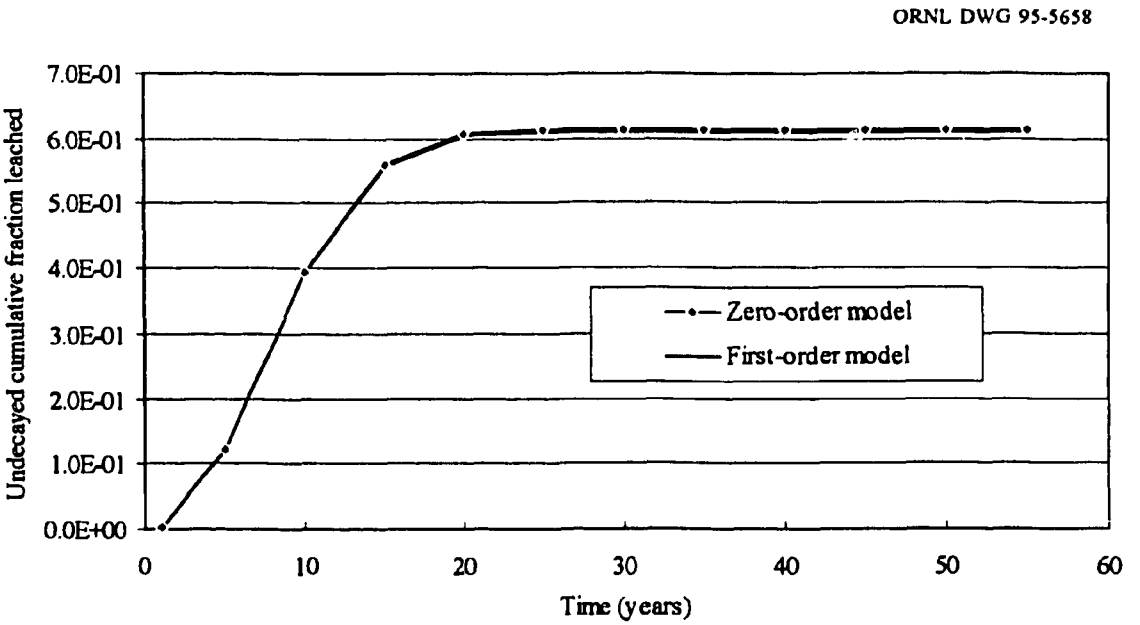

Fig. B.1. Comparison of the undecayed cumulative fraction of ^{3}H leached from a tumulus (SOURCE1) using zero-order and first-order advection models.

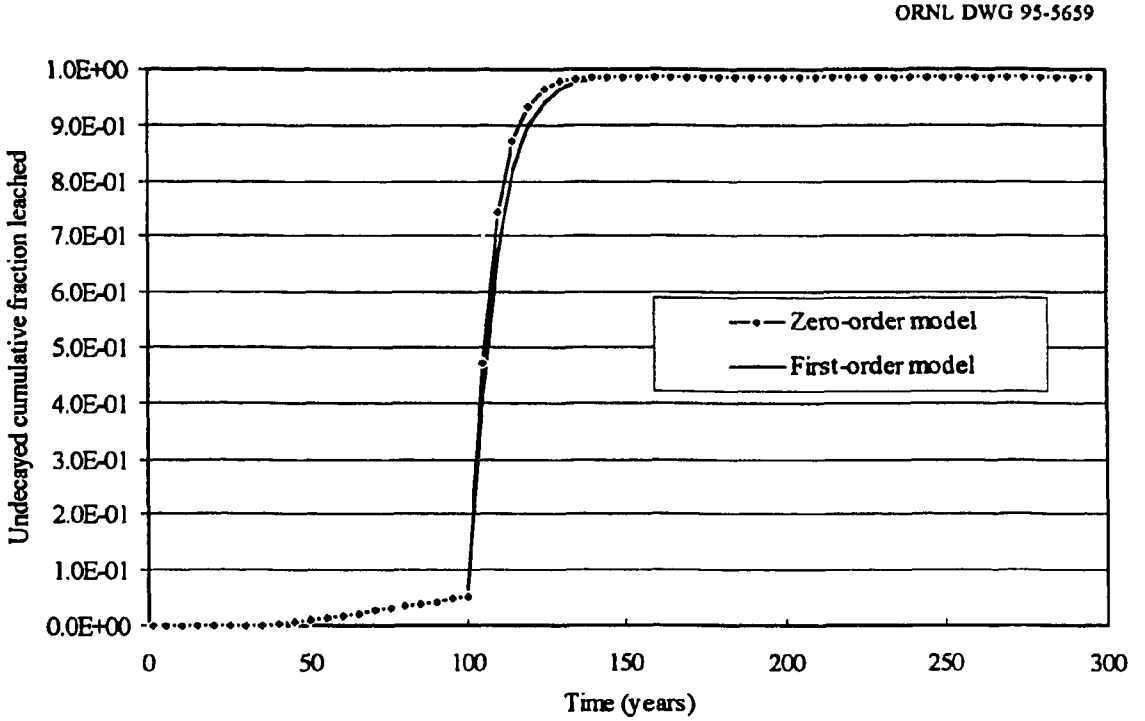

Fig. B.2. Comparison of the undecayed cumulative fraction of ^{14}C leached from a tumulus (SOURCE1) using zero-order and first-order advection models.

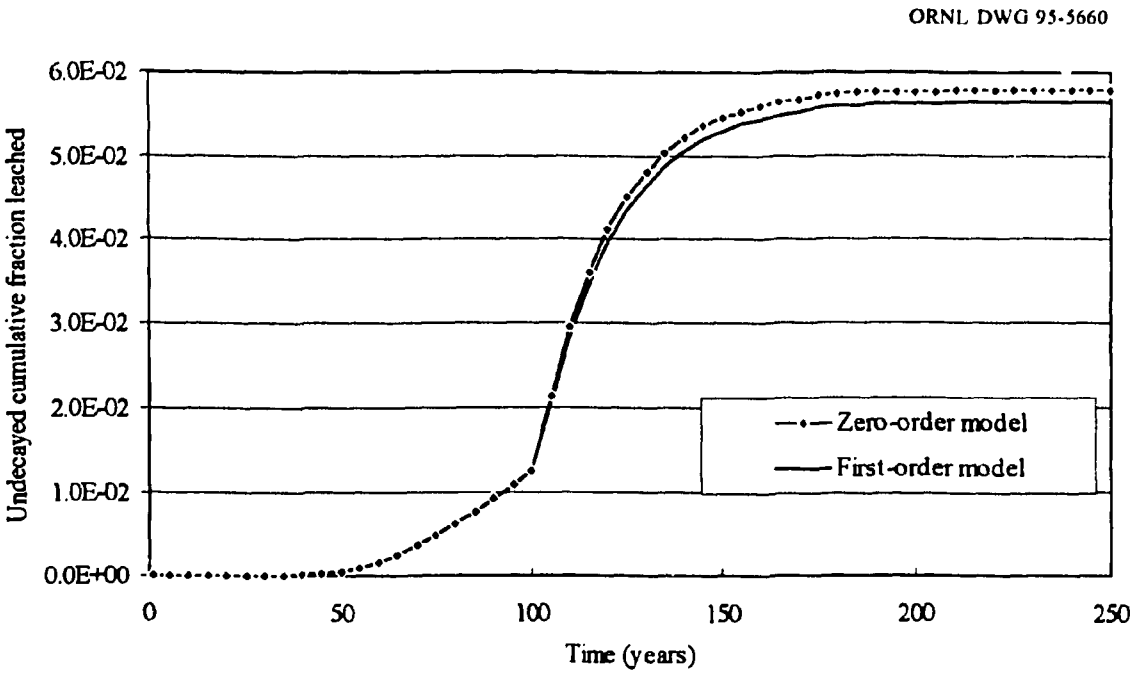

Fig. B.3. Comparison of the undecayed cumulative fraction of ^{90}Sr leached from a tumulus (SOURCE1) using zero-order and first-order advection models.

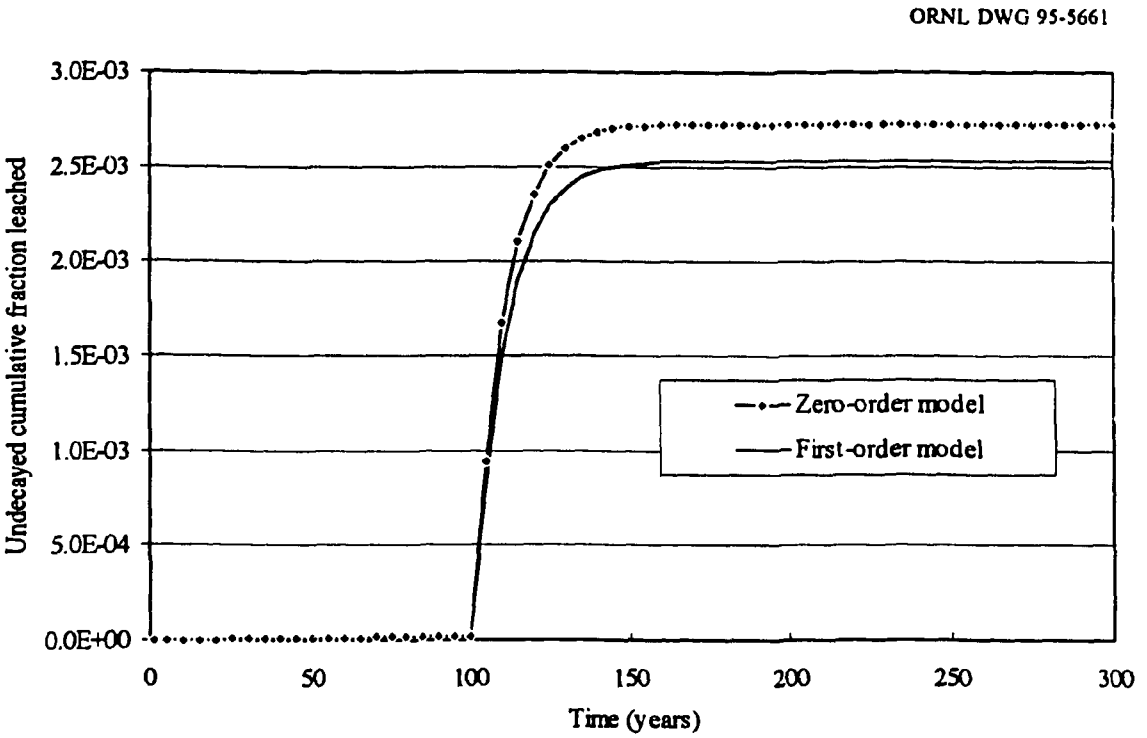

Fig. B.4. Comparison of the undecayed cumulative fraction of ^{152}Eu leached from a tumulus (SOURCE1) using zero-order and first-order advection models.

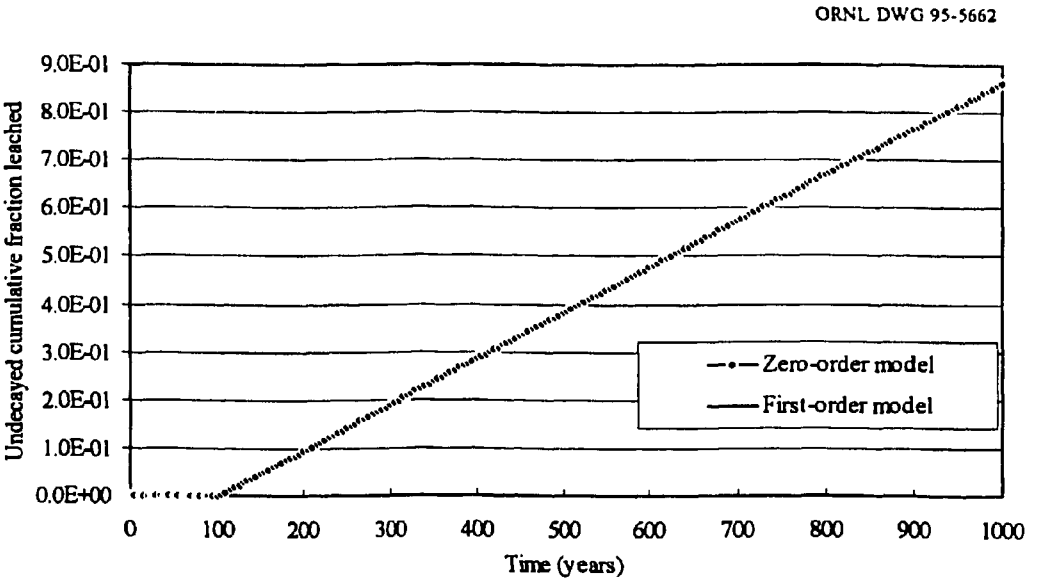

Fig. B.5. Comparison of the undecayed cumulative fraction of ^{238}U leached from a tumulus (SOURCE1) using zero-order and first-order advection models.

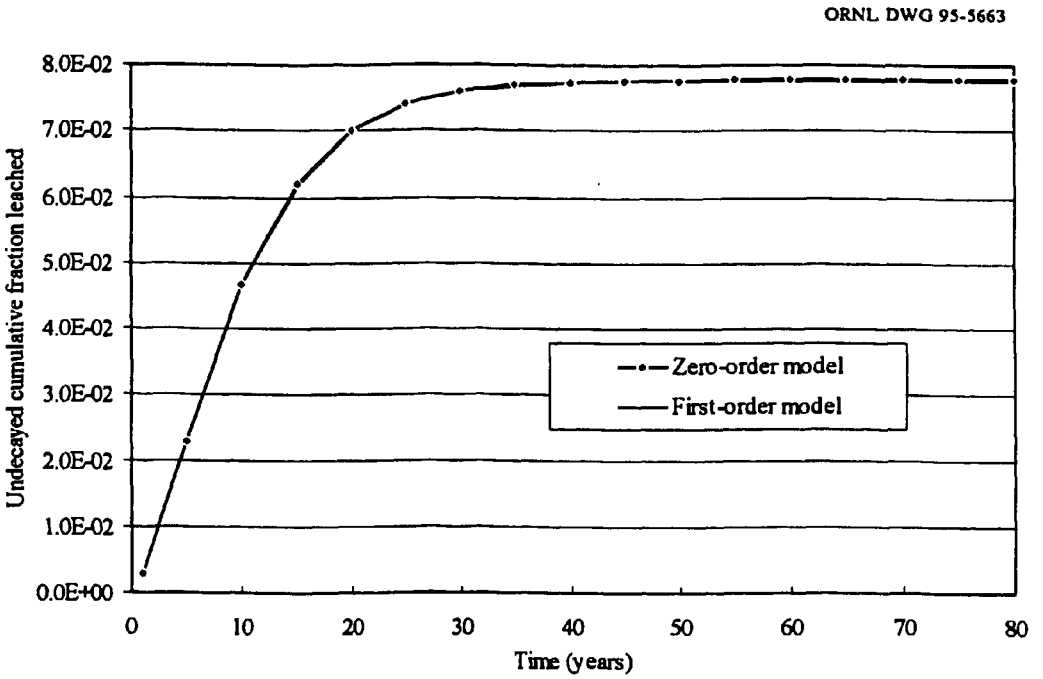

Fig. B.6. Comparison of the undecayed cumulative fraction of ^{3}H leached from a silo (SOURCE2) using zero-order and first-order advection models.

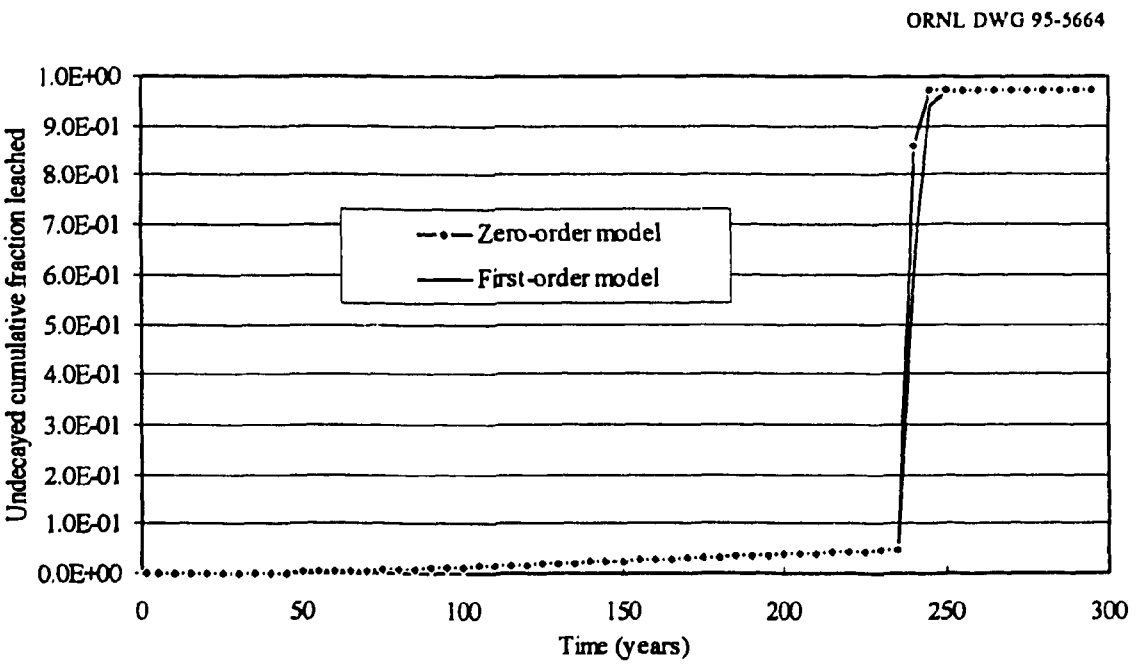

Fig. B.7. Comparison of the undecayed cumulative fraction of ^{14}C leached from a silo (SOURCE2) using zero-order and first-order advection models.

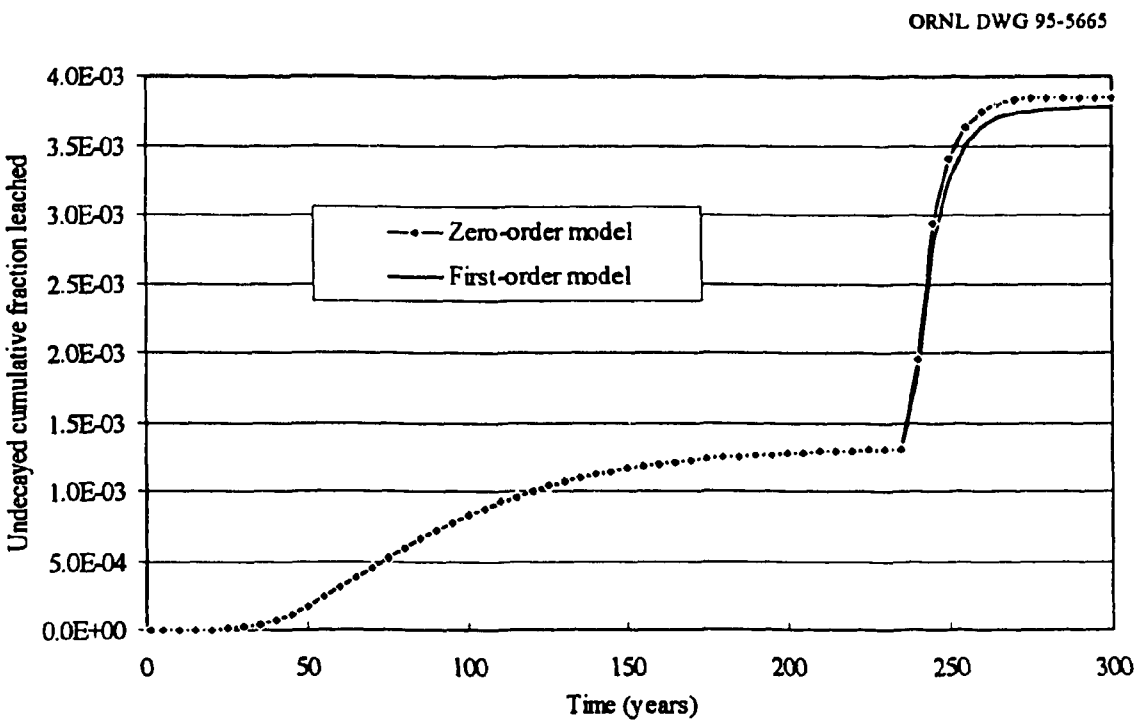

Fig. B.8. Comparison of the undecayed cumulative fraction of ^{90}Sr leached from a silo (SOURCE2) using zero-order and first-order advection models.

ORNL DWG 95-5666

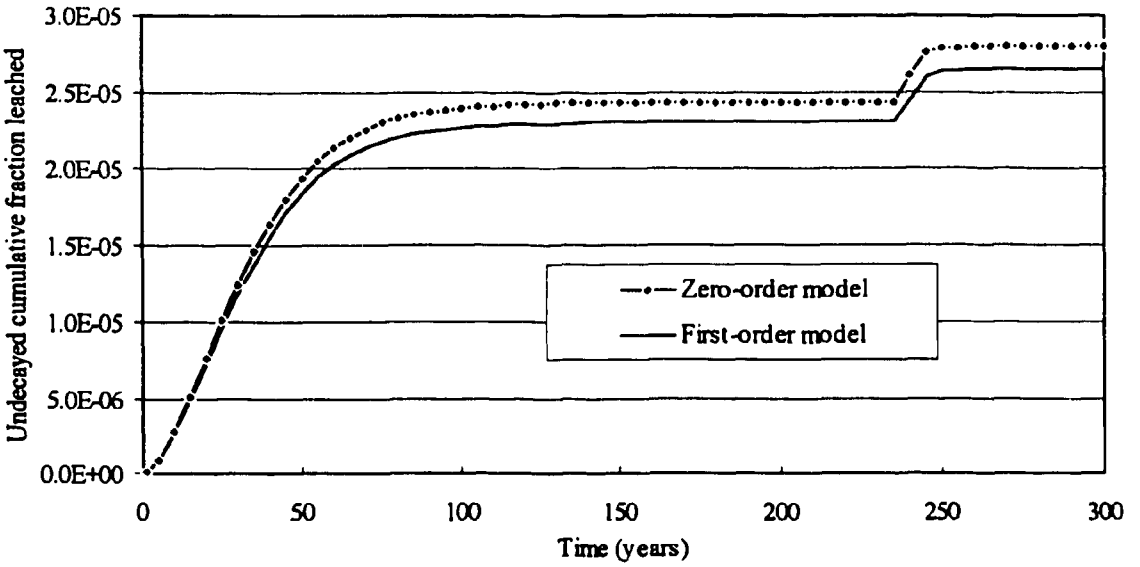

Fig. B.9. Comparison of the undecayed cumulative fraction of ^{152}Eu leached from a silo (SOURCE2) using zero-order and first-order advection models.

ORNL DWG 95-5667

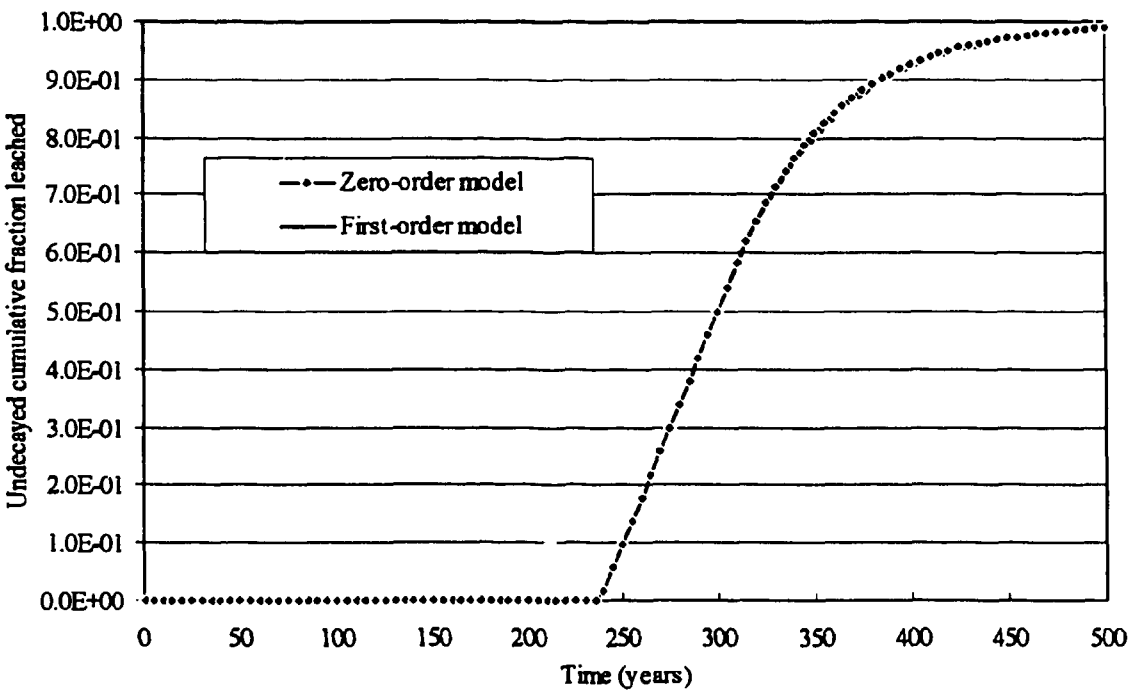

Fig. B.10. Comparison of the undecayed cumulative fraction of ^{238}U leached from a silo (SOURCE2) using zero-order and first-order advection models.

ORNL DWG 95-5668

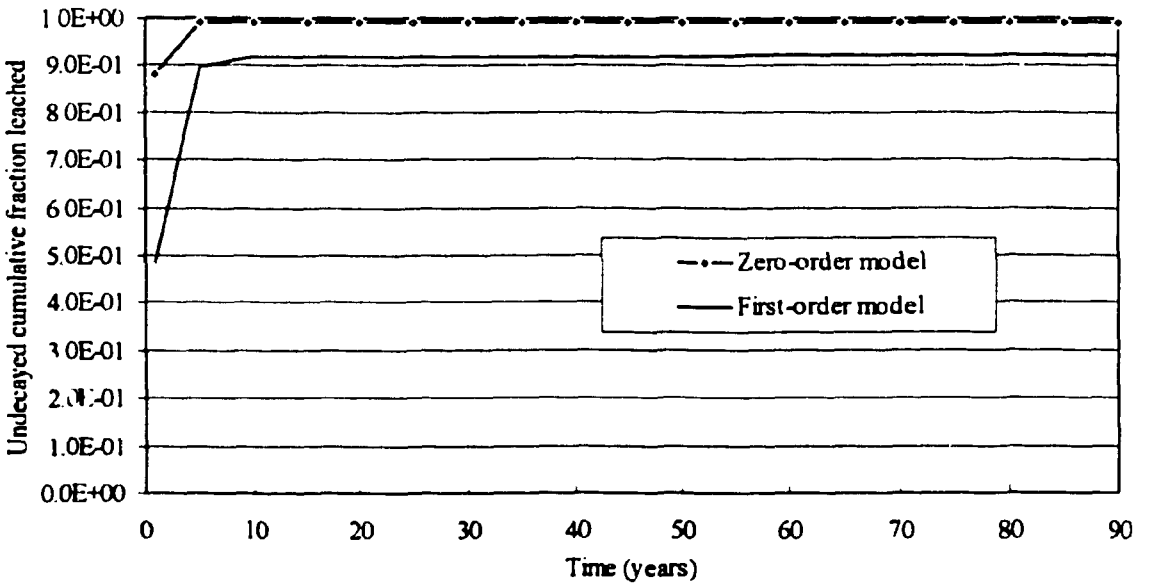

Fig. B.11. Comparison of the undecayed cumulative fraction of ^{3}H leached from an unlined trench (SOURCE2) using zero-order and first-order advection models.

ORNL DWG 95-5669

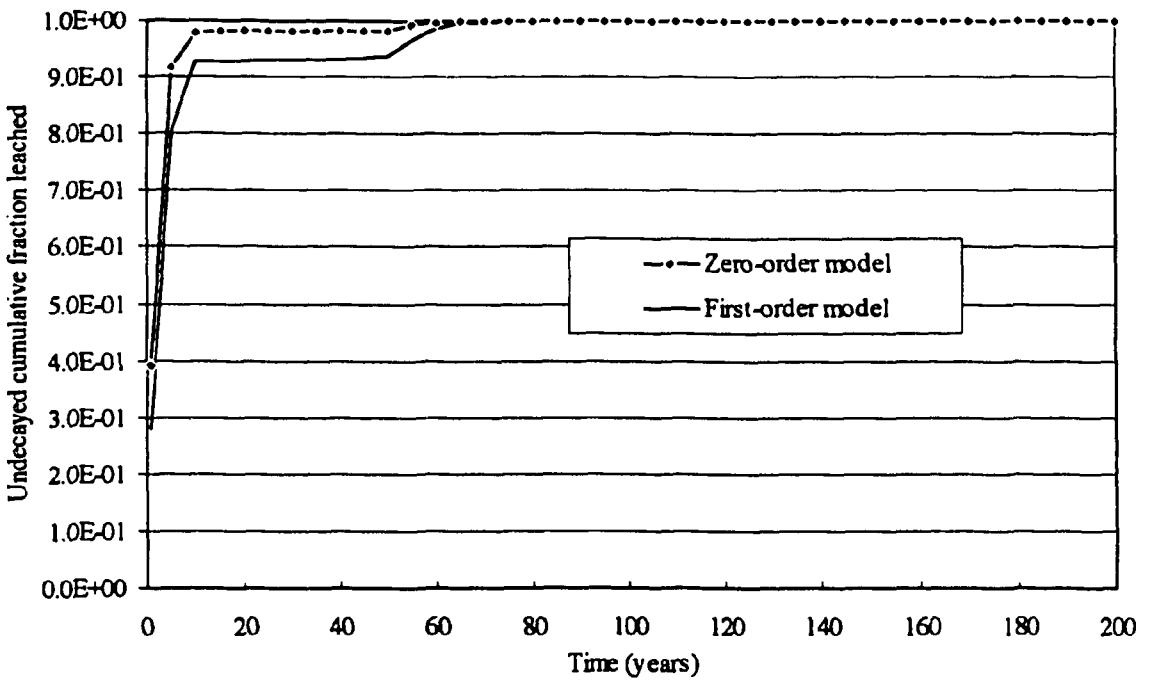

Fig. B.12. Comparison of the undecayed cumulative fraction of ^{14}C leached from an unlined trench (SOURCE2) using zero-order and first-order advection models.

ORNL DWG 95-5670

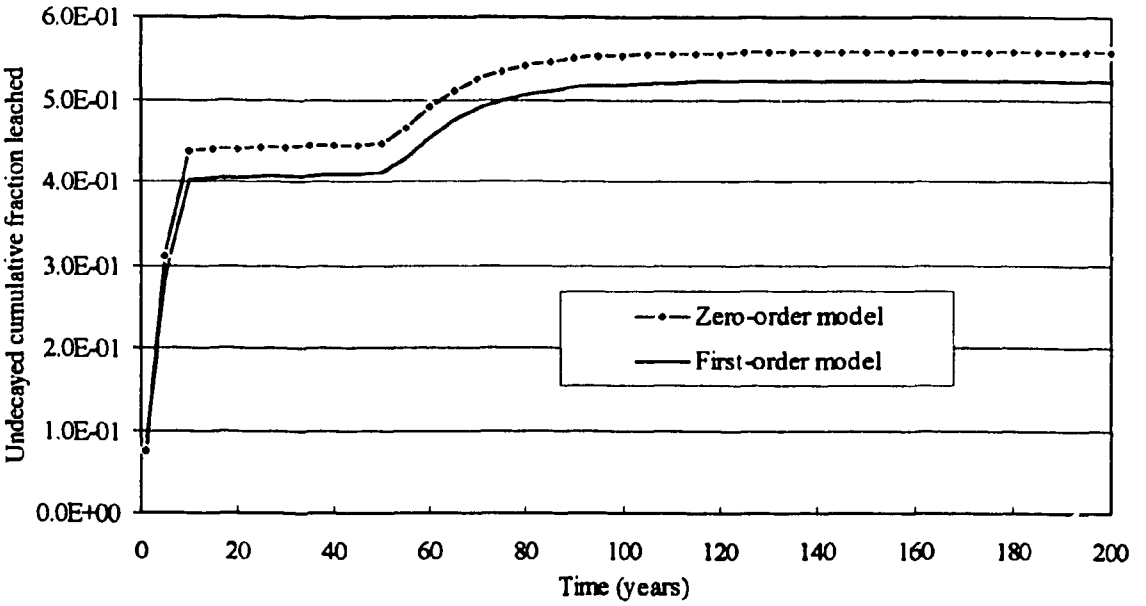

Fig. B.13. Comparison of the undecayed cumulative fraction of ^{90}Sr leached from an unlined trench (SOURCE2) using zero-order and first-order advection models.

ORNL DWG 95-5671

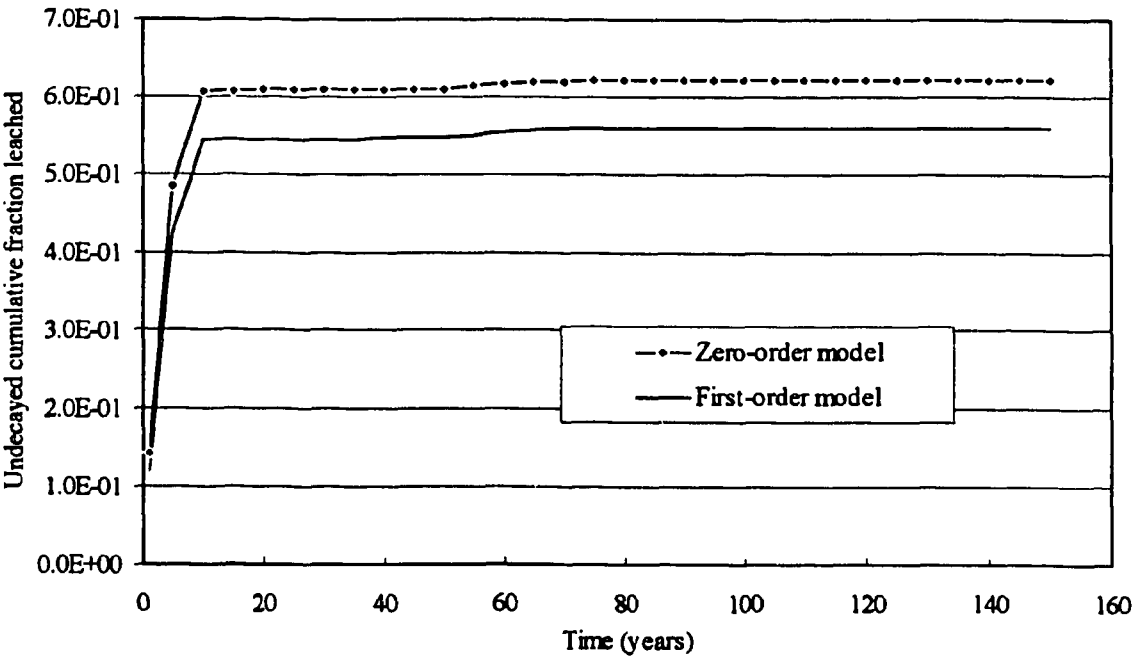

Fig. B.14. Comparison of the undecayed cumulative fraction of ^{152}Eu leached from an unlined trench (SOURCE2) using zero-order and first-order advection models.

ORNL DWG 95-5672

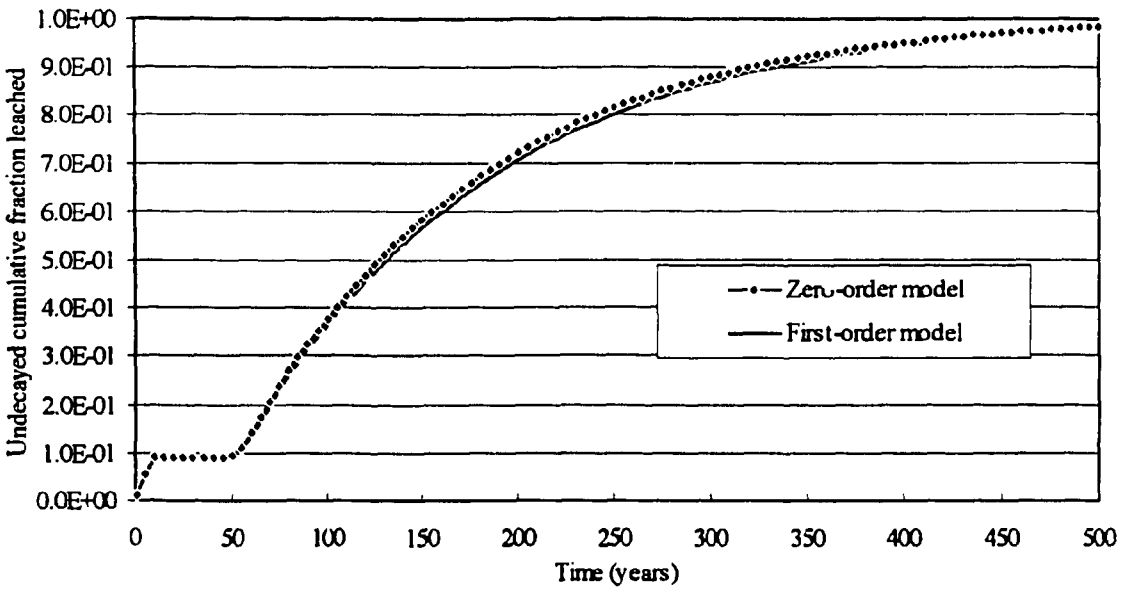

Fig. B.15. Comparison of the undecayed cumulative fraction of ^{238}U leached from an unlined trench (SOURCE2) using zero-order and first-order advection models.

INTERNAL DISTRIBUTION

1. R. C. Ashline
2. J. M. Begovich
3. G. R. Cunningham
4. D. L. Daugherty
5. J. R. Forgy, Jr.
6. H. W. Godbee
7-11. A. S. Icenhour
12. J. A. Klein
13. D. C. Kocher
14. M. W. Kohring
15. D. W. Lee
16. S. L. Loghry
17. R. J. Luxmoore
18. B. C. McClelland
19. L. E. McNeese
20. D. E. Reichle
21. R. Salmon
22. T. F. Scanlan
23. R. W. Sharpe
24. R. D. Spence
25. S. N. Storch
26. F. J. Sweeney
27. J. D. Tauxe
28. L. M. Tharp
29. M. W. Tull
30. M. W. Yambert
31. Central Research Library
32. Document Reference Center
33. ORNL Patent Section
34-35. ORNL Laboratory Records
36. ORNL Laboratory Records, RC
37. Y-12 Document Reference Section

EXTERNAL DISTRIBUTION

38. L. F. Miller, University of Tennessee, Department of Nuclear Engineering, Knoxville, TN 37996
39. R. Shuman, Rogers and Associates Engineering Corporation, P. O. Box 330, Salt Lake City, UT 84110-0330
40. Office of Assistant Manager, Energy Research and Development, DOE-OR, P.O. Box 2001, Oak Ridge, TN 37831
41-42. Office of Scientific and Technical Information, P.O. Box 62, Oak Ridge, TN 37831